

FLOW THROUGH COMPRESSIBLE POROUS MEDIA:
SHORT-TIME FILTRATION, WALL FRICTION IN COMPRESSION-
PERMEABILITY CELLS, AND RHEOLOGICAL MODELS

A Dissertation
Presented to
the Faculty of the Department of Chemical Engineering
University of Houston

In Partial Fulfillment
of the Requirements for the degree
Doctor of Philosophy in Chemical Engineering

by
Stewart Haynes, Jr.

June 1966

ACKNOWLEDGEMENTS

I am most deeply indebted to Dr. Frank M. Tiller for his assistance in formulating the problem and for his continued invaluable guidance which contributed so much to this thesis.

I would also like to acknowledge the helpful advice and guidance given by the faculty and staff of the Cullen College of Engineering, particularly Dr. Ardis H. White for his help in the design and manufacture of the force transducer.

Finally it can truly be said that this thesis could not have been written without the understanding, help, and encouragement of my wife, Jacquelyn, and therefore I dedicate this thesis to her.

FLOW THROUGH COMPRESSIBLE POROUS MEDIA:
SHORT-TIME FILTRATION, WALL FRICTION IN COMPRESSION-
PERMEABILITY CELLS, AND RHEOLOGICAL MODELS

An Abstract of a Dissertation
Presented to
the Faculty of the Department of Chemical Engineering
University of Houston

In Partial Fulfillment
of the Requirements for the Degree
Doctor of Philosophy in Chemical Engineering

by
Stewart Haynes, Jr.

June 1966

ABSTRACT

Both theoretical and experimental studies were made to elicit a better understanding of the process of filtration.

Flow equations were established for rotary drum filtration. Rotary drum filtration is characterized by short filtration times, low pressure differentials and generally by high slurry concentrations. In the development of the flow equations cognizance was taken of two effects; (1) the variation of flow rates throughout the cake due to the changes in cake porosity; and (2) the simultaneous flow of liquid and solids towards the medium. Operating and feed parameters were studied using the equations.

A modified compression-permeability cell was used to determine the degree of friction which exists between the filter cake and the side-wall of the cell. A simplified equation was derived and tested which described the frictional effect. Using this equation, factors were derived which correct the measured porosity and specific resistance for side-wall friction. Although the correction factor for porosity is not usually large, a measurable error would result if this effect were to be neglected. The correction for specific resistance is considerably larger and normally should not be neglected.

Further experimental studies were made to determine

the effect of primary compression on filter cakes. Several rheological models were compared with the experimental results. A Kelvin model was found to adequately describe the primary compression.

TABLE OF CONTENTS

CHAPTER	PAGE
I. INTRODUCTION	1
Importance of the Study	1
Description of Filtration	2
Object of the Work	4
II. DEVELOPMENT OF FILTRATION THEORY	5
Statement of the Problem	5
Review of the Literature	5
Equations for Flow Through Compressible	
Porous Solids	10
Basic assumptions	11
Equation of continuity	17
Final filtration equation	24
III. ROTARY DRUM FILTRATION	28
Literature Survey	28
Types of Rotary Filtration	30
Characteristics of Rotary Drum Filtration	30
Filtration Pressure	32
Equation for Rotary Drum Filtration	38
Comparison of Present Theory with Prior	58
Results and Discussion	68
Effect of operating variables	69
Effect of Slurry Concentration	72

CHAPTER	PAGE
Determination of R_m and α	79
IV. RELATING POROSITY TO TIME AND PRESSURE	83
Rheological Models	88
Models Used to Describe Primary Compression	92
Solutions of the Models	98
Testing of the Models	103
V. SIDE-WALL FRICTION IN COMPRESSION-PERMEABILITY	
TESTING	113
Significance of Side-wall Friction	114
Previous Investigators	115
Development of the Theory	116
Correction Factors for Porosity and Specific	
Cake Resistances	124
Testing Results	127
VI. SPECIFIC CAKE RESISTANCE VERSUS TIME	137
Experimental Studies of Specific Cake	
Resistance	139
Results and Discussion	140
VII. EQUIPMENT AND PROCEDURE	148
Materials	148
Equipment	150
Testing Procedure	156
VIII. DISCUSSION AND CONCLUSIONS	164

CHAPTER	PAGE
IX. RECOMMENDATIONS FOR FUTURE WORK	167
NOMENCLATURE	169
BIBLIOGRAPHY	174
APPENDIX	178
A. Computer Program for Numerical Calculation for Rotary Drum Filtration Theory	179
B. Ruth Program for Rotary Drum Filtration with Correction for Hydrostatic Pressure of Slurry.	185
Program for Determining Coefficients	188
Subroutine Program for Gaussian Elimination	189
Results of Calculations of Ruth Program	191
C. Calculations for Kelvin Rheological Model	192
D. Computer Output of Experimental Results	200

LIST OF TABLES

TABLE	PAGE
I. Correction Factors for Side-wall Friction . . .	135
II. Physical Properties of the Materials	149
II. Data for Rotary Drum Filtration	184
IV. Results of Calculations from Ruth Program . . .	191

LIST OF FIGURES

FIGURE	PAGE
II-1 Compressive Force Within a Filter Cake . . .	13
II-2 Schematic Diagram of a Filter Cake	16
III-1 Salient Features of a Rotary Drum Filter . . .	31
III-2 Pressure Variation for Talc	34
III-3 Pressure Variation for Hong Kong Pink Kaolin	35
III-4 Pressure Variation for Super Cel	36
III-5 Schematic Cross Section of Rotary Drum Filter	39
III-6 Total Filtrate Recorded	56
III-7 Variation of the Internal Flow Rate	57
III-8 Comparison of the Present Study with Prior Work	67
III-9 Effect of Applied Vacuum on q_f	70
III-10 Effect of Drum Submergence on q_f	71
III-11 Effect of Rotational Speed on q_f	73
III-12 Effect of Slurry Concentration on Production Rate	78
III-13 To Determine R_m and α	82
IV-1 Variation of Porosity with Time	84
IV-2 A Compression-permeability Cell Filter Cake	86
IV-3 Elements of Rheological Models	90

FIGURE	PAGE
IV-4	Rheological Models 93
IV-5	Response of Models 95
IV-6	Analog of a Kelvin Model 99
IV-7	Values for d and Δd for Runs 65 and 130 . . . 107
IV-8	Comparison of Kelvin Model to Run 65 109
IV-9	Comparison of Kelvin Model to Run 130 110
IV-10	Comparison of the Predicted Results to the Experimental 112
V-1	Schematic Diagram of a Layer of Filter Cake . 118
V-2	Typical Calibration Run 129
V-3	The Applied Force versus the Transmitted Force 132
V-4	Comparison of Steel and Teflon Lined Cylinders 134
VI-1	Variations of Specific Cake Resistance with Time 141
VI-2	Specific Cake Resistance versus Pressure . . . 143
VI-3	Variations of α with Time and Pressure . . . 146
VII-1	Caking Piston 151
VII-2	Free-floating Wall Effect Piston 153
VII-3	Compression-permeability Cell 155
VII-4	Test Cell System 157
VII-5	Caking System 158
VII-6	Block Diagram of a Strain-Gauge Indicator . . 161

CHAPTER I

INTRODUCTION

Even though the process of filtration is as old as nature itself, it has been only in the last few years that experimental and theoretical investigations have begun to elucidate the basic phenomena involved. The majority of these investigations have been for lengthy filtrations where porosity was assumed to reach an equilibrium value with respect to compressive pressure. While this assumption is valid in many situations, it may not be true for short-time operations. During short-time operations, compressive pressures within the filter cake increase quickly, and the porosities begin to decrease, requiring varying periods of time to attain their final values. Cake resistances do not reach equilibrium values during this transient stage.

The process of filtration begins with the deposition of some solid particles from a slurry onto the surface of a porous support, called the septum. As more and more of these particles are deposited, a wet solid mass is developed which is referred to as a filter cake.

Since filtration is a continuous process, slurry is admitted to the apparatus and the liquid portion of the slurry is withdrawn constantly. Thus at any instant of time,

slurry flows towards the interface of the filter cake. At this interface the solids are deposited onto the cake, immediately becoming an integral part of it and consequently increasing its thickness. A portion of the liquid in the slurry is simultaneously deposited together with the solid material to form a porous mass. The remaining portion of the liquid flows through the cake interface and passes through a tortuous path formed by the interstices of the cake and the septum particles.

As it flows through the cake, the liquid exerts a frictional drag on each particle. In turn this frictional drag produces an accumulative, compressive force on each successive element of the filter cake. Thus, the force on each elemental area of the cake, or the solid pressure at each element of the cake, increases from a minimum at the cake interface to a maximum value at the septum. This increase in pressure causes a parallel decrease in the intraparticle distance or the porosity of the cake, from a maximum value at the interface to a minimum at the septum. Furthermore, as the interstices of the cake are always liquid full, the decrease in porosity is accompanied by an increase in the absolute velocity as the liquid flows towards the septum. This increase in liquid flow is in addition to the increase in the superficial velocity brought about by the squeezing action.

If the cake is being deposited very rapidly because of either a large amount of solids in the slurry or high values of the permeability of the solid deposit, then a lag in time will occur before the porosity, permeability, and solids pressure will reach an equilibrium value. Since the mechanism of filtration is a continuous one, then theoretically as long as the fluid flows, the equilibrium values will never be attained.

Rotary filtration is used for filtering operations in which there is a high percentage of solids and where the cost of labor must be kept low. Basically there are four types of rotary filtration devices; rotary drum, rotary disk, rotary belt and string and rotary pan. By far the most common of these is the rotary drum filter. Rotary drum filtration is characterized by short filtration times, low pressure differentials, and generally by high slurry concentrations.

One of the first major contributions to rotary drum filtration was the theory reported by Ruth and Kempe (39). The development of their equations was based on three assumptions: (1) constant pressure differential across the cake, (2) constant filtration resistance, and (3) constant ratio of wet to dry cake. They also assumed that the flow rate throughout the cake was constant at any instant of time. Tiller

(61) and Shirato and co-workers (44) have shown that this is not valid.

It is the object of this work to:

1. Establish equations for rotary drum filtration which will account for the variation in flow rate (superficial velocity) within the cake. In addition, these equations will include the cocurrent movement of the solids and the filtrate toward the medium as has been reported by Shirato and co-workers (44).
2. Refine the established flow equations to account for non-equilibrium behavior of the fluid and solid during filtration.
3. Establish a basis for a better understanding of the variation of porosity and cake resistance with time.
4. Study the effect that side-wall friction has on permeability and porosity measurements obtained in a compression-permeability cell.

CHAPTER II

DEVELOPMENT OF FILTRATION THEORY

It is proposed to derive the dynamical flow equations for filtration which will account for the time effects of the fluid and solids which occur during the rapid filtration of an easily compressed material from a highly concentrated slurry.

I. REVIEW OF THE LITERATURE

Modern day filtration theory can be traced back to the hydrodynamical theories of Hagen (15), Poiseuille (35), and Darcy (9). These theories were applied by King (27) and Slichter (45) to describe the flow of liquids through regularly packed spherical particles, sands, etc., and were found to hold remarkably well for these systems. In the early twentieth century, Almy and Lewis (1) and Baker (2) experimentally studied the filtration of compressible sludges in commercial equipment. All of these investigators postulated that the rate was proportional to a driving force divided by a resistance. The difference between their various theories was in the definition of the driving force and the resistance.

Shortly after 1900 Sperry (49) performed small scale filtration under accurately controlled conditions and deter-

mined that the flow rate of liquid was proportional to the one-half power of the applied pressure drop. In addition, he discussed the necessity for developing a factor to modify the pressure term to compensate for the compression of the porous solids.

Underwood, in a series of articles (68, 69), reviewed published experimental data and postulated that the resistance of compressible precipitates was a linear function of the applied filtration pressure. Kozeny (29) in 1927, developed an equation governing the flow of fluids through a porous mass. For his model, he assumed a modification of the Poiseuille equation for capillary flow and developed an equation involving porosity, specific surface and hydraulic radius. This last term was expressed as a quotient of the surface area of the channels divided by the cross-sectional area available for flow. By this means, he arrived at an equation relating the flow rate to the applied pressure. Carman (6) also developed a filtration equation relating the flow rate through a compressible porous solid to a specific resistance. This average specific resistance was found to be solely a function of the pressure drop across the filter cake, whether the pressure drop resulted from a vacuum or a positive pressure. In differential form, Carman's filtration is similar to Kozeny's and is thus

called the Kozeny-Carmen equation,

$$s_c \frac{dp_x}{dx} = -k\mu \frac{(1-\epsilon)^2 s_o^2}{\epsilon^3} q \quad (\text{II-1})$$

As $\frac{dp_x}{dx}$ represents the point slope, this equation describes point conditions within a compressible precipitate.

In a series of articles published by Ruth (37, 38, 39) the idea of specific resistance, α_R , was developed. Ruth wrote the basic flow equation in the following form of rate equals driving force divided by resistance:

$$q = \frac{s_c p}{\mu(\alpha_R w + R_m)} \quad (\text{II-2})$$

The quantity α_R is an average, overall value expressed on the basis of resistance per unit mass of dry cake. The filtration resistance of Ruth is related to the permeability of Darcy and the Kozeny-Carman equation by:

$$\alpha = \frac{1}{k \rho_s (1-\epsilon)} = \frac{k (1-\epsilon)^2 s_o^2}{\epsilon^3} \quad (\text{II-3})$$

Between the time of Ruth's and Carman's work and that of Grace and Tiller there were no significant advances in the mathematical treatment of filtration.

Grace reported an extensive investigation of the filter properties of some seventeen different precipitates in

a series of papers (11,12,13). In addition, he correlated local coefficients obtained in a compression-permeability cell with average resistance coefficients of the Ruth type obtained from constant pressure filtration data.

Probably the most extensive series of papers analyzing published data and extending the theory of filtration has been written by Tiller and co-authors (57,58,59,60,61,62,63,64,65). In his first article he showed that the filtration equation proposed by Ruth did not describe the actual behavior of a constant pressure filtration process during the initial period of time. In Ruth's derivation, it was assumed that the average α was constant throughout the filtration. Tiller showed that there were two reasons why Ruth's assumption was false. First, in the idealized case in which the local α_x is known either through a relation such as Equation II-3 or through direct experimental data, the integrated average α is a constant only when the pressure drop across the cake is constant. However, in constant pressure filtration with medium resistance, the pressure drop across the cake varies with time. When the first drop of liquid flows through the filter unit, the entire pressure drop is across the medium. As time goes on and the rate decreases, the pressure drop across the cake increases. Consequently, the average α_R of the cake increases with time contrary to the assumption of Ruth.

Second, equations like II-3 do not correctly represent the cake resistance. They are based on the assumption that

$\alpha_x = f(p_g)$, that is the value of p_g reaches an equilibrium value, instantaneously, on the application of pressure.

The lag in reaching equilibrium values will be felt in filtration by changing α_x with respect to time. Thus there are two effects which cause the average cake resistance to vary with time, (1) changing pressure drop across the cake and (2) failure of α_x to be a function of p_g alone.

Although previous investigators had assumed that the rate of liquid flow throughout the cake was constant, Tiller and Cooper (61) have shown that such an assumption is not valid. By examining the liquid flow over a differential section of the cake, they found the following relationship

$$\left(\frac{\partial q}{\partial x} \right)_{\theta} = \left(\frac{\partial \epsilon}{\partial \theta} \right)_x \quad (\text{II-4})$$

This fact can be established from a consideration of the hydrodynamical equation for continuity. The same equation was proposed much earlier by Terzaghi (56).

In one of his latter articles, Tiller and Shirato (64) proposed that the filtration resistance is a function of the slurry concentration

$$\alpha_T = J \alpha_R \quad (\text{II-5})$$

where

$$J = f(s;p) \quad (\text{II-5a})$$

With regard to the latter function, Shirato and Okamura (42) and Toro (67) have confirmed experimentally that the cake resistance is a function of the slurry concentration.

Finally, Tiller has presented data (57) which show that the consolidation of the cake, as measured by the changes in porosity, continues for several minutes, even under moderately high compressive pressures.

Thus, filtration theory has progressed from equations based on semi-empirical bulk principles of Hagan, Poiseuille, and Darcy to the refined theoretical approaches of Kozeny-Carman, Ruth, Tiller, and Shirato.

II. EQUATIONS FOR FLOW THROUGH COMPRESSIBLE POROUS SOLIDS

Fundamental to the understanding of filtration is the theory of flow through compressible porous solids. The theory of flow through compressible porous solids seeks to interrelate volume of throughput, overall pressure differential, rate of flow, average bed porosity, mass of solids deposited, and time. A closer examination of the physics of a filter cake will yield a better understanding of the

filtration process. In this examination a number of basic assumptions are made, they are:

Basic Assumptions

1. The flow through the porous material is one-dimensional and viscous. The flow is single phase.
2. Solid particles and flowing liquid are incompressible.
3. There is point contact between particles.
4. The porosity and the specific filtration resistance have the same values for both filter cake and confined solids in a compression-permeability cell. The correspondence of equality can be assumed when the solids compressive pressure in a filter cake, as defined by $p_s = p - p_1$, equals the applied mechanical pressure in the compression-permeability cell. Essentially this assumption is based upon the belief that compressive forces produced by frictional drag are equivalent to those resulting from mechanical loading.

During filtration, liquid flows through the interstices of the compressible bed of solids exerting a compressive force on each element of the total filter cake. Since flow in most filtrations is viscous, the frictional drag and hydraulic pressure drop could be calculated theoretically by

the use of the Navier-Stokes equation of motion. However, the solution of such equations requires an exact geometric definition of the boundary conditions and restraints. Graton and Fraser (14) contributed a classic article to the literature of particle configuration in 1935. While others have written on the same subject, the complexity of internal geometrical arrangements of uniform spherical particles has led to as yet unsolved flow problems in a closed analytical form, it would seem futile to approach the greatly more difficult case of random distribution of irregularly shaped particles. Happel and Brenner have discussed the difficulty involved in this problem of random distribution. Also this problem was briefly discussed by Scheidegger (40). Recently Snyder and Stewart (48) have presented a system of differential equations which describe the velocity and pressure profiles for creeping flow of a constant property, Newtonian fluid through a bed of spheres arranged in regular cubic close-packing. An approximate solution to this system of differential equations was obtained using Galerkin's method (26). Nevertheless no theoretical solution of the flow through porous solids is possible without a complete understanding of the internal geometry of those solids and the changes which result from flocculation, particle migration, fluid shear, etc.

In Figure II-1 the particles composing the filter cake

COMPRESSIVE FORCES WITHIN A FILTER CAKE

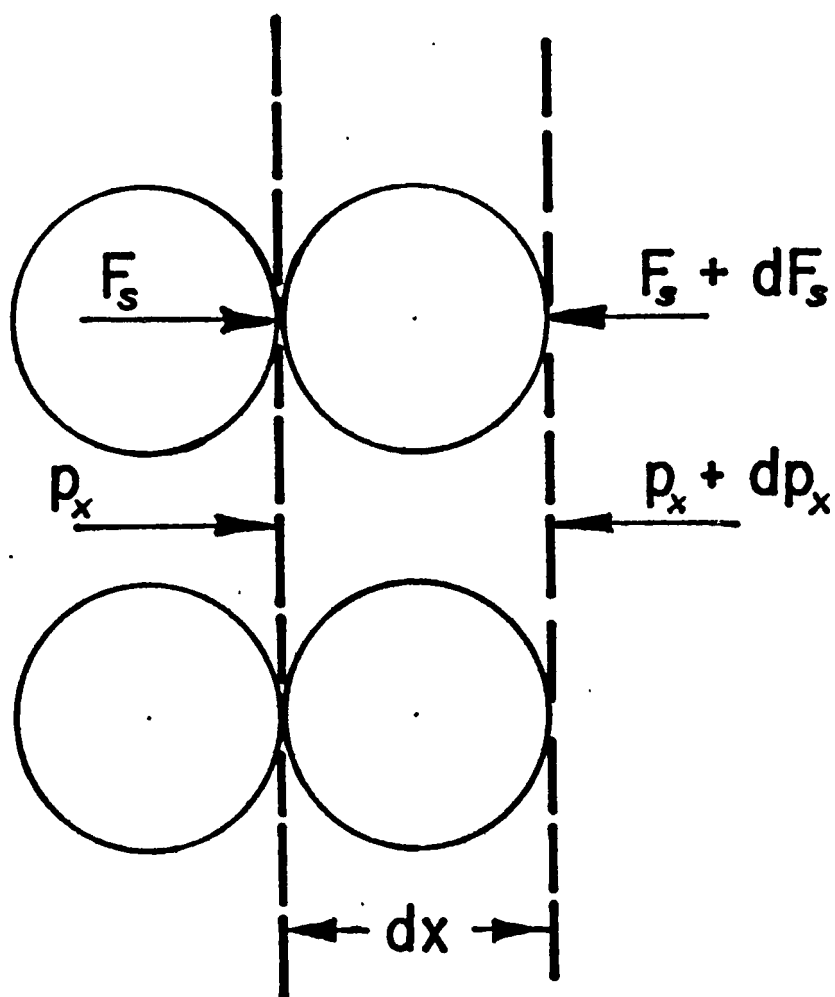


FIGURE II-1

are shown to be regularly arrayed and in point contact with one another. Actually, it is not necessary to the discussion to have regularly arrayed particles, but it is shown so as to illustrate the principles discussed. There is the necessity of assuming point contact, assumption 3, because with the particles in point contact, the hydraulic pressure, p_x , is effective over the entire cross-section of the cake. A further discussion of this point was made by Tiller and Huang (63). Considering, then, the forces on the total mass within a differential distance, dx , the summation of forces is given by

$$\sum = F_s + dF_s + A(p_x + dp_x) - F_s - Ap_x \quad (\text{II-6})$$

This net force is equal to the product of the mass within the elemental volume times the acceleration of the particles within. But, although the solids composing the cake do move towards the medium, their acceleration is actually so small as to be negligible. Thus, the equation can be rewritten as

$$dF_s + Adp_x = 0 \quad (\text{II-7})$$

and defining the solids compressive pressure as

$$dp_s = \frac{dF_s}{A} \quad (\text{II-8})$$

then,

$$dp_s + dp_x = 0 \quad (\text{II-9})$$

In Figure II-2 is presented a schematic diagram of a compressible filter cake. At a distance x from the medium is an elemental volume of the filter cake, Adx . This elemental volume of the cake is composed of the porous solid and the liquid phase which entirely fills the interstices of the porous solid. This liquid phase is flowing towards the septum. The fundamental differential equation for the pressure drop in the liquid phase brought about by this flow can be represented by Kozeny's equation

$$s_c \frac{dp_x}{dx} = -k s_o^2 \frac{(1-\epsilon)^2 \mu q}{\epsilon^3} \quad (\text{II-10})$$

A relationship exists between the porosity ϵ , Kozeny-Carman's permeability coefficient, k , and Ruth's specific filtration resistance, α_x , in the form

$$\alpha_x = \frac{k s_o^2 (1-\epsilon)}{\rho_s \epsilon^3} \quad (\text{II-11})$$

SCHEMATIC DIAGRAM OF A FILTER CAKE

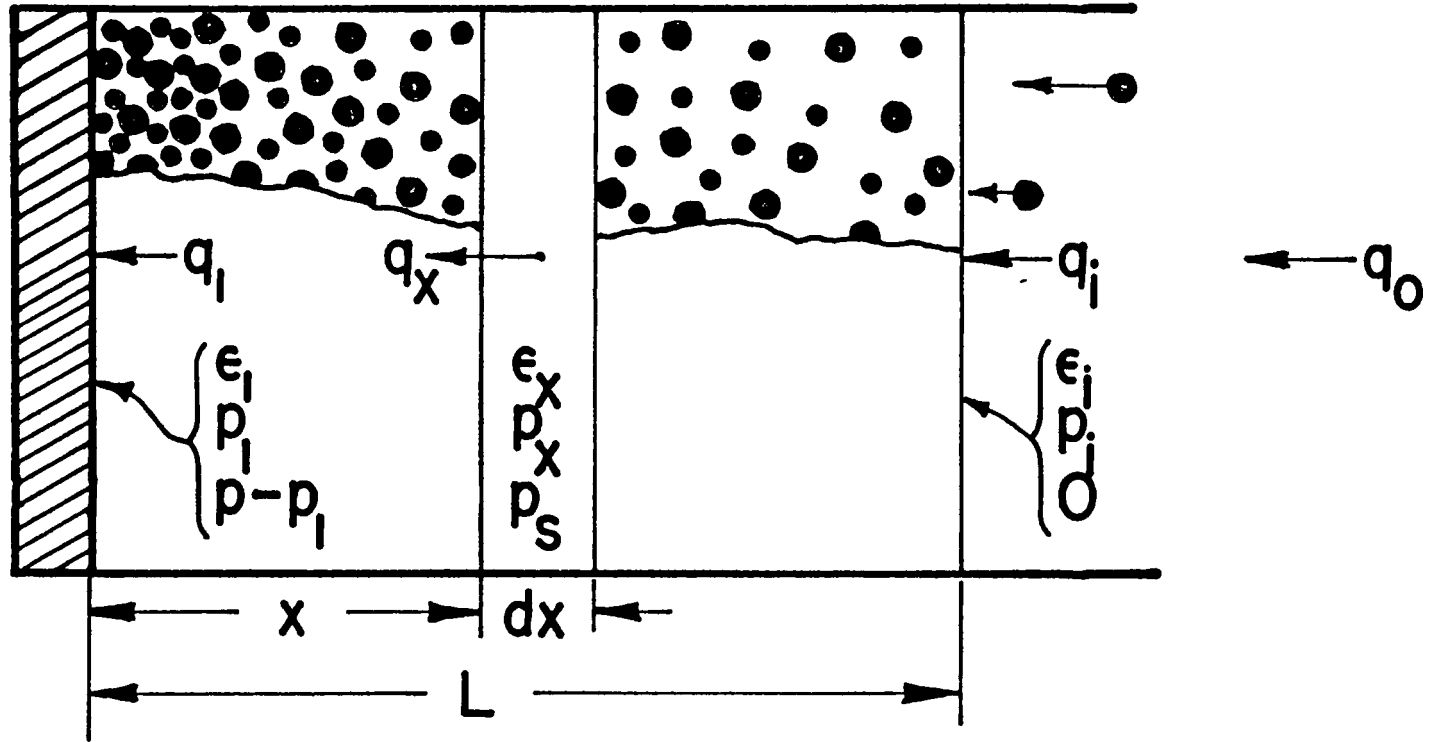


FIGURE II-2

Upon substituting this relationship into the Kozeny differential equation, one obtains the equation as modified by Tiller (61)

$$s_c \frac{dp_x}{dx} = -\rho_s \alpha_x (1 - \epsilon) \mu q \quad (\text{II-12})$$

The latter equation can be differentiated with respect to x to give

$$s_c \frac{d^2 p_x}{dx^2} = -\rho_s \mu \alpha_x (1 - \epsilon) \left(\frac{\partial q}{\partial x} \right)_\theta - \rho_s \mu q \left(\frac{\partial}{\partial x} [\alpha_x (1 - \epsilon)] \right)_\theta \quad (\text{II-13})$$

This is the differential flow equation which describes the changes in cake property with distance. Its final form depends upon the form of the equation of continuity assumed. The development of this latter equation is discussed next.

Equation of Continuity

The equation of continuity as given by Tiller and Cooper (61) and Terzaghi (56) relates the change of the rate of fluid flowing past a point within the cake, at a point x -distant from the septum, to the change in the porosity of the cake with time, as

$$\left(\frac{\partial q}{\partial x}\right)_{\theta} = \left(\frac{\partial \epsilon}{\partial \theta}\right)_x \quad (\text{II-14})$$

Heretofore, there has been a general assumption that equilibrium porosity is reached instantaneously, but as reported by Tiller (57) this is not true. For some materials it has been found that it takes about ten minutes to reach an initial equilibrium, after which a gradual creep continues for quite some time. With other materials such as clays, initial equilibrium was not reached for many hours with creep going on continually. Very few data on time effect have been published. Nevertheless, the time effect is important in that porosity is a maximum at the time the filter bed is laid down, and therefore, the cake resistance is at a minimum. In the initial stage of cake deposition, resistances are smaller than those obtained after the primary consolidation has been effected. Still larger resistances will occur when the secondary creep proceeds. Thus, the porosity may be defined as a function of both time and solids pressure

$$\epsilon = \epsilon (\theta, p_s) \quad (\text{II-15})$$

Porosity is usually determined experimentally in a compression-permeability cell, wherein the cake undergoes

compression. Intimately related to the cake compression is the nature of the cake materials, the void distribution, the flow rates, and pressure drops. This compression is a very complex process involving the basic ideas of friction, transmission of forces, and distribution of the resultant stresses. With regard to the idea of friction there are two types which must be differentiated. The first is the particle-to-particle friction and the second, liquid-to-particle.

A large amount of work has been devoted to the study of particle-to-particle friction in numerous fields such as soil mechanics, rock mechanics, lubrication, metallurgy, theoretical mechanics, and fluid mechanics. In soil mechanics particle-to-particle friction is separated into two components, one due to the cohesion between the particles and the other to the friction between the particles. The true cohesion of the particles is produced by the actual bond which develops at the surface of contact of the particles as a result of electrochemical forces; these forces are dependent on a great number of factors which are still being studied. The study of friction between particles includes the study of contact surfaces of the particles involved and the normal forces with which they are pressed together.

A meager amount of theoretical work has been reported on the liquid-to-particle friction which is developed when a

porous solid is undergoing compression. Recently several articles, by Brandt and Johson (5), Famularo and Happel (10) and Isaakyan and Gasparyan (21), have appeared which indicate the understanding of this frictional phenomenon is still incomplete. Some theoretical work has been published in the fields of hydrology, geophysics, and petroleum engineering; however, these works concern fixed beds of solid particles which were not undergoing compression.

Compression depends upon squeezing out liquid contained in the interstices of the compressible porous solid. Terzaghi (56) assumed that the only factor effecting compression was the frictional flow of the liquid through the porous solid. He also assumed that at each solids pressure p_s there was a corresponding equilibrium porosity which was a function of the compressive pressure and not the time.

Tiller and Cooper (62) have shown that a priori prediction of the effect of pressure on the porosity is difficult and not entirely dependent on the compressibility of the solid. In this prediction they used an analytical expression relating equilibrium porosity to the solids pressure which expression was obtained by an analysis of experimental equilibrium porosity data.

Similarly, an analytical expression may be found which will give the form of the function ϵ in Equation (II-15) by the analysis of experimental data for porosities obtained under

conditions where time effects, as well as solids pressure, have been studied.

A total differential of Equation (II-15) will be

$$d\epsilon = \left(\frac{\partial \epsilon}{\partial p_s} \right)_{\theta} dp_s + \left(\frac{\partial \epsilon}{\partial \theta} \right)_{p_s} d\theta \quad (\text{II-16})$$

By dividing the total differential by the differential, $d\theta$, the derivative of porosity with respect to time then becomes

$$\left(\frac{\partial \epsilon}{\partial \theta} \right)_x = \left(\frac{\partial \epsilon}{\partial p_s} \right)_{\theta} \left(\frac{\partial p_s}{\partial \theta} \right)_x + \left(\frac{\partial \epsilon}{\partial \theta} \right)_{p_s} \quad (\text{II-17})$$

This expression indicates that the change in porosity with time at a given point within the filter cake is composed of two effects. The first effect, which expresses the change in porosity due to the velocity with which the solids pressure at that point within the filter cake is changing with time, is a product of two factors, $\left(\frac{\partial \epsilon}{\partial p_s} \right)_{\theta} \left(\frac{\partial p_s}{\partial \theta} \right)_x$. The first of these factors, $\left(\frac{\partial \epsilon}{\partial p_s} \right)_{\theta}$, indicates the change in porosity with solids pressure, at a constant time, and is multiplied by the second of the factors which is the change in pressure with time at the given point in the cake, $\left(\frac{\partial p_s}{\partial \theta} \right)_x$. The first effect is that which results from primary compression of a filter cake. The second effect, which indicates that there is a change of porosity with time which is independent of

any changes in the solids pressure at the given point within the filter cake, $\left(\frac{\partial \epsilon}{\partial \theta}\right)_{P_S}$, is the creep factor which has been evidenced in a compression-permeability cell. It is this latter factor which has been neglected in the field of filtration.

Although this creep effect has been evidenced in compression-permeability cell testing, it has not been separated from other effects in an actual filtration process. To transfer the concepts of the behavior of a filter cake, as expressed in Equation (II-16) and (II-17) to an actual filtration process would require more knowledge of the function given in (II-15) than is presently available.

In the compression-permeability cell experiment, the total fixed amount of cake is compressed simultaneously, whereas in a filtration process the amount of cake w is constantly being added to by the deposition of an increment dw of cake at a time θ' . At the instant an incremental amount of cake is deposited, the same action occurs as would occur in a compression-permeability cell, with one major exception. It is this exception that causes the difficulty in applying compression-permeability cell data to an actual filtering cake in a filtration process. The major difficulty is that there are two different scales of time θ and θ' . The first time scale θ would refer to the total time that the filtration process has been operating; whereas, the

other scale, θ' , refers only to that time since an increment of cake dw , was deposited. In a compression-permeability cell, there is no distinction between the two time scales, because no cake is being deposited, thus $\theta' = \theta$. In filtration, $\theta' \neq \theta$, because the filter cake is being continuously deposited. If the form of Equation (II-17) were known it might be possible to establish a theory relating the behavior in a filter cake to that observed in a compression-permeability cell cake by the establishment of a function of the type, say

$$\left(\frac{\partial \epsilon}{\partial \theta}\right)_{dw} = \left(\frac{\partial \epsilon}{\partial p_s}\right)_{\theta'} \left(\frac{\partial p_s}{\partial \theta}\right)_{dw} + \left(\frac{\partial \epsilon}{\partial \theta'}\right)_{p_s} \quad (\text{II-17a})$$

At the present time such a function has not been developed, thus Equation (II-15), (II-16), and (II-17) must be restricted to describing the behavior within a compression-permeability cell. To describe the behavior of the filtration cake, with the present understanding, porosity must be assumed to reach equilibrium instantaneously. Thus porosity is a function of p_s alone, and Equation (II-14) may be rewritten as

$$\left(\frac{\partial \epsilon}{\partial \theta}\right)_x = \left(\frac{d\epsilon}{dp_s}\right) \left(\frac{\partial p_s}{\partial \theta}\right)_x \quad (\text{II-18})$$

This is the modified continuity equation.

Final Filtration Equation

Substituting the modified continuity Equation (II-18) into the differential flow equation (II-13) will yield the following

$$\begin{aligned} \epsilon_c \frac{\partial^2 p_x}{\partial x^2} = & -\rho_s \mu a_x (1 - \epsilon) \left[\frac{d\epsilon}{dp_s} \left(\frac{\partial p_s}{\partial \theta} \right)_x \right] \\ & - \rho_s \mu a \left[\frac{\partial \{a_x (1 - \epsilon)\}}{\partial x} \right] \end{aligned} \quad (\text{II-19})$$

Referring to Equation (II-9), it has been shown that the resultant sum of changes in the solids pressure and liquid pressure is zero. Thus, differentiation of the solids pressure twice with respect to x yields

$$\frac{\partial^2 p_s}{\partial x^2} = - \frac{\partial^2 p_x}{\partial x^2} \quad (\text{II-20})$$

Upon substituting these results into the previous equation for fluid flow, Equation (II-19), will give

$$\begin{aligned} \epsilon_c \frac{\partial^2 p_g}{\partial x^2} = & \rho_s \mu a_x (1 - \epsilon) \left[\frac{d\epsilon}{dp_s} \left(\frac{\partial p_s}{\partial \theta} \right)_x \right] \\ & + \rho_s \mu a \left[\frac{\partial \{a_x (1 - \epsilon)\}}{\partial x} \right] \end{aligned} \quad (\text{II-21})$$

However, the flow rate at a given point within the filter cake has been related by Equation (II-12). Rearrangement

of this equation gives

$$q = \frac{-\epsilon_c \frac{dp_x}{dx}}{\rho_B \mu \alpha_x (1-\epsilon)} = \frac{\epsilon_c \frac{dp_s}{dx}}{\rho_B \mu \alpha_x (1-\epsilon)}$$

Thus, the expression for the flow is now given in terms of the change of the solids pressure. Substitution of this equation into the previous filtration Equation (II-21), gives

$$\begin{aligned} \epsilon_c \frac{\partial^2 p_s}{\partial x^2} &= \rho_B \mu \alpha_x (1-\epsilon) \left[\frac{d\epsilon}{dp_s} \left(\frac{\partial p_s}{\partial \theta} \right)_x \right] \\ &+ \frac{\epsilon_c \frac{dp_s}{dx}}{\alpha_x (1-\epsilon)} \left[\frac{\partial \{ \alpha_x (1-\epsilon) \}}{\partial x} \right] \end{aligned} \quad (\text{II-23})$$

The mass of solids per unit area at a distance x from the septum can be defined as

$$w_x = \frac{W}{A} = \frac{\rho_s (1-\epsilon) x}{A} \quad (\text{II-24})$$

Upon differentiation of this equation with respect to the solids pressure, the change in solids pressure can be related to the change in the mass of cake with distance

$$\frac{dp_s}{dx} = \rho_s (1 - \epsilon) \frac{dp_s}{dw_x} \quad (\text{II-25})$$

The last expression can be differentiated with respect to x and upon a change of variables, the following expression can be obtained

$$\begin{aligned} \frac{d^2 p_s}{dx^2} = \rho_s (1 - \epsilon) \frac{\partial^2 p_s}{\partial w_x^2} \frac{dw_x}{dx} \\ + \rho_s \frac{\partial p_s}{\partial w_x} \frac{\partial (1 - \epsilon)}{\partial p_s} \frac{dp_s}{dx} \end{aligned} \quad (\text{II-26})$$

The change in the mass of cake with respect to a change in distance can be defined by differentiation of Equation (II-24) with respect to distance. The results of this differentiation substituted into the above Equation (II-26) will yield the following expression

$$\begin{aligned} \frac{\partial^2 p_s}{\partial x^2} = \rho_s^2 (1 - \epsilon) \frac{\partial^2 p_s}{\partial w_x^2} \\ + \rho_s^2 (1 - \epsilon) \frac{\partial (1 - \epsilon)}{\partial p_s} \frac{dp_s}{dx} \end{aligned} \quad (\text{II-27})$$

which is the desired equation for the change in solids pressure with cake thickness in terms of the mass of the cake.

When this equation is substituted into Equation (II-21) and the resulting equation divided through by $\epsilon_0 \rho_s^2 (1 - \epsilon)^2$ the following equation is obtained

$$\frac{\partial^2 p_s}{\partial w_x^2} = \frac{\mu a_x}{\rho_s (1 - \epsilon)} \left[\frac{d\epsilon}{dp_s} \left(\frac{\partial p_s}{\partial \theta} \right)_x \right] + \frac{1}{\rho_s^2 a_x (1 - \epsilon)} \frac{\partial [\alpha_x (1 - \epsilon)]}{\partial p_s} \left(\frac{\partial p_s}{\partial x} \right)^2 - \frac{1}{(1 - \epsilon)} \frac{\partial (1 - \epsilon)}{\partial p_s} \left(\frac{\partial p_s}{\partial w_x} \right)^2 \quad (\text{II-28})$$

Since it has already been shown that

$$\left(\frac{\partial p_s}{\partial x} \right)^2 = \rho_s^2 (1 - \epsilon)^2 \left(\frac{\partial p_s}{\partial w} \right)^2 \quad (\text{II-29})$$

then substituting this relationship into Equation (II-28) and simplifying will yield

$$\epsilon_0 \frac{\partial^2 p_s}{\partial w_x^2} = \frac{\mu a_x}{\rho_s} \left[\frac{\partial \ln(1 - \epsilon)}{\partial p_s} \right] \left(\frac{\partial p_s}{\partial \theta} \right)_x + \epsilon_0 \left(\frac{\partial \ln a_x}{\partial p_s} \right) \left(\frac{\partial p_s}{\partial w_x} \right)^2 \quad (\text{II-30})$$

which has been previously reported by Tiller and Cooper (62):

CHAPTER III

ROTARY DRUM FILTRATION

I. LITERATURE SURVEY

One of the first major contributions to rotary drum filtration was reported by Ruth and Kempe (39). The development of their equations was based on three assumptions: (a) constant filtration resistance, (b) constant ratio of wet to dry cake, and (c) constant pressure differential across the cake. Mondria (34), in elaborating on the data of Ruth and Kempe, derived a dimensionless equation suitable for estimating changes in the effect of pressure, filtration time, and medium resistance on filtration performance. Sjenitzer (46) revised Mondria's equation using better expressions for the filtration resistance, but he continued to neglect the effect of the medium. Schepman, Martin, and Dalstrom (41) presented data indicating that the resistance of the medium could be neglected.

This neglect of the resistance of the medium was based upon the extrapolation of the flow rate back to zero time. Tiller and Cooper (61) have shown that, in the evaluation of the medium resistance from experimental data, great care must be employed in this extrapolation. According to conventional theory, such curves should yield straight lines

if α , m , and R_m were constant. However, they have shown that variations in filtration resistances and average porosities during the very initial periods of time cause a marked deviation from the expected straight lines. Thus, if a linear extrapolation were to be used, then an incorrect value for the medium resistance could result. Many assumptions made in the past must be modified if a correct understanding of rotary drum filtration is to be attained. For example, in all the previous theories the flow rate throughout the cake was assumed to be constant at any instant of time. Tiller and Cooper (61) and Shirato (44) have shown that this assumption is not valid. Furthermore, the earlier authors neglected the effect of the variations in total filtration pressure due to the hydrostatic head of the slurry. Moreover, these authors did not include in their theories the effect of the variable filtration resistance brought about by the variation in total filtration pressure.

Therefore, it is the purpose of this chapter to establish equations for rotary drum filtration which will account for the variations in flow rate and to include the changes in total filtration pressure and the variations in the filtration resistance. This essentially will take the present published theory as far as possible. In this respect, the theory to be developed will not take into account the time lag for cake resistance and porosity to reach equilibrium

values at the applied pressure. Discussion of time effects are presented in Chapter IV.

II. TYPES OF ROTARY FILTRATION

Rotary filtration is, in general, used for filtering operations in which there is a high percentage of solids, the process is continuous, and where the cost of labor must be kept low. Basically there are four types of rotary filtration devices, namely (1) rotary pan, (2) rotary disk, (3) rotary belt or string, and (4) rotary drum. By far the most common of these is the rotary drum filter.

III. CHARACTERISTICS OF ROTARY DRUM FILTERS

Rotary drum filtration is characterized by short filtration times, low pressure differentials, and generally by high slurry concentrations. The salient features of a rotary drum filter are shown in Figure III-1. These features consist of a rotary drum, a vacuum source, a slurry level, and a knife. The latter is used to remove the filter cake. The rotary drum contains a sliding, multiported valve which connects certain segments of the medium at the periphery to the vacuum source. The vacuum is opened to the segment after it is completely submerged beneath the slurry level. as this particular segment progresses through the slurry, the filter cake builds up in the manner shown in the figure.

ROTARY DRUM FILTER

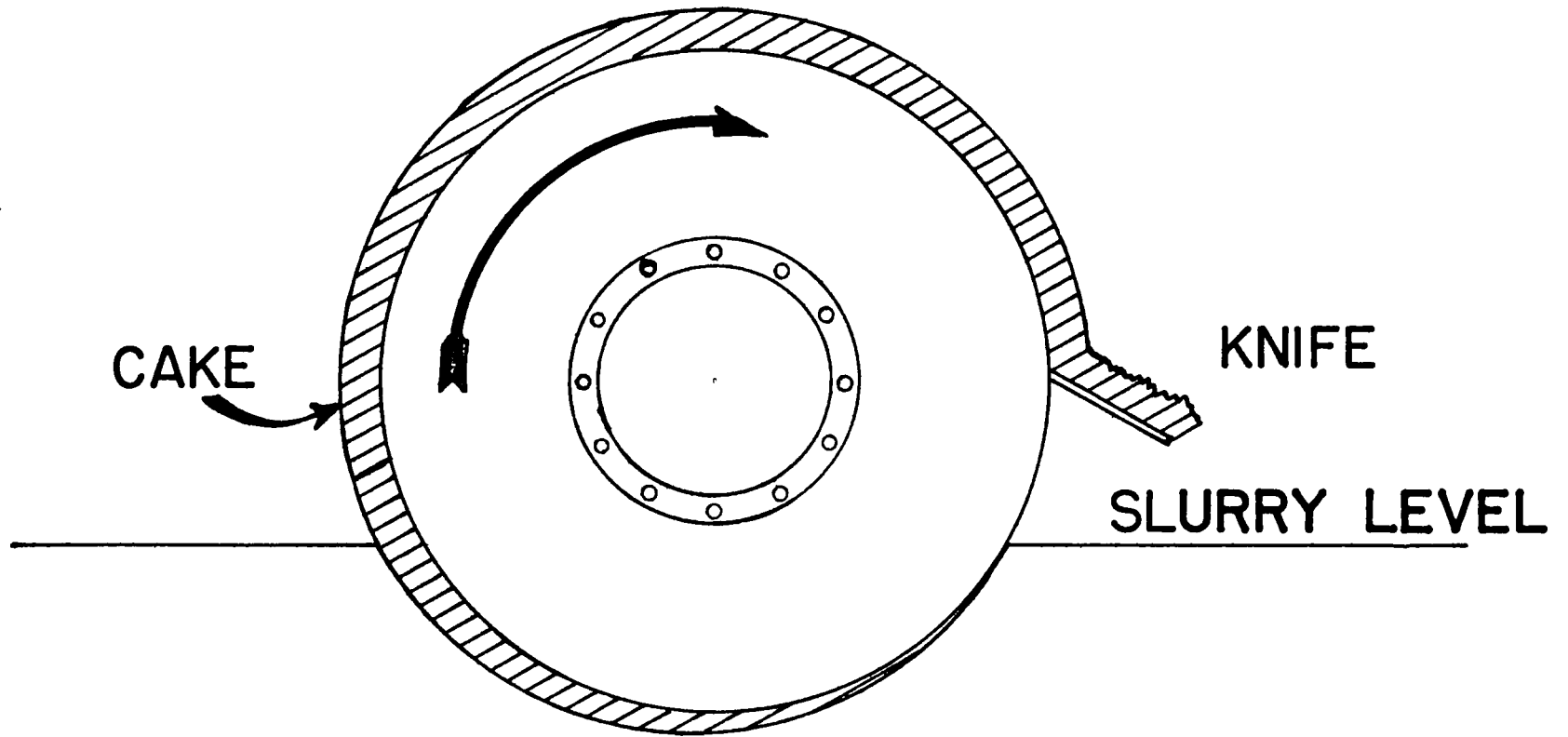


FIGURE III-1 SALIENT FEATURES OF A ROTARY DRUM FILTER

Just prior to the instant that this part of the filter cake emerges from the slurry, the multiported valve disconnects that particular segment from the vacuum. This is necessary so that the vacuum pump will not have to handle large volumes of air which would be sucked through the cake. In addition to the applied vacuum, each point on the periphery of the drum will be subjected to the static head of the slurry above it.

The usual commercial filter is operated with a submergence of one-third to one-half of the drum surface. Rotational speeds rarely exceed 1 r.p.m. and the diameter of these drums are usually from 6 to 14 feet.

Continuous rotary filters give a definite volume of filtrate per unit of time or per revolution. Thus, it would appear, upon first analysis, that the process is a constant rate filtration. However, if a differential area of the periphery is considered as it passes through the slurry, it is immediately apparent that the filtration occurs under neither constant pressure nor constant rate. At each angle α_1 is constant, but as the angle changes from one spot to another so will q_1 .

IV. FILTRATION PRESSURE

An illustration of the pressure variation as a function

of time is presented in Figure III-2. The upper curve shows the total head which consists of the vacuum plus the hydrostatic effect due to the slurry. It will be noted that this hydrostatic effect reaches the maximum at the middle of the cycle or when the segment is at the lowest point of submergence in the slurry. Initially, as the drum segment enters the slurry, the entire pressure drop is across the medium, which may include a precoat. As time progresses, the pressure drop across the cake increases and reaches a maximum after which a decrease may be evident.

By referring to Figure III-2 the pressure variations for talc may be seen; Figure III-3 and Figure III-4 present similar results for Hong Kong pink kaolin and super cel.

If the filtrate is removed as fast as it is formed, there will be a variable head of liquid aiding in the filtration. Referring to Figure III-5, the total pressure, p , at any point on the submerged part of the drum surface is equal to the sum of the pressure differential due to the vacuum, p_v , plus the hydrostatic head effect due to the liquid slurry, p_h , thus

$$p = p_v + p_h \quad (\text{III-1})$$

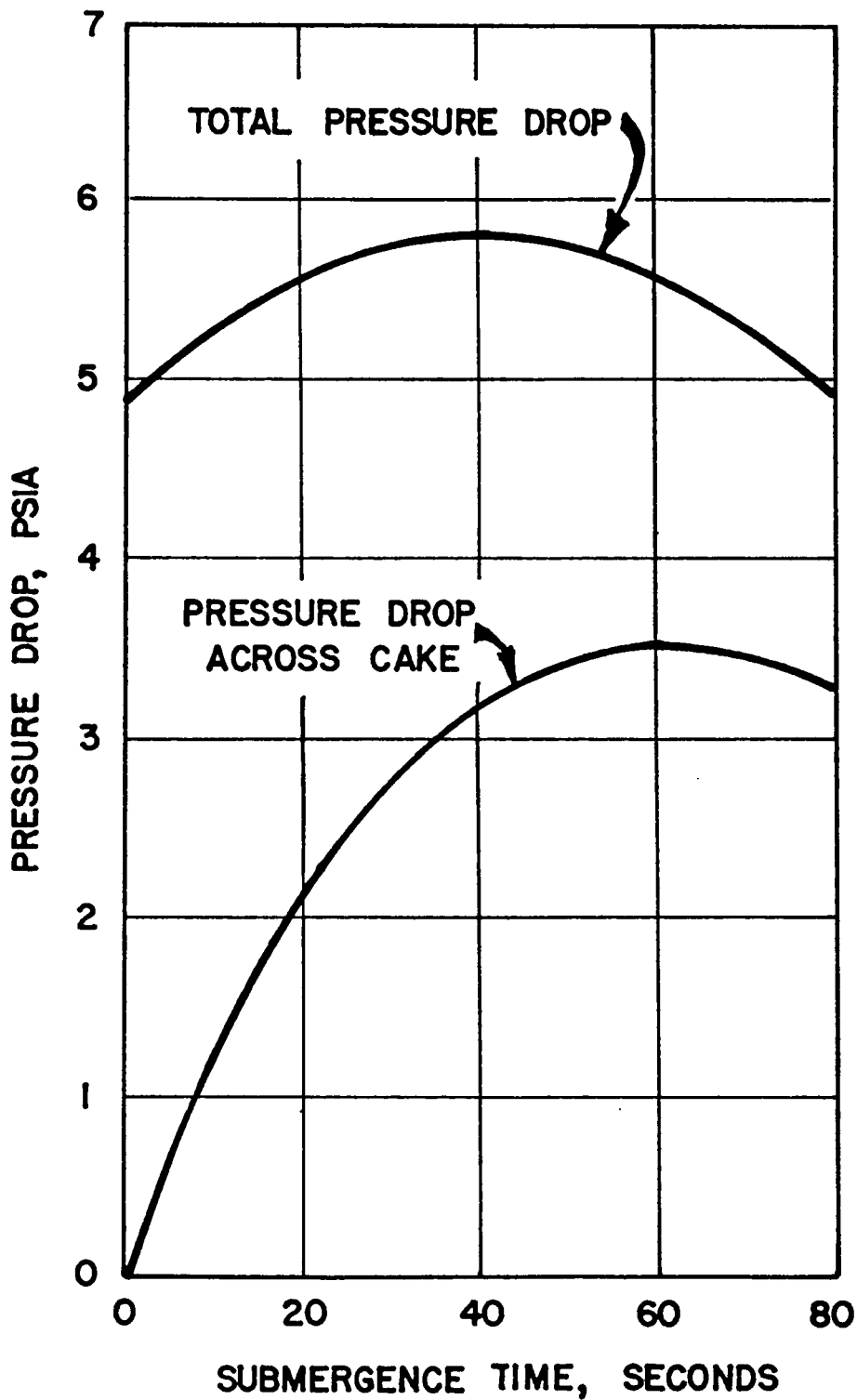


FIGURE III-2 PRESSURE VARIATION FOR TALC

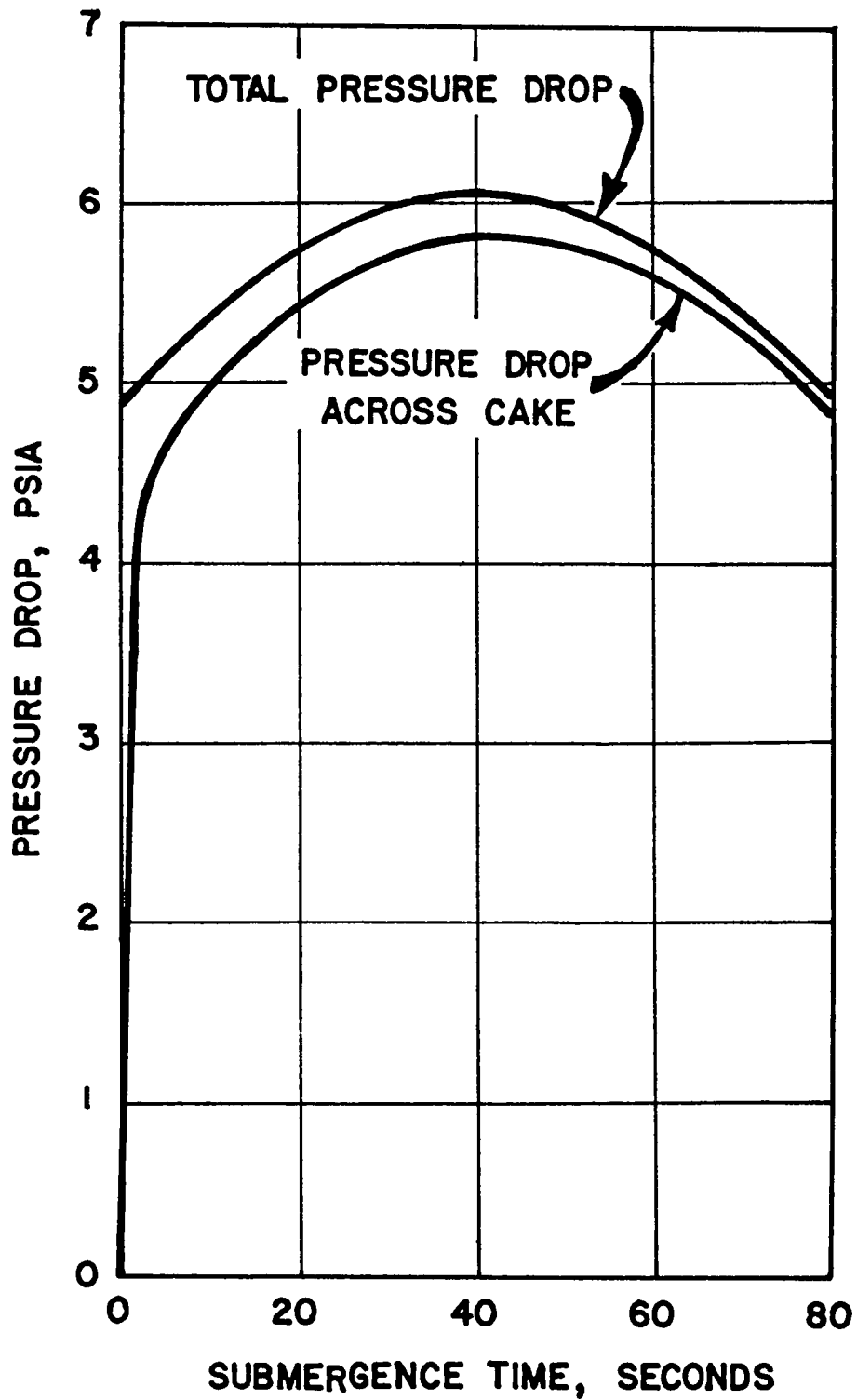


FIGURE III-3 PRESSURE VARIATION FOR HONG KONG PINK KAOLIN

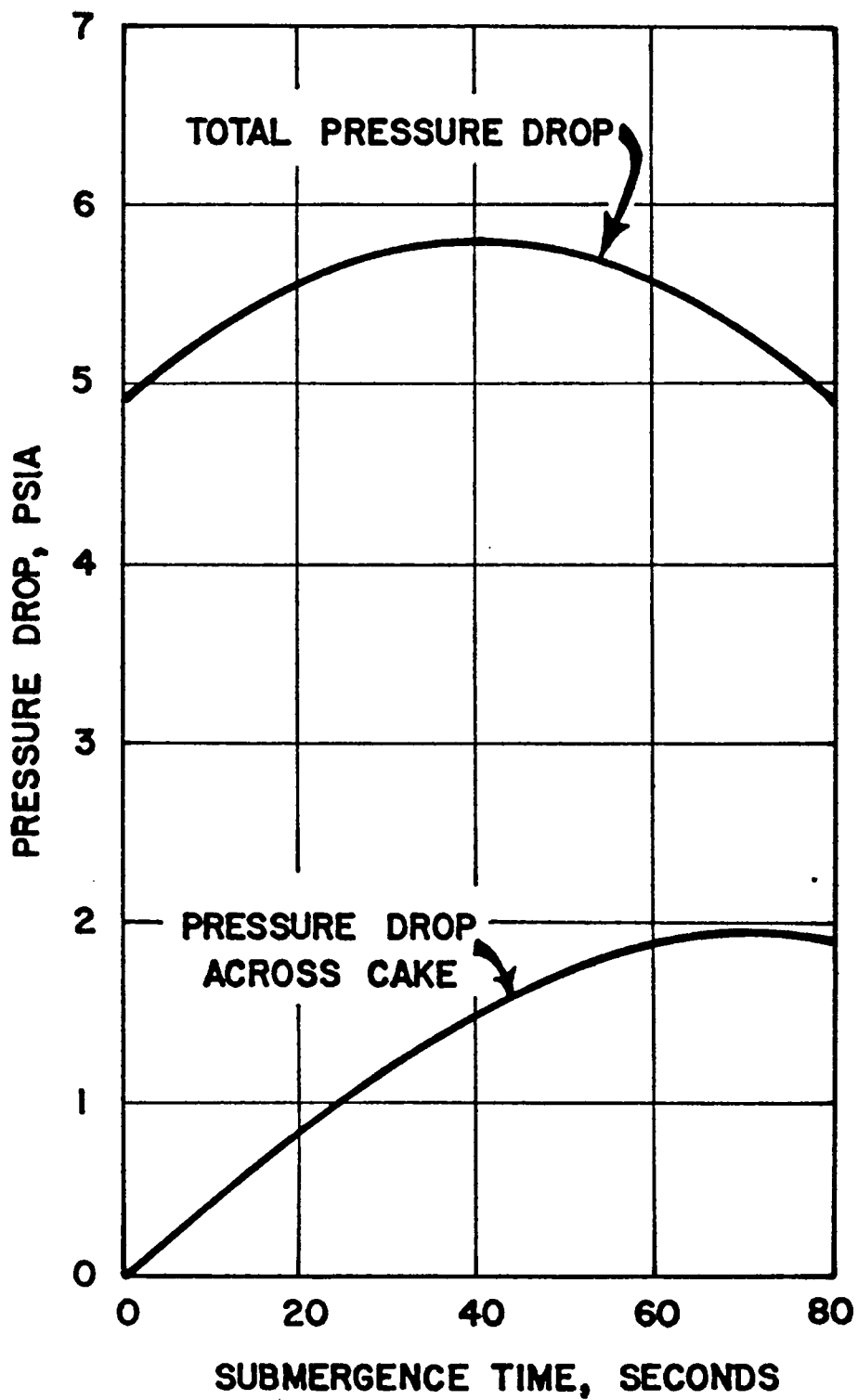


FIGURE III-4. PRESSURE VARIATION FOR SUPER GEL

Referring to the same figure, the distance h represents the variable head at any angle ϕ . The value for p_h was given by Mondria (34) as

$$p_h = \rho_f \frac{g}{g_c} h \quad (\text{III-2})$$

where ρ_f is the slurry density in lb-mass/cu.ft., and h is the variable head, CD - CE in Figure III-5. This variable head may be related by trigometric identities to the drum radius and the angle of submergence

$$p_h = \frac{g}{g_c} \rho_f R \left[\cos(\phi_0 - \phi) - \cos \phi_0 \right] \quad (\text{III-3})$$

where R is the radius of the filter drum in feet, and ϕ_0 is one-half the total angle of submergence in radians

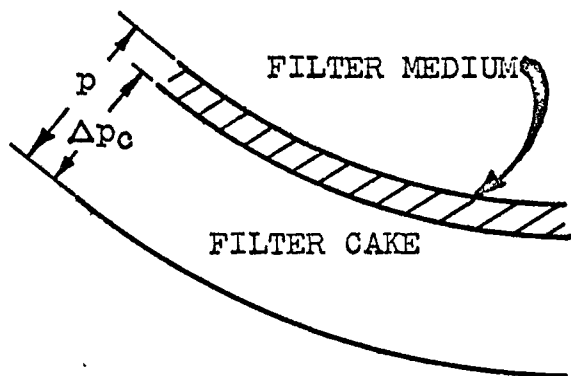
From the Carman-Kozeny equation, the flow rate q is related to the pressure drop across the filter cake as

$$q = - \frac{g_c \frac{dp}{dx}}{\mu w a_x} \quad (\text{III-4})$$

However, the total pressure differential defined in Equation (III-1) includes the pressure drop across the medium plus this differential across the cake. These differences between p and Δp can be seen by referring to the drawing on the next page. By definition (58) the pressure drop

across the medium is

$$\frac{\mu q_1 R_m}{\varepsilon_c} \quad (\text{III-5})$$



Thus, the pressure drop across the cake can be defined as:

$$\Delta P_c = p - \frac{\mu q_1 R_m}{\varepsilon_c} \quad (\text{III-6})$$

It is to this pressure difference that all the calculations in the following section refer.

V. EQUATIONS FOR ROTARY DRUM FILTRATION

The basic equation for flow through a porous solid has been given by Equation (III-4). The solution of this equation, subject to the equation of continuity as given by Tiller and Cooper (61), with the following conditions imposed: (1) concentrated slurry, (2) variable flow rate and specific cake resistance, (3) finite medium resistance, is the object of this chapter. In addition, these equations must include the cocurrent movement of the solids and the filtrate toward the medium as has been reported by Shirato and co-workers (44). In these derivations, equilibrium porosities

SCHEMATIC CROSS SECTION OF A ROTARY DRUM FILTER

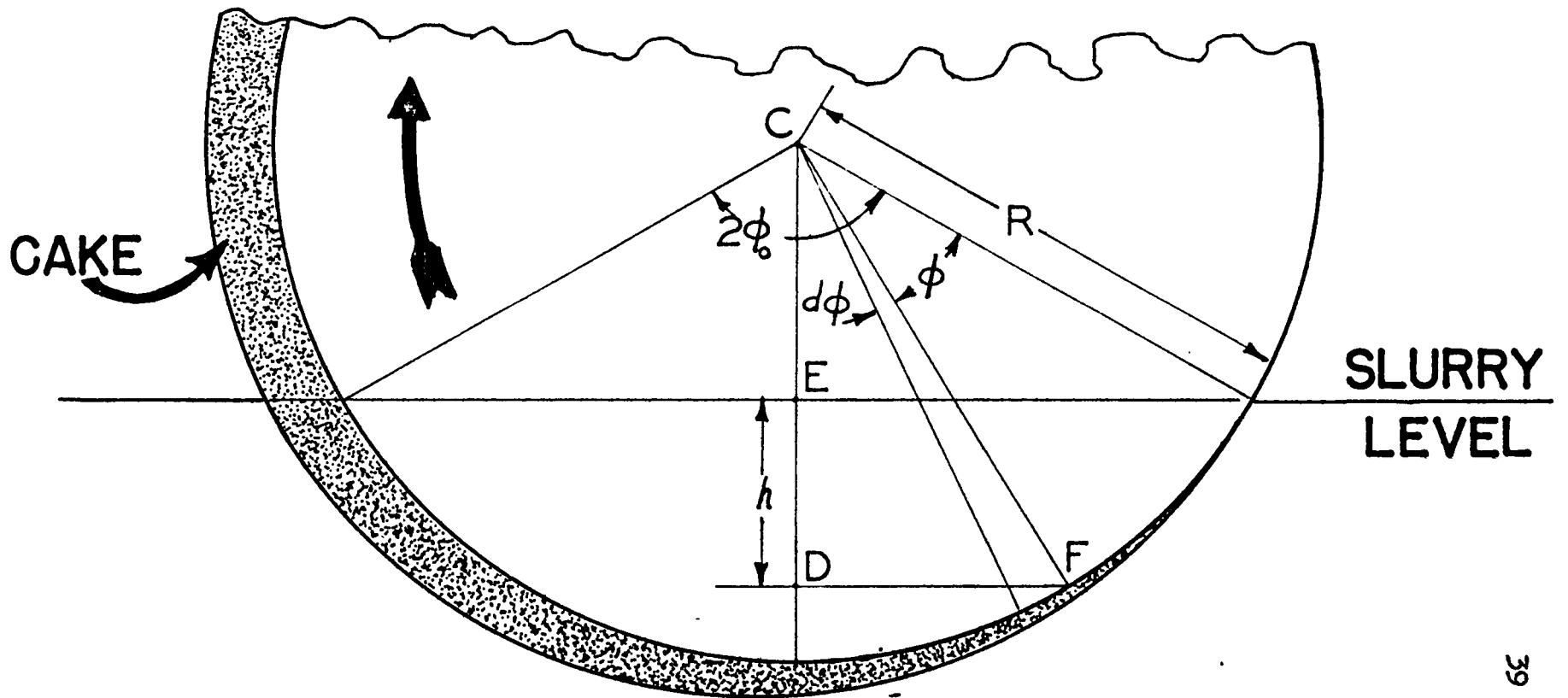


FIGURE III-5

and cake resistance are assumed to be attained instantaneously as has been discussed by Tiller (57).

Now assume as suggested by Tiller and Shirato (64) that the porosity is a function solely of the solids pressure and the dimensionless ratio of the distance from the septum as

$$\epsilon_x = f \left[p_s, (x/L) \right] \quad (\text{III-7})$$

Lu (31) simplified the porosity function, Equation (III-7), by assuming equilibrium porosity was a product of two functions $f_1(x/L)$ and $f_2(p_s)$ defined as

$$\epsilon = f_1(x/L) f_2(p_s) \quad (\text{III-7a})$$

The development will be continued by assuming that (III-7a) is identical with the form derived by Tiller and Cooper (61) for constant pressure filtration:

$$\epsilon_x = f_1(x/L) f_2(p_s) = \epsilon_0(p_s)^{-\lambda} \left[1 - (x/L) \right]^{\frac{-\lambda}{1-n-\beta}} \quad (\text{III-7b})$$

$$\epsilon_{x/L} = \left[1 - x/L \right]^{\frac{-\lambda}{1-n-\beta}}$$

$$\epsilon_{p_s} = \epsilon_0(p_s)^{-\lambda}$$

Lu, in his thesis (31), thoroughly discussed the limitations imposed by the use of this simplified porosity function, Equation (III-7a). He stated that the assumptions were probably adequate for filtrations which lasted more than a few minutes, i.e., porosity approached an equilibrium value within this time limit. Thus, if the pressure were increased slowly, Lu continued, it would not be unreasonable to expect that the porosity curves for variable pressure operations would approximate those for constant pressure filtration. Thus, in effect he assumed that the pressure function, $f_2(p_s)$, as obtained from constant pressure filtration would be the same for variable pressure filtration where p_s (constant pressure $R_m = 0$) equals $p - p_1$ for variable pressure filtration.

Tiller and Shirato (64) discussed at some length the reasons for assuming porosity is a function of the dimensionless ratio x/L . In turn, x/L and p_s are functions of time. The total differential of Equation (III-7) is

$$d\epsilon = \left(\frac{\partial \epsilon}{\partial (x/L)} \right)_{p_s} d(x/L) + \left(\frac{\partial \epsilon}{\partial p_s} \right)_{x/L} dp_s \quad (\text{III-8})$$

Upon differentiation with respect to time, θ , Equation (III-8) becomes

$$\left(\frac{\partial \epsilon_x}{\partial \theta}\right)_x = \left(\frac{\partial \epsilon_x}{\partial x/L}\right)_{p_s} \left(\frac{dx/L}{d\theta}\right)_x + \left(\frac{\partial \epsilon_x}{\partial p_s}\right)_{(x/L)} \left(\frac{dp_s}{d\theta}\right)_x \quad (\text{III-9})$$

This equation divides the total effect that time has upon porosity into two factors. The first factor refers to the change in porosity brought about by a change in cake thickness with time. The second factor describes the effect that the change in pressure with time has upon the porosity. However, since the cake thickness is a function of time the differential of the thickness ratio becomes

$$\left(\frac{dx/L}{d\theta}\right)_x = -\frac{x}{L^2} \frac{dL}{d\theta} \quad (\text{III-10})$$

Assuming that Equation (III-7b) defines the local porosity function the second term of Equation (III-9) can be written as:

$$\left(\frac{\partial \epsilon_x}{\partial \theta}\right)_{(x/L)} = \epsilon_{(x/L)} \frac{d\epsilon_{p_s}}{dp_s} \frac{dp_s}{d\theta} \quad (\text{III-11})$$

Upon substituting Equation (III-11) and Equation (III-10) into Equation (III-9), the change in porosity with time becomes

$$\left(\frac{\partial \epsilon_x}{\partial \theta}\right)_x = -\left(\frac{\partial \epsilon_x}{\partial (x/L)}\right)_{p_s} \frac{-x}{L^2} \frac{dL}{d\theta} + \epsilon_{x/L} \frac{d\epsilon_{p_s}}{dp_s} \frac{dp_s}{d\theta} \quad (\text{III-12})$$

Tiller and Cooper (61) have established, as a condition of continuity, the following equation

$$\left(\frac{\partial q_x}{\partial x} \right)_\theta = \left(\frac{\partial \epsilon_x}{\partial \theta} \right)_x \quad (\text{III-13})$$

The substitution of Equation (III-12) into the above (III-13), yields the differential equation

$$\left(\frac{\partial q_x}{\partial x} \right)_\theta = - \left(\frac{\partial \epsilon_x}{\partial (x/L)} \right)_{p_s} \frac{x}{L^2} \frac{dL}{d\theta} + \epsilon_{x/L} \frac{d\epsilon_{p_s}}{dp_s} \frac{dp_s}{d\theta} \quad (\text{III-14})$$

Since $\epsilon_x = \epsilon_{x/L} \epsilon_{p_s}$, Equation (III-7b) becomes

$$\left(\frac{d\epsilon_x}{d(x/L)} \right)_{p_s} = \epsilon_{p_s} \frac{d\epsilon_{x/L}}{d(x/L)} \quad (\text{III-15})$$

Therefore, Equation (III-14) may be written as

$$\left(\frac{\partial q_x}{\partial x} \right) = -\epsilon_{p_s} \frac{d\epsilon_{x/L}}{d(x/L)} \frac{x}{L^2} \frac{dL}{d\theta} + \epsilon_{x/L} \frac{d\epsilon_{p_s}}{dp_s} \frac{dp_s}{d\theta} \quad (\text{III-16})$$

Then for an instant of time, the change in flow rate is

$$dq_x = -\epsilon_{p_s} \frac{d\epsilon_{x/L}}{d(x/L)} \frac{x}{L^2} \frac{dL}{d\theta} dx + \epsilon_{x/L} \frac{d\epsilon_{p_s}}{dp_s} \frac{dp_s}{d\theta} dx \quad (\text{III-17})$$

if Equation (III-17) is integrated between the interface of medium and the distance x/L , the difference in flow rates

at these two positions may be determined, as

$$q_1 - q_x = \epsilon_{p_0} \frac{dL}{d\theta} \left(\epsilon_{x/L} - \epsilon_{aw/x/L} \right) \frac{x}{L} - \epsilon_{aw/x/L} L \frac{x}{L} \frac{d\epsilon_{p_0}}{dp_s} \frac{dp_s}{dL} \frac{dL}{d\theta} \quad (\text{III-18})$$

Rearranging

$$q_1 - q_x = \frac{x}{L} \left\{ \epsilon_x - \epsilon_{aw/x} - \frac{d\epsilon_{p_0}}{dp_s} \frac{dp_s}{dL} L \epsilon_{aw/x} \right\} \frac{dL}{d\theta} \quad (\text{III-19})$$

Similarly, integrating over the entire cake thickness will yield:

$$q_1 - q_i = \left[(\epsilon_i - \epsilon_{ar}) - L \frac{d\epsilon_{ar}}{dL} \right] \frac{dL}{d\theta} \quad (\text{III-20})$$

By the division of Equation (III-19) by (III-20) and rearrangement of the quotient, one may obtain the ratio of flow rates as Lu (31) has reported

$$\frac{q_x}{q_1} = 1 - \left(1 - \frac{q_i}{q_1} \right) \left(\frac{x}{L} \right) \left\{ \frac{(\epsilon_x - \epsilon_{aw/x}) - L \epsilon_{aw/x} \frac{d\epsilon_{p_0}}{dL}}{(\epsilon_i - \epsilon_w) - L \frac{d\epsilon_w}{dL}} \right\} \quad (\text{III-21})$$

As previously discussed, Lu (31) assumed that the equilibrium porosity was a product of two functions given by Equation (III-7b). The pressure dependent porosity function ϵ_{p_0} upon the substitution of Δp for p_s ,

becomes

$$\epsilon_{p_0} = \epsilon_{\Delta p} = \epsilon_0 \Delta p^{-\lambda} \quad (\text{III-22})$$

Differentiation of this pressure dependent function by means of the chain rule, will yield

$$\frac{d\epsilon_{p_0}}{dL} = \frac{d\epsilon_{\Delta p}}{d\Delta p} \frac{d\Delta p}{dL} = \epsilon_0 \left(\frac{-\lambda}{\Delta p} \right) \Delta p^{-\lambda} \frac{d\Delta p}{dL} \quad (\text{III-23})$$

or

$$\frac{d\epsilon_{p_0}}{dL} = \epsilon_{p_0} \left(\frac{-\lambda}{\Delta p} \right) \frac{d\Delta p}{dL} \quad (\text{III-24})$$

Substituting this expression Equation (III-24) into Equation (III-21) and simplifying, will produce the following equation for the ratio of the flow rates:

$$\frac{q_x}{q_1} = 1 - \left(1 - \frac{q_i}{q_1} \right) \left(\frac{x}{L} \right) \left\{ \frac{(\epsilon_x - \epsilon_{av,x}) + \lambda \epsilon_{av,x} \frac{d \ln \Delta p}{d \ln L}}{(\epsilon_i - \epsilon_{av}) - L \frac{d\epsilon_{av}}{dL}} \right\} \quad (\text{III-25})$$

By means of a material balance over the filter cake, filtrate, and slurry, it is possible to relate the volume of filtrate to the mass of solids deposited and the average

moisture content, as

$$v = \frac{1 - ms}{\rho_s} w \quad (\text{III-26})$$

Differentiation of this equation with respect to time will give the change in filtrate volume with time, or the flow rate of the filtrate as

$$\frac{dv}{d\theta} = q_1 = \left(\frac{1 - ms}{\rho_s} \right) \frac{dw}{d\theta} - \frac{w}{\rho} \frac{dm}{d\theta} \quad (\text{III-27})$$

By definition, the ratio of the mass of wet to the mass of dry cake is

$$m = 1 + \frac{\rho \epsilon_w}{\rho_s (1 - \epsilon_w)} \quad (\text{III-28})$$

Thus the change in the ratio of the mass of wet to dry cake is

$$\frac{dm}{d\theta} = \frac{\rho}{\rho_s (1 - \epsilon_w)^2} \frac{d\epsilon_w}{d\theta} \quad (\text{III-29})$$

Similarly, from the definition of the weight of dry solids per unit area of the filter cake, the changes in the mass of dry solids with time is

$$\frac{dw}{d\theta} = \rho_s(1 - \epsilon_w) \frac{dL}{d\theta} - \rho_s L \frac{d\epsilon_w}{d\theta} \quad (\text{III-30})$$

Thus upon the substitution of Equation (III-29) and Equation (III-30), Equation (III-27) becomes

$$q_1 = \left(\frac{1 - m_s}{\rho_s} \right) \rho_s \left[(1 - \epsilon_w) \frac{dL}{d\theta} - L \frac{d\epsilon_w}{d\theta} \right] - \frac{L}{(1 - \epsilon_w)} \frac{d\epsilon_w}{d\theta} \quad (\text{III-31})$$

The above equations must be modified to account for the flow of solids within the filter cake, towards the medium. These modifications are based upon the suggestions of Shirato and co-workers (44). He has stated that both the internal flow rate of the liquid and the internal migration rate of solids due to the squeezing action are not constant through the cake. Thus the flow of solids in the slurry approaching the cake surface is

$$r_0 = (1 - \epsilon_w) \frac{dL}{d\theta} - L \frac{d\epsilon_w}{d\theta} \quad (\text{III-32})$$

At the surface of the filter cake, the solid volume which remains in the infinitesimal surface layer is

$$r_1 = r_0 - (1 - \epsilon_1) \frac{dL}{d\theta} \quad (\text{III-33})$$

or

$$r_1 = (\epsilon_1 - \epsilon_w) \frac{dL}{d\theta} - L \frac{d\epsilon_w}{d\theta} \quad (\text{III-34})$$

Then the ratio of the apparent rate of flow of solids to the rate of filtrate flow can be obtained by dividing the above equation by Equation (III-31) to give

$$\frac{r_1}{q_1} = \frac{(\epsilon_i - \epsilon_w) \frac{dL}{d\theta} - L \frac{d\epsilon_w}{d\theta}}{\left(\frac{1 - m_s}{\rho_s}\right) \rho_s \left[(1 - \epsilon_w) \frac{dL}{d\theta} - L \frac{d\epsilon_w}{d\theta} \right] - \frac{L}{1 - \epsilon} \frac{d\epsilon_w}{d\theta}} \quad (\text{III-35})$$

The ratio of the relative velocity of liquid to solids in the infinitesimal surface layer to the relative velocity at the interface of the medium and cake can be represented by

$$\frac{q_i}{q_1} = \frac{1 - m_1 s}{1 - m_s} + \frac{\epsilon_i}{1 - \epsilon_i} \frac{r_1}{q_1} \quad (\text{III-36})$$

The substitution of Equation (III-35) into the above equation will give

$$\frac{q_i}{q_1} = \frac{1 - m_1 s}{1 - m s} + \frac{\epsilon_i}{1 - \epsilon_i} \left\{ \frac{(\epsilon_i - \epsilon_w) - L \frac{d\epsilon_w}{dL}}{\left(\frac{1 - m s}{\rho_s}\right)_s \left[(1 - \epsilon) - L \frac{d\epsilon_w}{dL} \right] - \frac{L}{1 - \epsilon_w} \frac{d\epsilon_w}{dL}} \right\} \quad (\text{III-37})$$

which may be simplified to yield

$$\frac{q_i}{q_1} = \frac{1 - m_1 s}{1 - m s} \left\{ 1 - \frac{(1 - m_1) s}{1 - m s} \frac{\left[(\epsilon_i - \epsilon_w) - L \frac{d\epsilon_w}{dL} \right]}{\left[1 - \epsilon_w - \left(L - \frac{L s (1 - m)}{(1 - m s) \epsilon_w} \right) \frac{d\epsilon_w}{dL} \right]} \right\} \quad (\text{III-38})$$

By use of the above equation, the ratio of the flow rates throughout the cake may be calculated from Equation (III-21). The change in average porosity with cake thickness $\frac{d\epsilon_w}{dL}$ is the only value not known; however, its value may be determined using the chain rule as

$$\frac{d\epsilon_w}{dL} = \frac{d\epsilon_w}{d\Delta p_c} \frac{d\Delta p_c}{dL} \quad (\text{III-39})$$

An approximate expression for $1 - \epsilon_w$ in terms of the pressure drop across the cake Δp_c was given by Lu (31) as

$$1 - \epsilon_w = \frac{B (1 - n - \beta) (\Delta p_c^{1-n} - n p_1^{1-n})}{(1 - n) [\Delta p_c^{1-n-\beta} - (n+\beta) p_1^{1-n-\beta}]} \quad (\text{III-40})$$

In order to obtain the cake thickness in terms of p , the fundamental filtration equation

$$\epsilon_c \frac{dp_x}{dx} = \mu q_x \alpha_x (1 - \epsilon_x) \rho_s \quad (\text{III-41})$$

is integrated to yield

$$L = \frac{\epsilon_c}{J_T \mu \rho_s q_1 (1 - \epsilon_{av})} \int_0^{\Delta p_c} \frac{dp_s}{\alpha_x} \quad (\text{III-42})$$

The specific cake resistance for a moderately compressible cake in the pressure range of 0 to 100 psia solids pressure can be determined, as reported by Tiller (60), by the relationships of

$$\left. \begin{aligned} \alpha_x &= \alpha_o p_s^n & p_s > p_1 \\ \alpha_1 &= \alpha_o p_1^n & p_s \equiv p_1 \end{aligned} \right\} \quad (\text{III-43})$$

Thus, it is possible to integrate the integral of Equation (III-42) as follows:

$$\int_0^{\Delta p_c} \frac{dp_s}{\alpha_x} = \frac{\Delta p_c^{1-n} - n p_1^{1-n}}{\alpha_o (1-n)} \quad (\text{III-44})$$

The cake thickness can then be determined by substituting the values found in Equations (III-43) and (III-44) into Equation (III-42) to give

$$L = \frac{\epsilon_c \left[\Delta p_c^{1-n-\beta} - (n+\beta) p_1^{1-n-\beta} \right]}{J_T \mu \rho_s \alpha_o B q_1 (1-n-\beta)} \quad (\text{III-45})$$

Upon differentiation with respect to pressure drop across the cake Δp_c , Equation (III-45) becomes

$$\frac{dL}{d\Delta p_c} = \frac{\varepsilon_c \left[(1-n-\beta) \Delta p_c^{-(n+\beta)} - \left[\Delta p_c^{1-n-\beta} - (n+\beta) p_1^{1-n-\beta} \right] \left(\frac{dJ_T}{J_T d\Delta p_c} + \frac{dq_1}{q_1 d\Delta p_c} \right) \right]}{J_T \mu \rho_s \alpha_o B q_1 (1-n-\beta)} \quad (\text{III-46})$$

which may be simplified by substituting the definition of the cake thickness Equation (III-45) for the appropriate terms in (III-46) to get

$$\frac{dL}{d\Delta p_c} = \frac{\varepsilon_c \Delta p_c^{-(n+\beta)}}{J_T \mu \rho_s \alpha_o B q_1} - \left[\frac{L}{J_T} \frac{dJ_T}{d\Delta p_c} + \frac{L}{q_1} \frac{dq_1}{d\Delta p_c} \right] \quad (\text{III-47})$$

Lu (31) has shown that the term $\left[\frac{L}{J_T} \frac{dJ_T}{d\Delta p_c} \right]$ can be neglected in comparison with the other terms; therefore, Equation (III-47) is approximated as

$$\frac{dL}{d\Delta p_c} = \frac{\varepsilon_c \Delta p_c^{-(n+\beta)}}{J_T \mu \rho_s \alpha_o B q_1} - \frac{L}{q_1} \frac{dq_1}{d\Delta p_c} \quad (\text{III-48})$$

where the last term can be approximated as

$$\frac{dq_1}{d\Delta p_c} \doteq \left[\frac{q_{1@0} - q_{1@0-\Delta\theta}}{\Delta p_{c@0} - \Delta p_{c@0-\Delta\theta}} \right] \quad (\text{III-49})$$

Differentiation of Equation (III-41) will yield as Lu (31)

has shown

$$\frac{d\epsilon_{sw}}{d\Delta p_c} = \frac{B(1-n-\beta)}{(1-n)} \frac{\left[(1-n)(\Delta p_c^{1-n-\beta} - [n+\beta] p_1^{1-n-\beta} \Delta p_c^{-n}) - (\Delta p_c^{1-n} - n p_1^{1-n})(1-n-\beta)\Delta p_c^{-(n+\beta)} \right]}{\left[\Delta p_c^{1-n-\beta} - (n+\beta) p_1^{1-n-\beta} \right]^2} \quad (\text{III-50})$$

This equation may be further simplified by the following procedure: the numerator of the right hand side of the equation is split into two portions

$$(1) \quad \frac{B(1-n-\beta)}{(1-n)} \frac{\left[(1-n)(\Delta p_c^{1-n-\beta} - (n+\beta) p_1^{1-n-\beta}) \Delta p_c^{-n} \right]}{\left[\Delta p_c^{1-n-\beta} - (n+\beta) p_1^{1-n-\beta} \right]^2}$$

$$(2) \quad - \frac{B(1-n-\beta)}{(1-n)} \frac{\left[(\Delta p_c^{1-n} - n p_1^{1-n})(1-n-\beta) \Delta p_c^{-(n+\beta)} \right]}{\left[\Delta p_c^{1-n-\beta} - (n+\beta) p_1^{1-n-\beta} \right]^2}$$

The first portion (1) above, can be reduced by the common factor, as seen in (1a) below; the second portion (2) seems to be a function of porosity as expressed in Equation (III-40); therefore, it may be reduced to that given in (2a).

$$(1a) \quad \frac{B(1-n-\beta)\Delta p_c^{-n}}{[\Delta p_c^{1-n-\beta} - (n+\beta)p_i^{1-n-\beta}]}$$

$$(2a) \quad \frac{(1-n-\beta)\Delta p_c^{-(n+\beta)}(1-\epsilon_w)}{[\Delta p_c^{1-n-\beta} - (n+\beta)p_i^{1-n-\beta}]}$$

These latter equations can be combined to yield

$$\frac{d\epsilon_w}{d\Delta p_c} = \frac{B(1-n-\beta)\Delta p_c^{-n}}{[\Delta p_c^{1-n-\beta} - (n+\beta)p_i^{1-n-\beta}]} \left[1 - \frac{(1-\epsilon_w)\Delta p_c^{-B}}{B} \right] \quad (III-51)$$

A computer program was written to solve the flow Equation (III-31). This program assumed that the change in the pressure drop across the filter cake is governed by the applied vacuum, the hydrostatic head of the slurry, and the pressure drop across the medium resulting from the filtrate flow. In arriving at the values for the filtrate flow, corrections for the apparent rate of flow of the solids in the filter cake towards the medium were made. This computer program is given in Appendix A. The data for the three materials tested are, also found in the same Appendix.

Values for q_1 as a function of the total time of submergence are obtained as one of the results of the computer program. If the entire periphery of the submerged portion of the rotary drum were divided into an infinite number of segments and the filtrate flowing through each of these segments were measured by small rotameters, the filtrate rate measured by these rotameters would be the value of q_1 . The position of these segments is fixed with respect to the submergence in the slurry. The integral of all of these rotameter readings or the sum of all of the filtrate passed through the medium during a single rotation is v the filtrate rate. If one were to follow a portion of the

drum as it revolved and were to record the amount of liquid that passed into these fixed segments, then the data obtained would be identical to that obtained from the computer program.

A set of these data are shown in Figure III-6. The results reported here were calculated for an eight foot diameter drum filter operating under ten inches of mercury vacuum with an angle of submergence of 120° filtering a ten per cent talc slurry. The drum speeds studied to obtain this figure were 2.0, 1.0, 0.5, and 0.25 revolutions per minute. The terminus of these solid lines is the total filtrate recorded during the entire time the drum was submerged. A dotted line connects the terminals. As shown by the solid lines, the flow-time relationship is the internal integral flow; the dotted line represents the external flow-time relationship obtained by integrating with respect to time the measurement of the large rotameter through which the entire liquid flow from all the smaller rotameters would pass. Thus, v is the integral of the entire flow.

In Figure III-7 the internal flow rate variation q_x/q_1 is plotted versus the normalized thickness x/L with the time of submergence as a parameter. It is evident that the value of q_x/q_1 is not only a function of the normalized

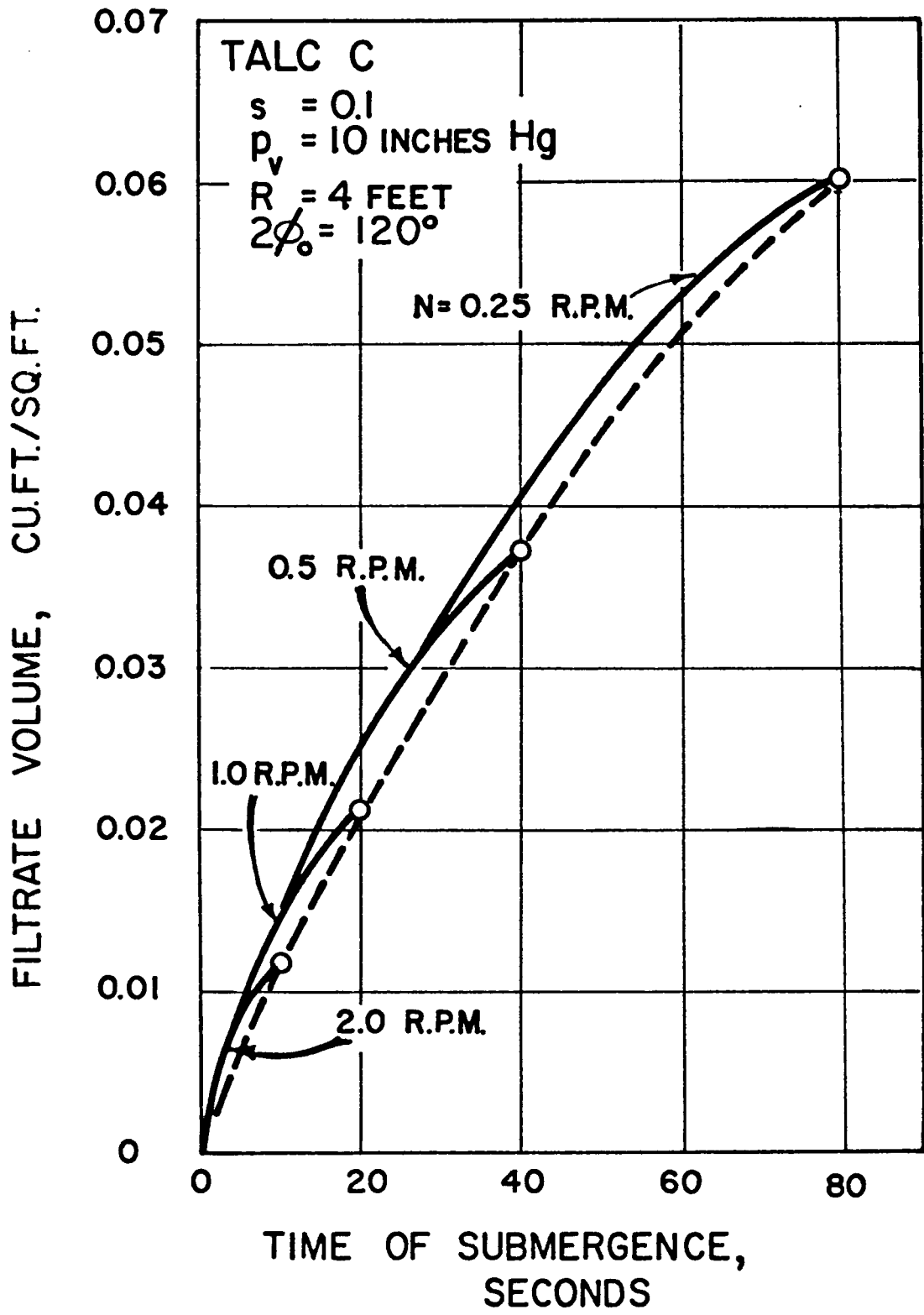


FIGURE III-6 TOTAL FILTRATE RECORDED

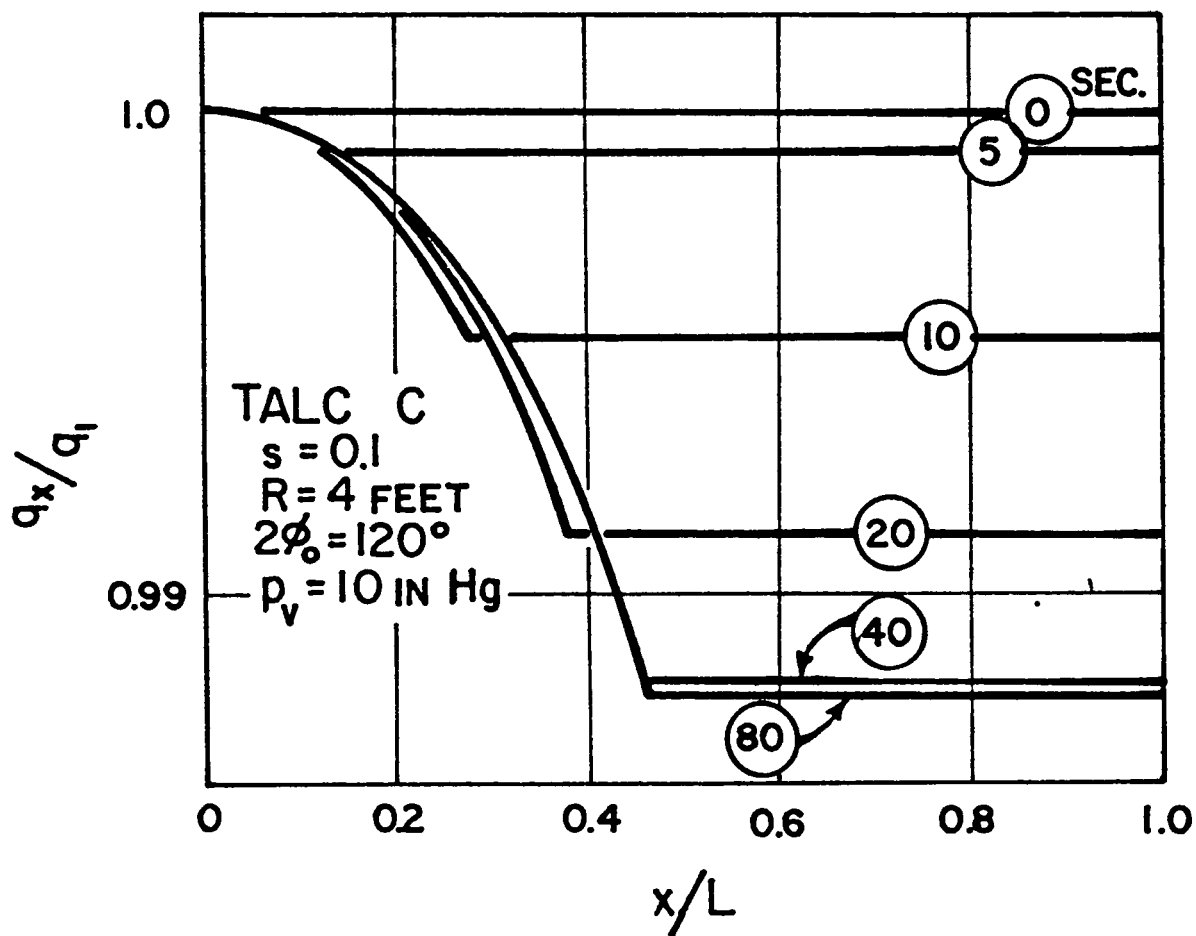


FIGURE III-7 VARIATION OF THE INTERNAL FLOW RATE

thickness, but is a function of the time of submergence. The latter dependence of internal flow rate with time of submergence is theoretically correct as can be seen by Equation (III-25). Pressure enters into this equation not only through the term $d \ln \Delta P_c / d \ln L$ but also through Equation (III-39) which indicates that the average porosity is dependent upon the pressure. Furthermore the ratio of the relative velocity q_i/q_1 as given by Equation (III-38) is likewise a function of the change in pressure drop across the cake through Equation (III-39). It is this latter function of pressure which governs the flow rate through the medium and hence determines the flow rate through the cake.

In Figure III-7 a region of constant q_x/q_1 is indicated by horizontal lines. This region of constant flow ratio results from the cake having a constant porosity ϵ_1 . The thickness of this constant porosity region as seen in this figure decreases as the time of submergence increases, which could be expected since the pressure drop across the cake will increase as the time of submergence increases. In turn this increase in pressure drop across the cake has been shown by Lu (31) to produce a decrease in the thickness of the constant porosity region.

VI. COMPARISON OF PRESENT THEORY WITH PRIOR THEORY

All theories for rotary drum filtration have been based upon the fundamental filtration equation as derived by Ruth (37). The major difference between these theories is the manner in which the pressure variations through out the cake and the variations in the total filtration pressure (the sum of the static pressure and the pressure difference delivered by the vacuum pump) have been accounted for. Typical of the prior theories for rotary drum filtration are those of Ruth and Kempe (39) and Cooper (7). Ruth and Kempe analytically solved the filtration equation assuming the total filtration pressure was a constant. Cooper numerically integrated the filtration equation assuming an empirically fitted relationship for average specific cake resistance and average porosity versus cake pressure differential. A comparison of these theories to that proposed in this chapter is given below.

In describing the flow through a porous solid material, Ruth developed the basic fundamental filtration equation, which relates the flow rate to the pressure gradient and a specific cake resistance as

$$q = \frac{s_c \frac{dp_s}{dw_x}}{\mu \alpha_x} \quad (\text{III-52})$$

In rotary drum filtration, the pressure drop across the cake,

Δp_c , is the difference between the total filtration pressure, p , and the pressure drop across the septum p_1 is given as

$$\Delta p_c = p - p_1 \quad (\text{III-6a})$$

By use of this definition of the pressure drop across the cake, the above filtration equation, (III-52), can be integrated between the limits of 0 and Δp_c to yield:

$$\int_0^{\Delta p_c} \frac{dp_s}{\alpha_x} = \frac{\mu}{g_c} \int_0^w q \, dw_x = \frac{\mu q w}{g_c} \quad (\text{III-53})$$

where

$$q = \frac{dv}{d\theta} \quad (\text{III-54})$$

In this integration several simplifying assumptions were introduced namely:

1. Equilibrium porosities were assumed to be attained instantaneously.
2. Filtrate flow was assumed to be constant throughout the cake and equivalent to the flow rate through the medium. In the filtration of dilute slurries the error resulting from this assumption will probably be quite small.

3. The resistance of the medium constant.
4. The flow resistance in the cake at any point is solely a function of the solids pressure p_s at that point.
5. Flow through the cake follows the laws for viscous flow or Newtonian fluids.
6. Changes in the average cake porosity brought about by time are ignored.

The volume of filtrate collected during the time that mass w of solids are deposited can be determined by means of a material balance around the entire cake, as

$$w = \frac{\rho_s v}{1 - m_s} \quad (\text{III-55})$$

The substitution of Equation (III-54) and (III-55) into Equation (III-53) will give

$$\int_0^{\Delta p_c} \frac{dp_s}{\alpha_x} = \frac{\mu_s \rho v}{g_c (1 - m_s)} \frac{dv}{d\theta} \quad (\text{III-56})$$

Ruth (37) defined the average specific cake resistance, α_{av} , in terms of the pressure drop across the cake, Δp_c , and the point specific cake resistances, α_x , as

$$\alpha_{av} = \frac{\Delta p_c}{\int_0^{\Delta p_c} \frac{dp_s}{\alpha_x}} \quad (\text{III-57})$$

Substituting Equation (III-57) into (III-56) will yield:

$$\frac{\Delta p_c}{\alpha_{av}} = \frac{\mu s \rho v}{\epsilon_c (1 - ms)} \frac{dv}{d\theta} \quad (\text{III-58})$$

A straight forward solution to Equation (III-58) could be obtained provided the pressure drop across the cake were a constant. Thus, a simplified solution could be written provided the pressure drop across the cake could be expressed in terms of the angle of rotation ϕ as

$$\Delta p_c = p_v + \frac{\epsilon \rho_f R}{\epsilon_c} \left[\cos(\phi_0 - \phi) - \cos \phi_0 \right] - \frac{\mu R_m \omega}{\epsilon_c} \frac{dv}{d\theta} \quad (\text{III-59})$$

A certain amount of difficulty can be avoided by using the suggestion of Ruth and Kempe (39). They suggested that an integrated static head correction factor could be added to the filtration pressure difference, p_v . The results they obtained integrating the static head correction factor, Equation (III-3), from $\phi = 0$ to $2\phi_0$ are as follows:

$$p_h = \frac{\epsilon R \rho_f}{\epsilon_c} \left[\frac{1}{\phi_0} \sin \phi_0 - \cos \phi_0 \right] \quad (\text{III-60})$$

Substitution of Equation (III-60) into (III-59) yields

$$\Delta p_c = p_v + \frac{\varepsilon R \rho_f}{\varepsilon_c} \left[\frac{1}{\phi_0} \sin \phi_0 - \cos \phi_0 \right] - \frac{\mu R_m \omega}{\varepsilon_c} \frac{dv}{d\theta} \quad (\text{III-61})$$

The basic differential equation for rotary drum filtration can then be obtained by the substitution of Equation (III-61) into (III-58) together with the definition of the rate of rotation, ω , of the drum as

$$\omega = \frac{d\phi}{d\theta} \quad (\text{III-62})$$

to yield

$$\frac{\alpha_{av} \mu s \rho \omega}{\varepsilon_c (1 - ms)} v \frac{dv}{d\phi} + \frac{\mu}{\varepsilon_c} R_m \omega \frac{dv}{d\phi} - \left\{ p_v + \frac{\varepsilon R \rho_f}{\varepsilon_c} \left[\frac{1}{\phi_0} \sin \phi_0 - \cos \phi_0 \right] \right\} = 0 \quad (\text{III-63})$$

Since it has been assumed that the medium resistance is constant and that the time changes in average cake porosity can be ignored, Equation (III-63) can be integrated with

the terms α_{av} , m , and R_m kept constant. The results of this integration is

$$\frac{\alpha_{av} \mu_s \rho \omega}{2 \epsilon_c (1 - m s)} v^2 + \frac{\mu R_m \omega}{\epsilon_c} v - \left\{ p_v + \frac{\epsilon R \rho}{\epsilon_c} \left[\frac{1}{\phi_0} \sin \phi_0 - \cos \phi_0 \right] \right\} \phi = 0 \quad (\text{III-64})$$

Equation (III-64) is the solution that Ruth used to describe the filtrate flow rate v as a function of the time of submergence, $\theta = \frac{\omega}{\phi_0}$. In using this equation the true values of α_{av} and m must be determined. Although the true values for α_{av} and m would depend upon the instantaneous solids pressure distribution, their values have been assumed constant for the derivation of Equation (III-64) and thus these values are assumed to be solely a function of the average pressure within the cake given by Equation (III-61). This assumption is a consequence of assumption 3 and 4 given previously.

A computer program was written to solve Equation (III-64). This program is given in Appendix B. In order to use this program, values for α_{av} and ϵ_{av} were needed. A series of values for these variables were obtained from the

results of a constant pressure filtration run. These values were plotted versus the filtration pressure across the cake. The smoothed values were read at even increments of the filtration pressure. In turn, these values were used to establish fourth degree polynomial equations which would permit α_{av} and ϵ_{av} to be calculated. The coefficients of these equations were found using a Gaussian elimination subroutine program which was written for this purpose and is, also, given in Appendix B.

Cooper (7) used a trial and error approximation to solve for the rate of filtration in a continuous drum process. The procedure used was based on the simultaneous solution of Equation (III-59) and the following equation:

$$\Delta p_c = p_v + p_s - p_l \quad (\text{III-65})$$

where p_s is approximated by his procedure as

$$\text{and } p_l = \frac{\mu}{g_c} q R_m = \frac{\mu}{g_c} R_m \omega \frac{dv}{do} \quad (\text{III-66})$$

The solution of expression (III-59) and (III-66) was accomplished by finding values of q and Δp_c which satisfied the expressions for a fixed value of v . He obtained his approximate solution as follows:

1. Incremental increases in filtrate volume were assumed.
2. Values of q which satisfy Equations (III-59) and (III-66) for some Δp_c defined by Equation (III-65) were found by approximating time, θ , by the expression

$$\theta = \int \frac{d v}{q} \quad (\text{III-67})$$

3. The filtrate volume, v , is increased by an additional increment and steps 1 and 2 are repeated until the accumulated filtration time, $\sum \Delta \theta$, equals the total submergence time, $\frac{\phi_a}{\omega}$.

Values for the flow of filtrate v were obtained using the proposed theory and the theories of Ruth and Kempe (37) and Cooper (7). The results of these calculations are plotted in Figure III-8. It may be observed that the rate of filtrate flow as predicted by Ruth's equation is appreciable lower than that predicted by either Cooper's or the present investigation.

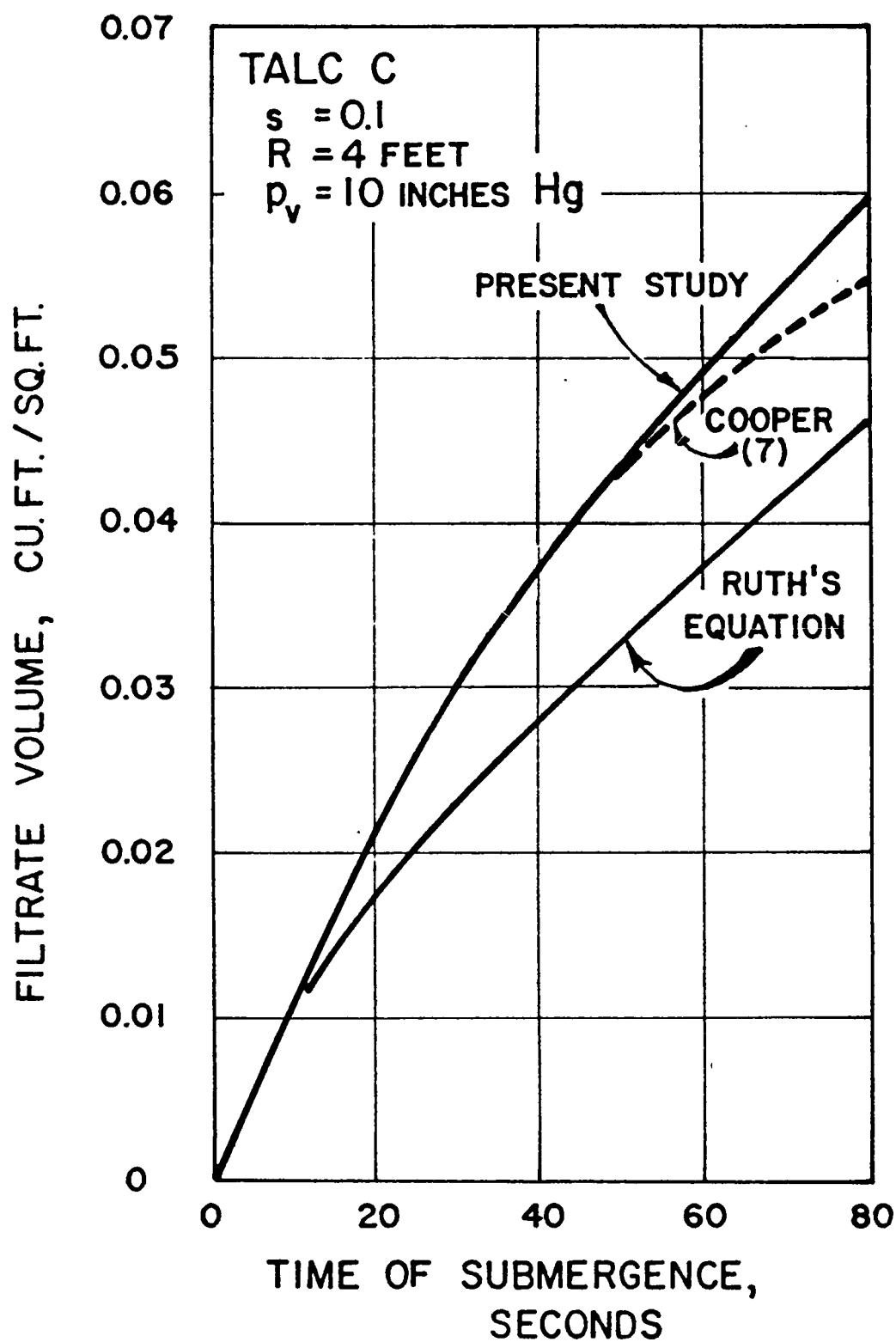


FIGURE III-8 COMPARISON OF THE PRESENT STUDY WITH PRIOR WORK

The differences between these results stem from the simplifying assumptions which were made in deriving the earlier theories. Previously the assumption was made that the rate of liquid flow throughout the filter cake was constant. In the case of Ruth's equation, the assumption was made that the pressure drop across the cake and medium was constant and equal to the integral average value. This assumption primarily accounts for the large difference between the filtrate values predicted by the equations of Ruth and Kempe and those values predicted by the other two.

The smaller difference between the present investigation and that of Cooper's may be attributed to the fact that both methods account for the variation in the pressure drop across the cake. However, the investigation provides for variation of m with changes in cake thickness. Also, the present investigation includes the effect of solids movement toward the medium within the cake itself based upon the suggestion of Shirato and Co-workers (44). The existence of this effect was not realized when Cooper's derivation was made.

VII. DISCUSSION AND RESULTS

Computer runs were made to predict the effect that

changes in rotary drum operating conditions had on filtrate flow and tonnage capacity. The physical dimensions of the rotary drum filter, such as the drum diameter and length, were assumed to be fixed. The range of operating conditions used are given below:

Slurry Concentrations	0.1, 0.15, 0.2
Angles of Submergence	60°, 90°, 120°
Drum Speeds	0.25, 0.5, 1.0, 2.0 r.p.m.
Applied Vacuum	5, 10, 15 inches of mercury

A tabulation of the results of these computer runs is given in Appendix A. An analysis of these results follow.

Effect of Operating Variables

The effect that changes in applied vacuum has on the filtration rate q_f is shown in Figure III-9. An increase in filtrate rate with increased vacuum is evident in this figure. Assuming that a design factor of eighty per cent of maximum capacity is used, a greater rotational speed will be permitted when 15 inches of vacuum is specified than if say five inches vacuum were to be specified. Furthermore, a greatly increased filtration rate can be attained by an increase in the drum submergence.

This latter effect is more easily seen by referring to Figure III-10. The filtrate flow is plotted in this figure

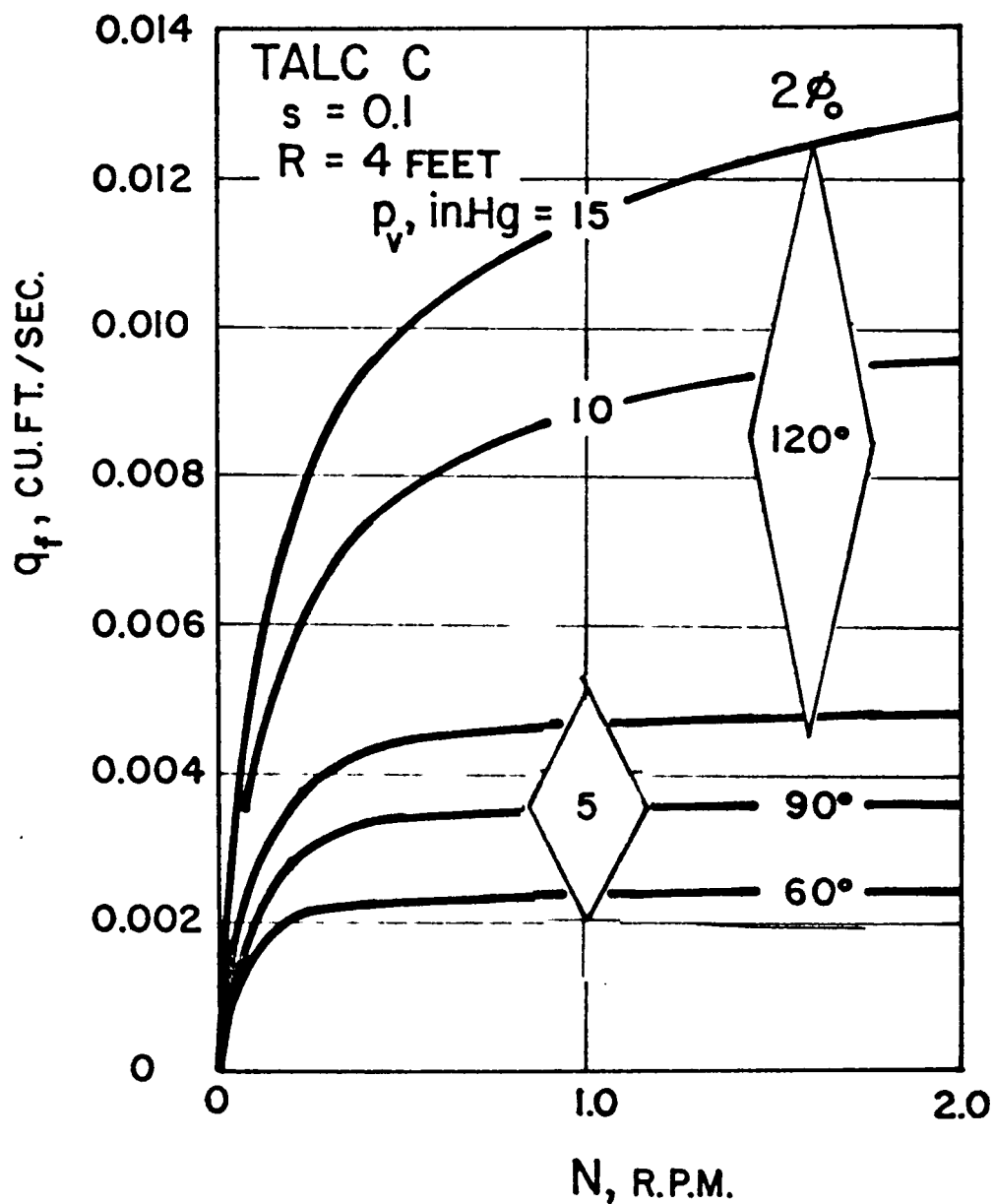


FIGURE III-9 EFFECT OF APPLIED VACUUM ON q_f

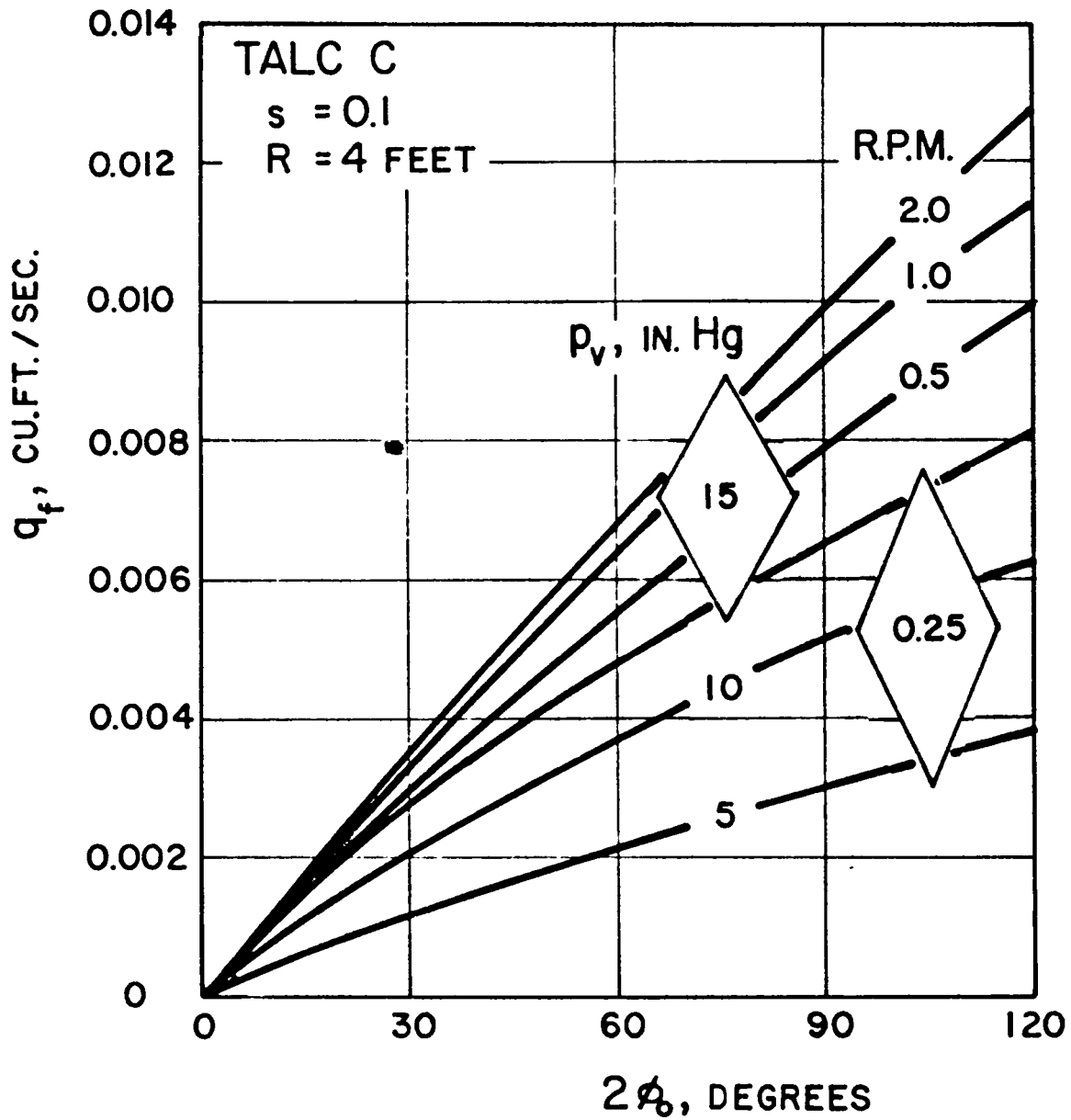


FIGURE III-10 EFFECT OF DRUM SUBMERGENCE ON q_f

as a function of the angle of submergence. The increase in filtrate rate with increased submergence is shown to be not quite linear as could be ascertained by reference to Ruth and Kempe's equation. A further effect shown here is the increase in filtrate rate with rotational speed. That effect is most noticeable for the case of 15 inches of mercury vacuum.

In Figure III-11 is shown the effect of rotational speed upon filtration rate. A greater rate is evidenced for the higher rotational speeds for all applied vacuums. However, as shown in Figure III-9 the effect of rotational speed is not the same for all pressure levels

Effect of Slurry Concentration

The tonnage capacity of a rotary drum filter is highly influenced by the solids concentration of the slurry feed. To determine the degree of that influence, let the filtration process be described in a slightly different manner (60) using the fundamental equation of Ruth's

$$q_1 = \frac{s_c p}{\mu(\alpha_w + R_m)} \quad (\text{III-68})$$

If q_1 is taken as a constant across the differential angle, $d\phi$, the total volume of filtrate per unit time may be

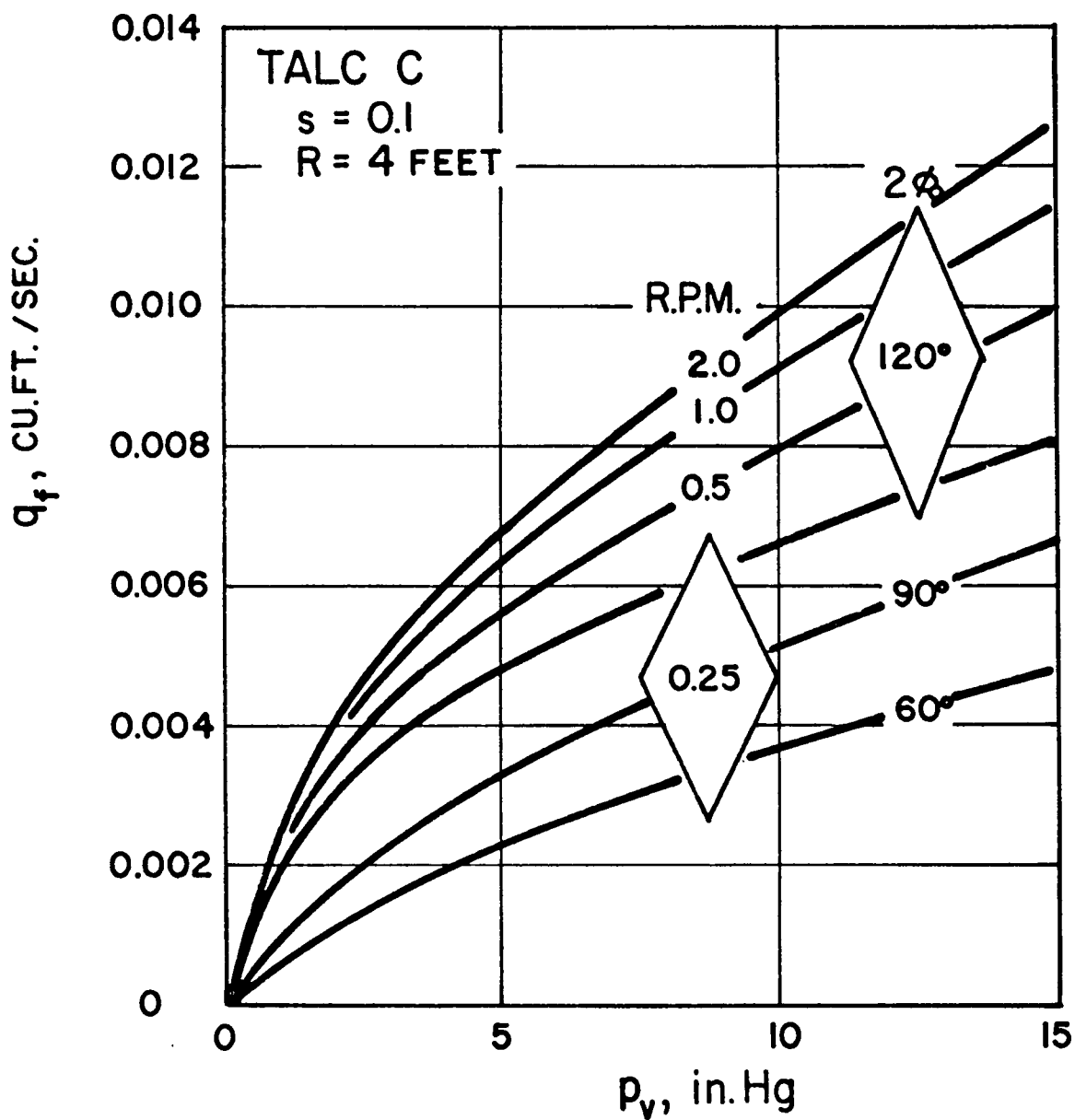


FIGURE III-11 EFFECT OF ROTATIONAL SPEED ON q_f

written as

$$q_f = \int_0^{2\phi} q_1 R L d\phi \quad (\text{III-69})$$

The weight of dry solids, dw , which is deposited from a differential volume of filtrate, dv , can be obtained from a material balance of the entire cake

$$dv = \frac{A (1 - ms)}{\rho_s} dw \quad (\text{III-70})$$

The incremental volume of filtrate, dv , can be expressed in terms of q_1 as

$$dv = q_1 A d\theta \quad (\text{III-71})$$

Since the differential angle $d\theta$ is defined as equal to $\omega d\phi$, Equations (III-70) and (III-71) can be combined to yield

$$dw = \frac{q_1 \rho_s}{\omega (1 - ms)} d\phi \quad (\text{III-72})$$

which can be integrated to give w in terms of q as

$$w = \frac{\rho_s}{\omega (1 - ms)} \int_0^{2\phi} q_1 d\phi \quad (\text{III-73})$$

By substituting this value for w , Equation (III-68) becomes

$$q_1 = \frac{g_c p}{\frac{\alpha \mu \rho_s}{\omega(1 - ms)} \int_0^{\phi} q_1 d\phi + \mu R_m} \quad (\text{III-74})$$

or

$$\frac{g_c p}{q_1} = \frac{\alpha \mu \rho_s}{\omega(1 - ms)} \int_0^{\phi} q_1 d\phi + \mu R_m \quad (\text{III-75})$$

Upon differentiation of the last equation with respect to ϕ , provided p is assumed constant, the equation may be written

$$\frac{\alpha \mu \rho_s}{\omega(1 - ms)} d\phi = - \frac{g_c p}{q_1^2} dq_1 \quad (\text{III-76})$$

Separating the variables and integrating between the limits of $\phi = 0$ and $\phi = \phi$, and $q = \frac{g_c p}{\mu R_m}$ and $q = q$ will yield upon rearrangement

$$q_1 = \sqrt{\frac{\omega}{\frac{2\alpha\mu\rho_s}{1 - ms}\phi + \left(\frac{\mu R_m}{g_c p}\right)^2 \omega}} \quad (\text{III-77})$$

Substituting the above value of q_1 into Equation (III-69) yields

$$q_f = RL \int_0^{2\phi_0} \frac{\omega \, d\phi}{\sqrt{\frac{2\alpha\mu\rho s}{1-ms} \phi + \left(\frac{\mu R_m}{\epsilon_c p}\right)^2 \omega}} \quad (\text{III-78})$$

Integration of (III-78) and subsequent simplification will produce

$$\left(\frac{q_f}{\omega}\right) = \frac{8R^2 L^2 \phi_0}{\left[\frac{2\alpha\mu\rho s}{1-ms}\right] q_f} - \frac{4RL \left(\frac{\mu R_m}{\epsilon_c p}\right)}{\left[\frac{2\alpha\mu\rho s}{1-ms}\right]} \quad (\text{III-79})$$

Since ω is defined as equal to $2\pi N$, Equation (III-79) becomes

$$\frac{1}{2\pi} \left(\frac{q_f}{N}\right) = \frac{8R^2 L^2 \phi_0}{\left[\frac{2\alpha\mu\rho s}{1-ms}\right] \left(\frac{1}{q_f}\right)} - \frac{4RL \left(\frac{\mu R_m}{\epsilon_c p}\right)}{\left[\frac{2\alpha\mu\rho s}{1-ms}\right]} \quad (\text{III-80})$$

Simplifying, Equation (III-80) is shown to be the equation of a straight line

$$\left(\frac{q_f}{N}\right) = \frac{4\pi R^2 L^2 (1-ms) 2\phi_0 \left(\frac{1}{q_f}\right)}{\alpha \mu \rho s} - \frac{4\pi R L R_m (1-ms)}{\alpha \rho s \epsilon_c p} \quad (\text{III-81})$$

where the slope is

$$\frac{4\pi R^2 L^2 (1-ms) 2\phi_0}{\alpha \mu \rho s} \quad (\text{III-82})$$

and the intercept on the ordinate at $\left(\frac{1}{\alpha_f}\right)=0$ is

$$-\frac{4\pi R L R_m (1 - ms)}{\alpha \rho^s \varepsilon_c p} \quad (\text{III-83})$$

In a similar manner, the definition for the tonnage capacity, w_f , in tons of solid per unit time per unit length of drum may be obtained by the following

$$\left(\frac{w_f}{N}\right) = -2\pi R \frac{R_m}{\alpha \varepsilon_c p} + 2\pi R \sqrt{\left(\frac{R_m}{\alpha \varepsilon_c p}\right)^2 + \frac{2\phi_o}{\pi \alpha N \mu} \frac{\rho^s}{(1-ms)}} \quad (\text{III-84})$$

The effect that slurry concentration has upon the production rate was calculated using the present theory. The results of these calculations are presented in Figure III-12. It may be observed that the tonnage production rate increases rapidly with slurry concentration. This rapid increase would approach an extremely large value as the reciprocal of slurry concentration approaches the mass fraction of solids in the wet cake or

$$s \rightarrow \frac{1}{m_i} \quad (\text{III-85})$$

In the same figure is drawn the idealization as represented by Equation (III-84), wherein the resistance of the medium is assumed to be zero.

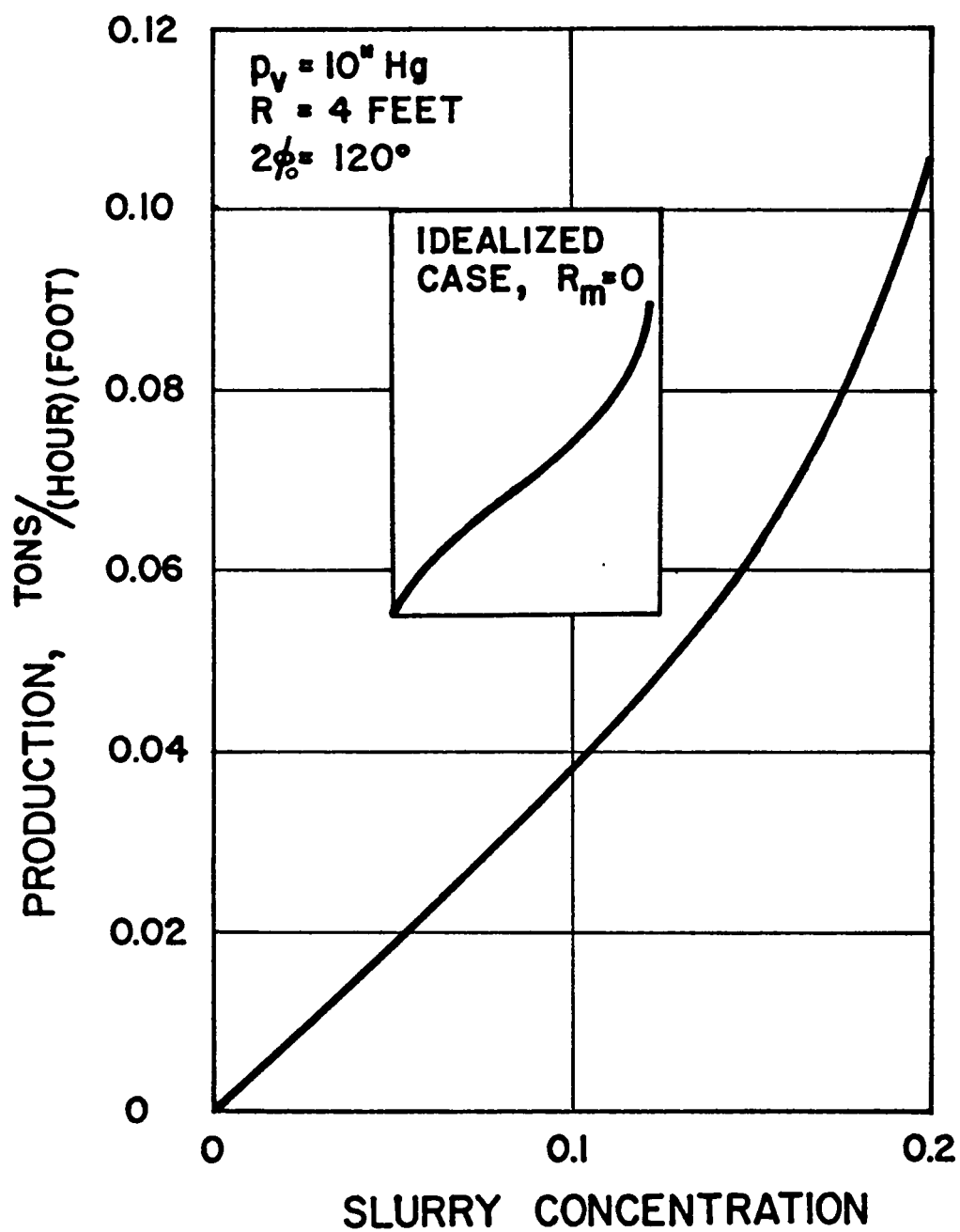


FIGURE III-12 EFFECT THAT SLURRY CONCENTRATION
HAS UPON PRODUCTION RATE

Determination of R_m and α

According to Ruth's theory it is possible to determine values of R_m and α from experimental rotary drum filtration data. Such experimental data would consist of the filtrate flow rate, q_f , obtained at a given set of drum rotational speeds, N . By combining these data to form the group q_f/N and plotting the value of this group versus $1/q_f$, a straight line would be produced according to Equation (III-81).

Referring to Equation (III-81), it can be seen that R_m may be calculated from such straight line relationships provided the intercept of the line with the abscissa, $1/q_f$, is known. From this intercept, R_m is calculated as

$$R_m = 2 \phi_o R g_c p (1/q_f)_{\text{intercept}} \quad (\text{III-86})$$

In a similar manner, an estimate of the specific cake resistance, α , can be made using the experimental rotary drum filtration data. The slope of the straight line which Equation (III-81) describes is given by Equation (III-82). Using the latter relationship and the slope of the experimental data curve, α can be calculated as

$$\alpha = \frac{4 \pi R L^2 (1-m_s) 2\phi_0}{\mu \rho_s (\text{slope})} \quad (\text{III-82a})$$

To test whether consistent values for R_m and α can be obtained from experimental data using Ruth's equation in the manner described on the previous page, a set of values for filtrate flow, q_f , at different drum speeds, N , are required. Based upon the numerical methods of this thesis, a set of calculated values of q_f versus N were plotted in the form q_f/N versus $1/q_f$ as shown in Figure III-13. Reasonably good straight lines could be drawn through the points.

At first, it might appear that the straight lines justify the simplified theory of Ruth. However, calculation of α and R_m from the straight lines in accord with Equations (III-82) and (III-82a) leads to values which differ from those assumed in making the numerical calculations. A summary of values of R_m and α obtained for different values of the angle of submergence follows:

$2\phi_0$	R_m	α
60°	1.95×10^{10}	1.04×10^{10}
90°	1.93×10^{10}	1.09×10^{10}
120°	1.84×10^{10}	1.29×10^{10}
assumed	2.0×10^{10}	

It is apparent that incorrect values of R_m would result from Ruth's analysis. Furthermore α was not constant during any of the assumed runs since the pressure drop across the cake varied with time.

It can be argued that Ruth's analysis of actual filtration data would likewise lead to incorrect values of α and R_m . Even though good straight lines would be drawn through the points, the values of the approximate slope and intercept would not lead to correct values of the parameters. If the same slurry and medium were employed in a different filter device such as a plate and frame press, different experimental values would be obtained for α and R_m in the two cases due to the weakness of the theory.

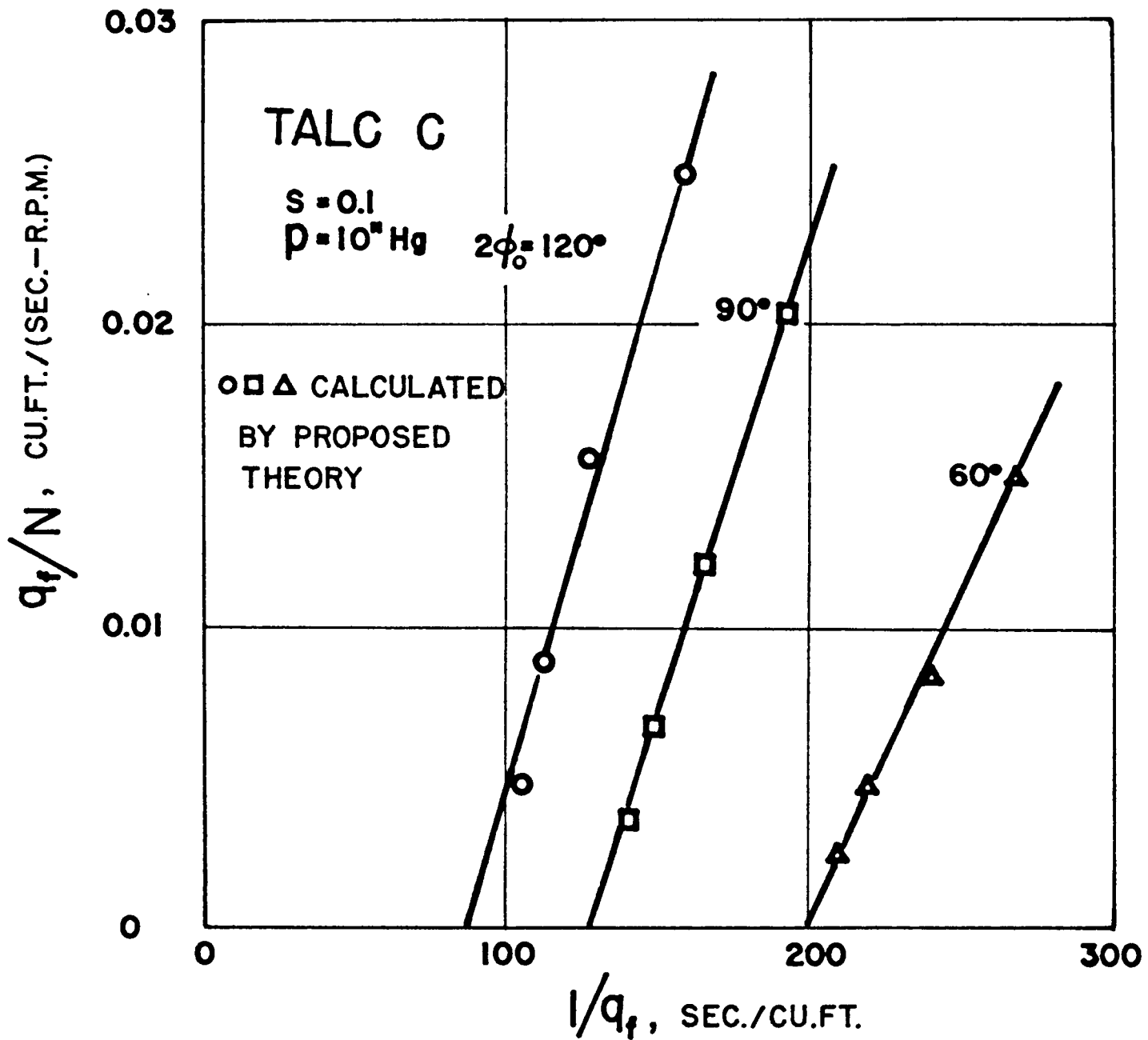


FIG. 7 III-1 TO BE PUBLISHED WITH F_m and α_{av}

CHAPTER IV

RELATING POROSITY TO PRESSURE AND TIME

Numerous authors have determined porosity as a function solely of applied pressure (11, 19, 28, 37,). Although these authors assumed that equilibrium porosity was attained instantaneously, Tiller (57) stated that this was not true. He indicated that a gradual creep would continue even after an initial quasi-equilibrium had been attained. To substantiate these conclusions he reported a plot of the variations of the porosity of crushed limestone with time for different applied pressures. This plot is reproduced in Figure IV-1. It can be seen in this figure that an initial equilibrium was reached in about 5 minutes, after which a gradual creep continued. Thus in the compression of a porous solid two time effects have been shown to exist; initial equilibrium and a creep effect.

These time effects were studied experimentally through the use of device called a compression-permeability cell disclosed by Ruth (38) in 1946. As a result of these studies it was found that porosity was a function of both time and pressure. The time dependency was evidenced by a decrease in porosity with time under a constant applied pressure.

Two time effects were found to occur simultaneously.

VARIATION OF POROSITY WITH TIME

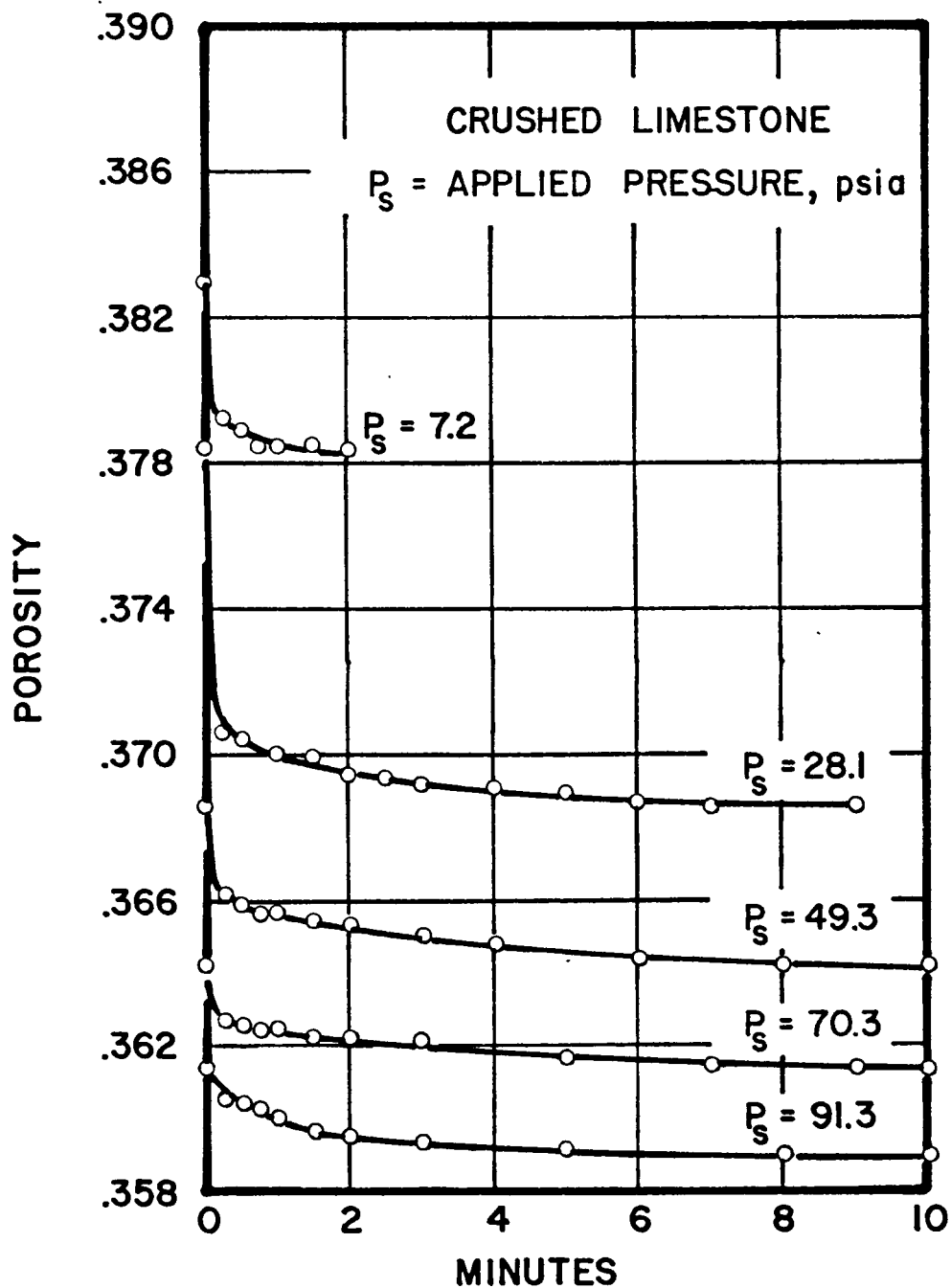


FIGURE IV-1

The first effect predominates up to the time initial equilibrium is attained and is called primary compression. This attainment of equilibrium occurs quickly, after which the creep effect becomes pronounced. Although the effect of creep may be of importance in other fields, primary compression is of chief importance in the field of filtration.

Primary compression is a time effect concerned with the initial expulsion of liquid from the interstices of the porous solid. This time effect may be described phenomenologically by combinations of mechanical analog models. These analog models are composed of elastic springs, dashpots, etc., and are termed rheological models. The rheological models can be converted to their electrical analogs and solved using circuit theory and Laplace transform theory.

The final solution of these Rheological models presents cake thickness as a function of the applied force and time. The cake thickness in turn must be related to porosity so that the function may be employed in filtration theory. Tiller (57, 58) has shown that porosity plays an important role in filtration. The relationship between cake thickness and porosity may be determined by use of a fictitious, but factually correct, representation of a compression-permeability filter cake as shown in Figure IV-2. In this figure, the solids are assumed to be inelastic and occupy a distinct layer

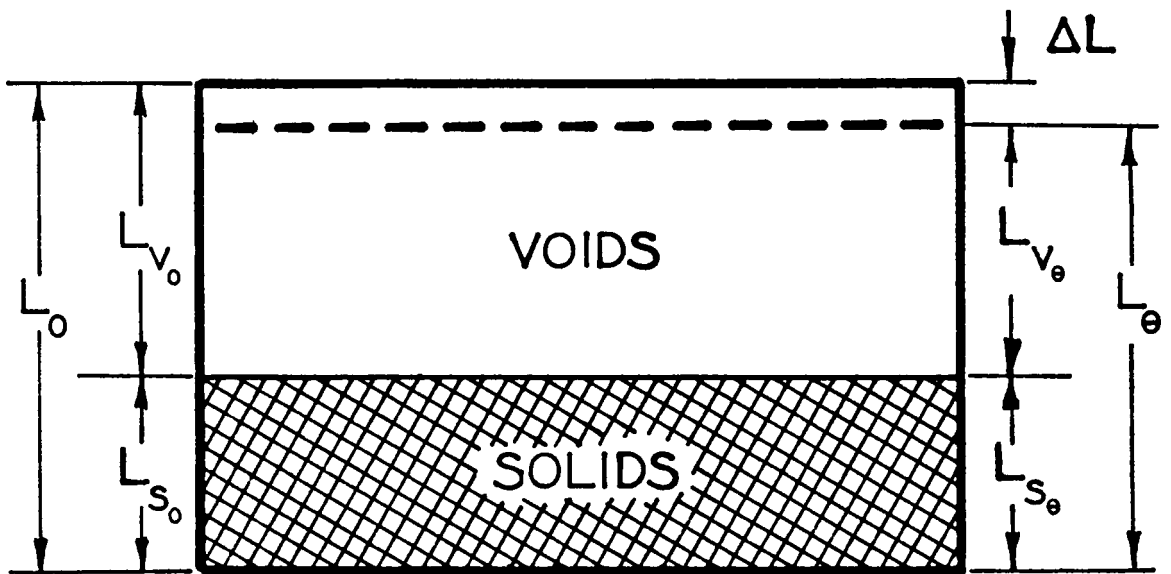


FIGURE IV-2 A COMPRESSION-PERMEABILITY FILTER CAKE

of thickness L_s . Since the initial cake thickness is L_1 , the porosity ϵ at that time is

$$\epsilon = \frac{L_0 - L_{s0}}{L_0} \quad (\text{IV-1})$$

Thus the porosity at any time is related to the cake height and the change in porosity can also be related to the change in cake height as

$$\epsilon_\theta = \frac{L_\theta - L_{s\theta}}{L_\theta} \quad (\text{IV-2})$$

Since $L_{s\theta} - L_{s0}$, which by Equation (IV-1) is

$$L_{s0} = L_0 (1 - \epsilon) \quad (\text{IV-3})$$

then

$$\epsilon = \frac{L_\theta - L_0 (1 - \epsilon)}{L_\theta} \quad (\text{IV-4})$$

Equation (IV-4) indicates that the porosity at any θ may be calculated provided the original cake thickness, the original porosity, and the final cake thickness are known. The cake thickness may be predicted by use of a rheological model which would describe the behavior of the cake as it under goes compression.

I. RHEOLOGICAL MODELS

Rheology is defined as the science of the deformation and flow of matter. A body is said to be deformed when application of an appropriate force system alters the shape or size of the body. A body is said to flow if its degree of deformation changes continually with time. Thus, it is the goal of rheology to predict the deformation or flow of matter which will result from the application of a given force system to that matter. One method of describing this rheological behavior is through the use of model theories.

These theories substitute a model which is supposed to behave analogously to that of the real matter. Admittedly the models consist of elements which have no counter part in the real material. That is, the filter cake in no wise is thought to be composed of actual physical springs and pistons. Rather it is through the analogy that the real matter and the model are related.

There are two kinds of model theories. One is entirely concerned with the relation between the real matter and the model through analogies. This kind is called "analogy-models". The second, is concerned with a closer approximation of the model to the real conditions. This latter is called a "structural-model".

The use of these models greatly aids in the development of a clearer understanding of the rheology of a material. As the rheology of the material becomes clearer, the studies using analog models are replaced by those of structural models and devolve to a point where an exact structural theory can be established.

The model of a filter cake to be developed in this section is one which will represent the overall behavior of the cake under primary compression. This model will serve as an indication for the differential model which will be fed into the filtration theory by future studies.

Two mechanical elements which are used in the rheological models to be described in this chapter are "Hookean" elements and "Newtonian" elements. Hookean elements may be visualized as perfectly elastic, weightless springs. An example of such a spring is shown in Figure IV-3a. Under no load, the spring will have an initial length L_0 . Under a load F , the spring will be compressed to a length $L_0 - \Delta L$. When the elastic property of the material is K' , then the compression may be written as

$$\Delta L = \frac{F}{K'} \quad (\text{IV-5})$$

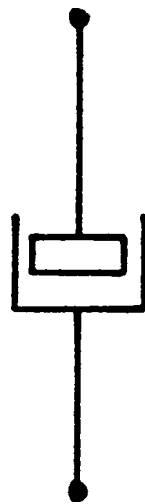
Newtonian elements are idealized as viscous dashpots; that is, as a porous plug or piston which moves within a closed

ELEMENTS OF RHEOLOGICAL MODELS



HOOKEAN
ELEMENT

a



NEWTONIAN
ELEMENT

b

FIGURE IV-3

cylinder filled with a viscous liquid. Such a dashpot, as presented in Figure IV-3b, has the property that its rate of compression is proportional to the applied force, and not on the total amount of the shear strain. Thus, the rate of compression is related as follows

$$\frac{\Delta L}{\Delta \theta} = \frac{F}{B'} \quad (\text{IV-6})$$

where B' is the dashpot constant, a characteristic of the material.

Separately, these model elements can represent certain classes of simple materials. The Hookean element can represent a solid having pure elasticity only. The Newtonian element represents a liquid possessing Newtonian viscosity alone. If the aim of model building were the description of these materials, the use of rheological models would be trivial indeed. It is, however, by the combination of these elements into more complex models that the desired understanding of the rheological behavior of a real substance can be attained. The combination of these elements can be made in any number of ways. Both elements can be combined either in series or in parallel. Furthermore, these combinations of elements can be combined with more elements or other combinations of elements. By this means, rather

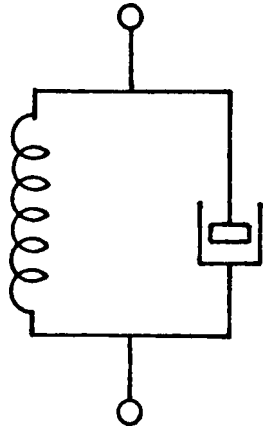
complex rheological models can be built which can describe the behavior of any sort of material.

II. MODELS USED TO DESCRIBE PRIMARY COMPRESSION

To describe the primary compression of a compressible porous solid, three different rheological models were devised. These were the Kelvin model, the Maxwell model, and what Jaeger (22) calls "the General Linear Substance" model.

The Kelvin model is represented by a spring connected in parallel with a dashpot. This representation is shown in Figure IV-4a. This model is one which might be expected to apply to a cellular elastic material containing voids or holes filled with viscous liquid. Under an applied load, the model instantly begins to compress. However, the action of the spring is retarded by the parallel acting dashpot. The dashpot, at the instant of loading, assumes the total amount of the load. Upon assuming this load the dashpot is compressed, causing a movement of the piston inside the closed cylinder. Under this movement of the piston, the spring begins to compress and through this compression, begins to assume a portion of the total applied load. Thus as time progresses, the total load originally assumed by the dashpot is transferred to the spring, so that at some infinite

RHEOLOGICAL MODELS



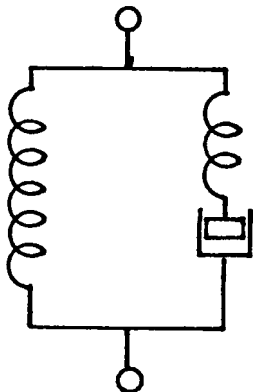
KELVIN MODEL

IV-4a



MAXWELL MODEL

IV-4b



LINEAR MODEL

IV-4c

FIGURE IV -4

time, the total applied load is then assumed by the compression of the spring. When this transfer of load is completed, further compression is prevented and motion ceases. A graphical representation of the compression of this model under applied load may be seen by reference to Figure IV-5a.

The Maxwell model is represented by a spring connected in series with a dashpot, as shown in Figure IV-4b. This model has been used in the study of materials which must behave elastically for short times, but at the same time may flow very slowly under continuously applied stress. If this model is suddenly loaded, it instantaneously compresses so that the spring at this time assumes the total load. Simultaneously with this compression, the dashpot begins to be compressed; however, unlike the Kelvin model, the Maxwell model does not have a mechanism whereby the stress on the spring can be shared by the action of the dashpot. Thus, in the case of the Maxwell model, the material will possess an instantaneous elastic strain, followed by a linearly increasing strain. The compression of this model under an applied load is graphically represented in Figure IV-5b.

The General Linear Substance model consists of a spring in parallel with a Maxwell model, as shown in Figure IV-4c.

RESPONSE OF MODELS

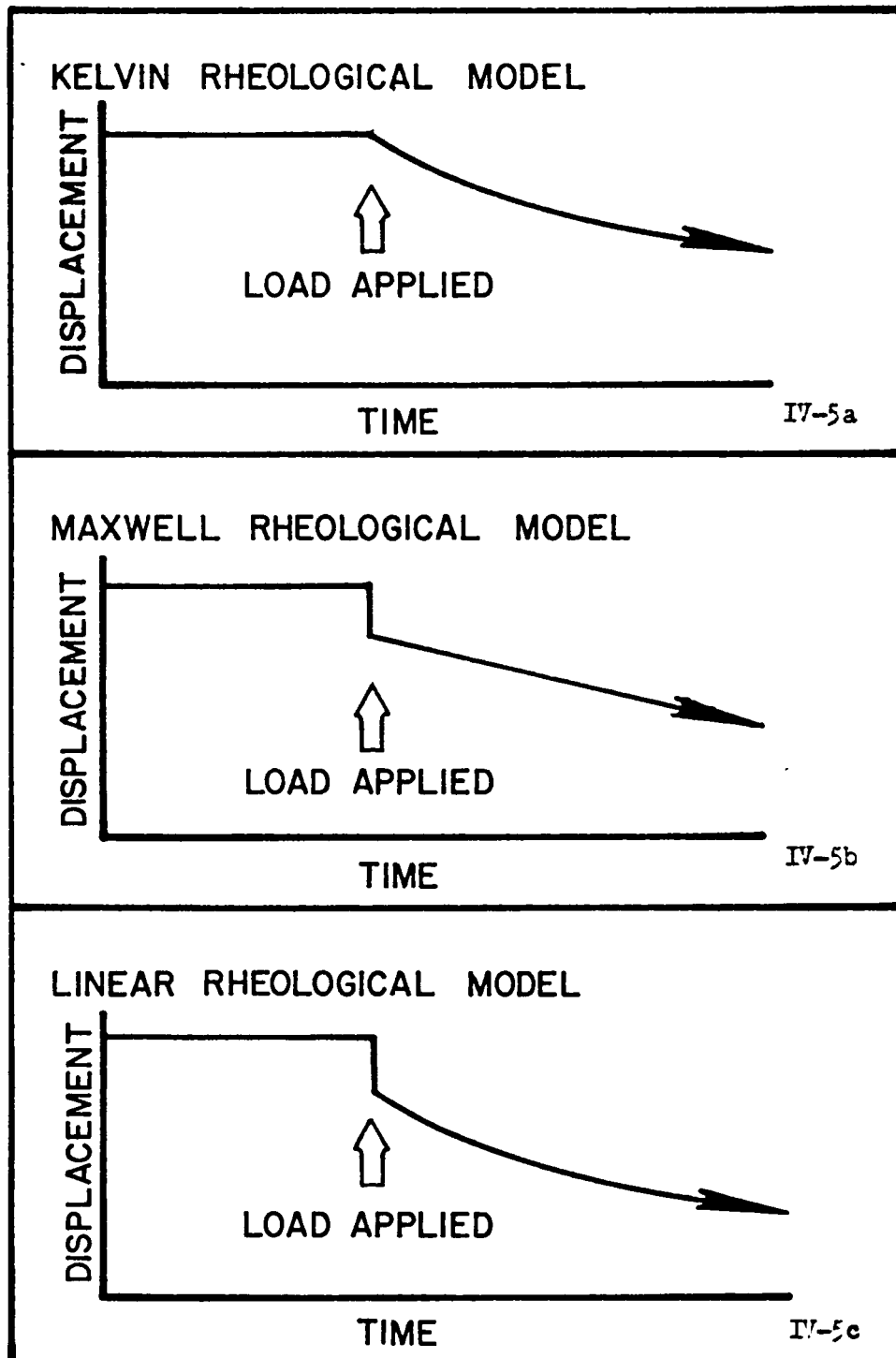


FIGURE IV-5

Under a suddenly applied load, the model elastically compresses such that the total load is taken up by the two springs. As soon as the load is applied to the spring of the Maxwell branch of the model, the dashpot starts to move, thus relaxing the stress applied to the spring of that branch. With this relaxation the other parallel spring must assume the additional load. In effect, the load assumed by the Maxwell branch is slowly transferred to the parallel spring. Once the total load is assumed by the latter spring, motion will cease. Since the rate that the load will be transferred is dependent upon the arresting motion of the dashpot, and this motion is arrested only at very long times, then the stress relaxation or the strain (compression) continues for an infinite length of time. The above described reactions of this model to an applied load is shown in Figure IV-5c.

A mathematical analysis of the above described models was made and compared with the compression found by experiment. The results of this comparison will be shown later in this chapter. The first step in the solution of a rheological model is the development of an electrical analog model.

The basic law governing the behavior of springs and dashpots are given above as Equations IV-5 and IV-6. It is the principle of analogs that systems represented by equations

having the same form can be substituted for one another. In this manner, a more familiar phenomenon may be studied instead of the former, less familiar one.

The variables involved in rheological systems are force, distance, velocity, and material constants. An analogous electrical system has as the equivalent variables, current, voltage, time derivatives of current, and resistance and conductance. Thus, Equations (IV-5) and (IV-6) may be rewritten in terms of the electrical behavior as

$$V' = \frac{i}{K'} \quad (\text{IV-5a})$$

$$V' = \frac{1}{B'} \frac{di}{d\theta} \quad (\text{IV-6a})$$

where V' is the voltage, i is the current, and $\frac{1}{K'}$ and $\frac{1}{B'}$ are the resistance and conductance, respectively.

By use of Laplace transform theory, the corresponding equations are converted to the transforms:

$$\mathcal{L}\{V'\} = V'_{(s)} = \frac{s i(s)}{K'} \quad (\text{IV-5b})$$

$$\mathcal{L}\{V'\} = V'_{(s)} = \frac{i(s)}{B'} \quad (\text{IV-6b})$$

As an illustration of the use of this method, the solution for the Kelvin model is detailed next.

III. SOLUTIONS OF THE RHEOLOGICAL MODELS

The procedure used to solve these rheological models is to operate on the analogous electrical system and to determine the function by application of Laplace Transform theory.

The Kelvin model is redrawn in Figure IV-6. Its analogous electrical circuit is shown in the same figure. The impedance \bar{Z} of the circuit can be determined as follows:

$$\bar{Z} = \frac{1}{B' + \frac{K'}{s}} = \frac{s}{B's + K'} \quad (\text{IV-7})$$

Let it now be assumed that a constant force is applied instantaneously to the rheological model. This is signified by the application of a constant current in the electrical analog model. Such an instantaneously applied current is represented by a step function, defined as:

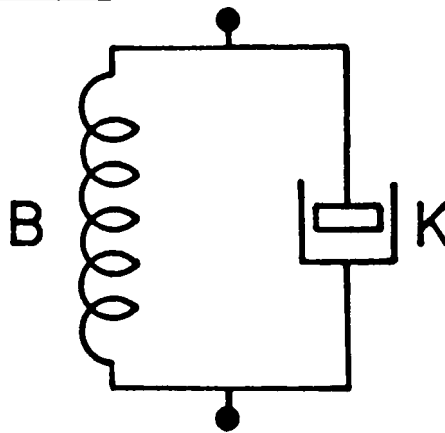
$$\left. \begin{array}{ll} i = 0 & \theta < 0 \\ i = I & \theta > 0 \end{array} \right\} \quad (\text{IV-8})$$

The corresponding Laplace transform of this step function is:

$$\mathcal{L}\{i\} = \frac{F'}{s} \quad \text{for } \theta = 0 \quad (\text{IV-8a})$$

ANALOG OF MODEL

RHEOLOGICAL MODEL



ELECTRICAL ANALOG MODEL

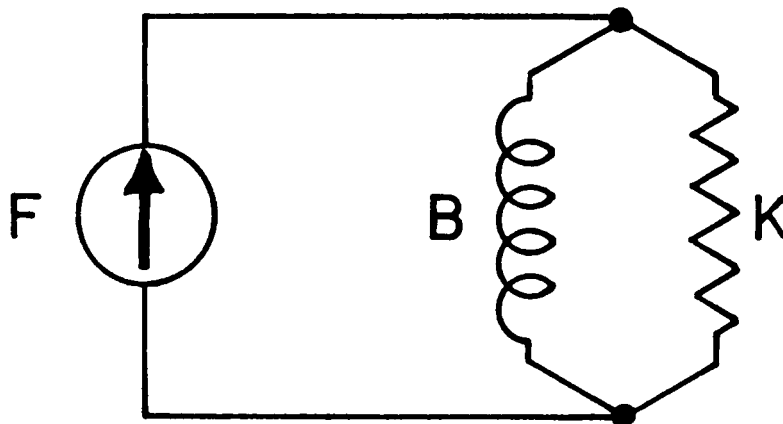


FIGURE IV-6 ANALOG OF A MAXWELL MODEL

The displacements within the rheological model corresponds to the voltage of an analogous electrical model. Thus the transformed displacement corresponds to the analogous transformed voltage according to Ohm's law

$$V'_{(s)} = \int \left\{ 1 \right\} \bar{Z}(s) \quad (\text{IV-9})$$

The transformed instantaneous current is given by Equation (IV-8) and the impedance, \bar{Z} , has already been given by Equation (IV-7). Upon substituting these values into the above equation, the transformed voltage is found to be

$$V'_{(s)} = \frac{F}{s} \left[\frac{s}{Bs + K'} \right] = \frac{F}{B's + K'} \quad (\text{IV-10})$$

The velocity of the displacement can now be obtained by taking the inverse Laplace transform of Equation (IV-10).

This will give

$$\int^{-1} \left\{ V'_{(s)} \right\} = v' = \frac{dx}{d\theta} = \int^{-1} \left\{ \frac{F/B'}{s + K'/B'} \right\} \quad (\text{IV-11})$$

$$\frac{dx}{d\theta} = \frac{F}{B'} e^{-\frac{K'}{B'}\theta}$$

The displacement or the change in cake thickness is obtained by integrating Equation (IV-11) as

$$\int_{L_0}^{L_\theta} dx = \frac{F}{B'} \int_0^\theta e^{-\frac{K'}{B'}\theta} d\theta$$

$$L_0 - L_\theta = \frac{F}{K'} \left[1 - e^{-\frac{K'}{B'}\theta} \right] \quad (\text{IV-12})$$

or

$$L_{\theta} = L_0 \left[1 - \frac{F}{K' L_0} \left(1 - e^{-\frac{K'}{B'} \theta} \right) \right] \quad (\text{IV-12a})$$

Equation (IV-12) is the solution to the Kelvin model.

The solution for the other two rheological models may be found in a similar manner. The details of their solution are outlined next.

The Maxwell model shown in Figure IV-4b can be represented as a analogous electrical circuit having a resistor and a conductance connected in series to a current source. The impedance \bar{Z} of this circuit is

$$\bar{Z} = \frac{1}{B'} + \frac{s}{K'} \quad (\text{IV-13})$$

To this circuit, let a step functional current be applied. The Laplace transform of this function has been discussed earlier and was found to be

$$\mathcal{L} \left\{ 1 \right\} = \frac{F}{s} \quad (\text{IV-14})$$

Thus, the application of Ohm's law yields

$$V'_{(s)} = \mathcal{L} \left\{ 1 \right\} \bar{Z} = \frac{F}{s} \left[\frac{1}{B'} + \frac{s}{K'} \right] \quad (\text{IV-15})$$

or

$$V'_{(s)} = F \left[\frac{1}{B' s} + \frac{1}{K'} \right] \quad (\text{IV-15a})$$

and the inverse Laplace transform, the voltage or the velocity is

$$\mathcal{L}^{-1} \left\{ V'_{(s)} \right\} = v' = \frac{dx}{d\theta} = \mathcal{L}^{-1} \left\{ F \left[\frac{1}{B' s} + \frac{1}{K'} \right] \right\} \quad (\text{IV-16})$$

$$\frac{dx}{d\theta} = F \left[\frac{1}{B'} + \frac{\delta(\theta)}{K'} \right]$$

where $\delta(\theta)$ is the Dirac Function.

The displacement may be found by integrating between the appropriate limits to yield

$$\int_{L_0}^{L_0} dx = F \int_0^0 \left[\frac{1}{B'} + \frac{\delta(\theta)}{K'} \right] d\theta \quad (\text{IV-17})$$

$$L_\theta - L_0 = F \left[\frac{\theta}{B'} + \frac{1}{K'} \right]$$

For the so called "General Linear Substance" model, Figure IV-4c, the analogous electrical circuit is a resistor (K_2) in parallel with a branch made of another resistor K_1 , connected in series with a conductance. The impedance for this circuit is

$$\bar{Z} = \frac{1}{\frac{B' K_1}{K_1 + B' s} + \frac{K_2}{s}} \quad (\text{IV-18})$$

The transformed voltage is hence

$$V'_{(s)} = F \left[\frac{K_1 + B' s}{K_1 K_2 + (K_1 + K_2) B' s} \right] \quad (\text{IV-19})$$

When Equation (IV-19) is inverted using the Laplace transform theory, this voltage is found to be

$$V' = \frac{F}{K_1' + K_2'} \left[(\theta) + \frac{(K_1')^2}{B'(K_1' - K_2')} e^{-\frac{K_1' K_2' \theta}{B'(K_1' + K_2')}} \right] \quad (IV-20)$$

Since the voltage is also the velocity of the compression $dz/d\theta$ then integration of the resulting differential equation in terms of time θ will yield

$$L_\theta - L_0 = \frac{F}{K_1' + K_2'} \left\{ 1 + \frac{K_1'}{K_1'} \left[1 - e^{-\frac{K_1' K_2' \theta}{B'(K_1' + K_2')}} \right] \right\} \quad (IV-21)$$

IV. TESTING OF THE MODELS

Each of the models, as expressed by Equations (IV-12a), (IV-17), and (IV-21) describe a possible compression of a filter cake. In order to determine which best describes the actual compression, a series of laboratory experiments using solka floc were performed to determine the cake height and porosity as a function of time.

The procedure used in getting these data is detailed in Chapter VII. In brief it consisted of preparing a filter cake in the compression-permeability cell, in situ; compressing the cake under a given load, measuring the height of the cake periodically; and at given intervals increasing the

amount of the load applied to the cake. In this manner, the cake height was determined as a function of time for a given applied load. The interval between applications of an increment of load was varied from 6 seconds in some runs to as much as 10 minutes in others. Several longer time runs were made, these results are described in Chapter VI. For the shorter time periods instantaneous cake height readings were recorded simultaneously with the corresponding time using a movie camera. After the film was developed, the recorded cake height and time could be easily determined. The results of the test are given in Appendix D. These results must be transformed in order to determine the suitability of a given model to describe the actual behavior of the filter cake.

The mathematical description of the three models are given in Equation (IV-12) for the Kelvin; Equation (IV-17) for the Maxwell; and Equation (IV-21) for the "General Linear Substance" model. A comparison of the experimental results to these models is given next.

For the Kelvin model, let the following definitions be made so that Equation (IV-12) can be modified

$$\begin{aligned} d &= L_0 - L_\theta & ; & \quad a = \frac{F}{B'} \\ \Delta d &= L_\theta - L_{\theta + \Delta\theta} & ; & \quad b = \frac{K'}{B'} \end{aligned}$$

Thus, Equation (IV-12) becomes

$$d = \frac{a}{b} (1 - e^{-b\theta}) \quad (\text{IV-22})$$

and

$$\Delta d = \frac{a}{b} (1 - e^{-b\theta}) - \frac{a}{b} (1 - e^{-b(\theta - \Delta\theta)}) \quad (\text{IV-23})$$

This latter equation can be simplified to yield

$$d = \frac{a}{b} e^{-b\theta} (1 - e^{-b\Delta\theta}) \quad (\text{IV-24})$$

From Equation (IV-22) a value for $e^{-b\theta}$ can be obtained. Substituting this value into Equation (IV-24) the latter equation then becomes

$$\Delta d = -(1 - e^{-b\Delta\theta}) d + \frac{a}{b} (1 - e^{-b\Delta\theta}) \quad (\text{IV-25})$$

This equation is a linear relationship between d and Δd ; hence, a plot of Δd versus d will yield a straight line having a slope equal to

$$-(1 - e^{-b\Delta\theta})$$

and an intercept equal to

$$\frac{a}{b} (1 - e^{-b\Delta\theta})$$

For the Maxwell model a similar transformation of Equation (IV-17) will yield

$$\Delta d = -d + a\Delta\theta \quad (\text{IV-26})$$

Which is the equation of a straight line, also. In this case the intercept will be $a\Delta\theta$ and the slope of the line will be -1 .

Finally, a transformation of Equation (IV-21) for the "General Linear Substance" model will yield the linear relationship

$$\Delta d = \left(-e^{-\frac{bc}{b+c}\Delta\theta} \right) d + \frac{a}{c} \left(1 + e^{-\frac{bc}{b+c}\Delta\theta} \right) \quad (\text{IV-27})$$

where

$$c = \frac{K_2'}{B'}$$

A short computer program was written to calculate d and Δd from the experimental values. This program, together with several sample results are given in Appendix C.

In Figure IV-7 are plotted the results of two experimental runs, numbers XVII-65 and XVII-130. The applied force for run XVII-65 was 15.3 pounds; the force for run XVII-130 was 100.3 pounds. Since the data from each of these runs show a linear form, all the models are acceptable on the basis of this linearity. However, a further comparison of the models with the

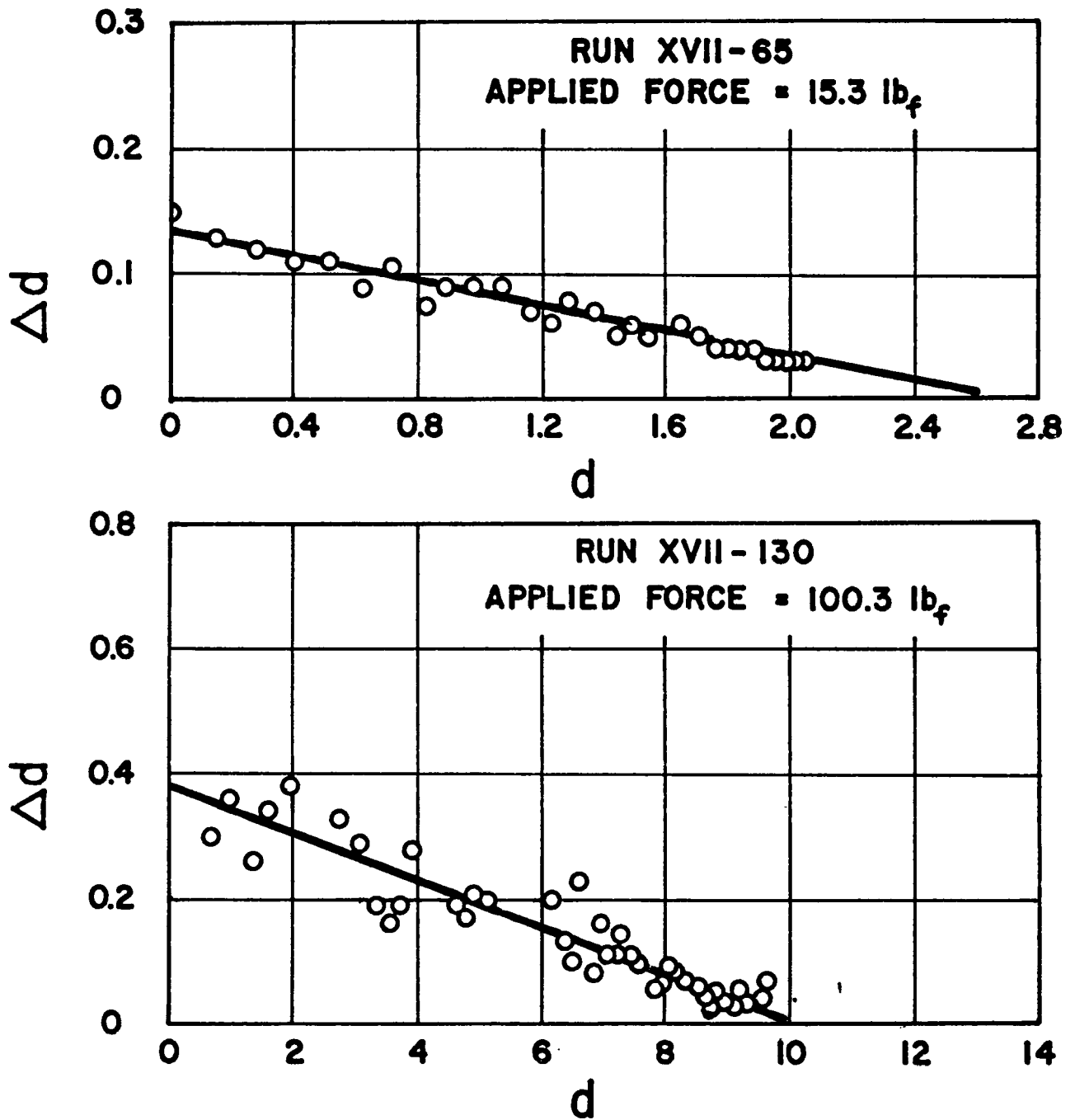


FIGURE IV-7

linear plots show that the Maxwell model can be discarded because the slope of none of the lines is minus one. This leaves as acceptable models either the Kelvin or the "General Linear Substance". Since either of these are acceptable and the available data does not indicate that one is more sufficient than the other, the Kelvin model will be assumed to be sufficient to describe the primary compression. From the slope and intercepts obtained from the lines drawn in Figure IV-7, values of a and b , and hence values of K' and B' could be determined using Equation (IV-25). The results of these evaluations are listed below:

<u>Run</u>	<u>F'</u>	<u>B'</u>	<u>K'</u>
XVII-65	15.3	5.69	4.969
XVII-130	100.3	9.933	6.374

The ability of these constants to reproduce the experimental data are shown in Figures IV-8 and IV-9. In these figures the cake thickness predicted using the Kelvin model is shown in Figures IV-8 and IV-9. In these figures the cake thickness predicted using the Kelvin model is shown as a solid line, whereas, the experimental data are shown as circles. The agreement between data and the predicted values is good.

An additional test of these rheological constants was

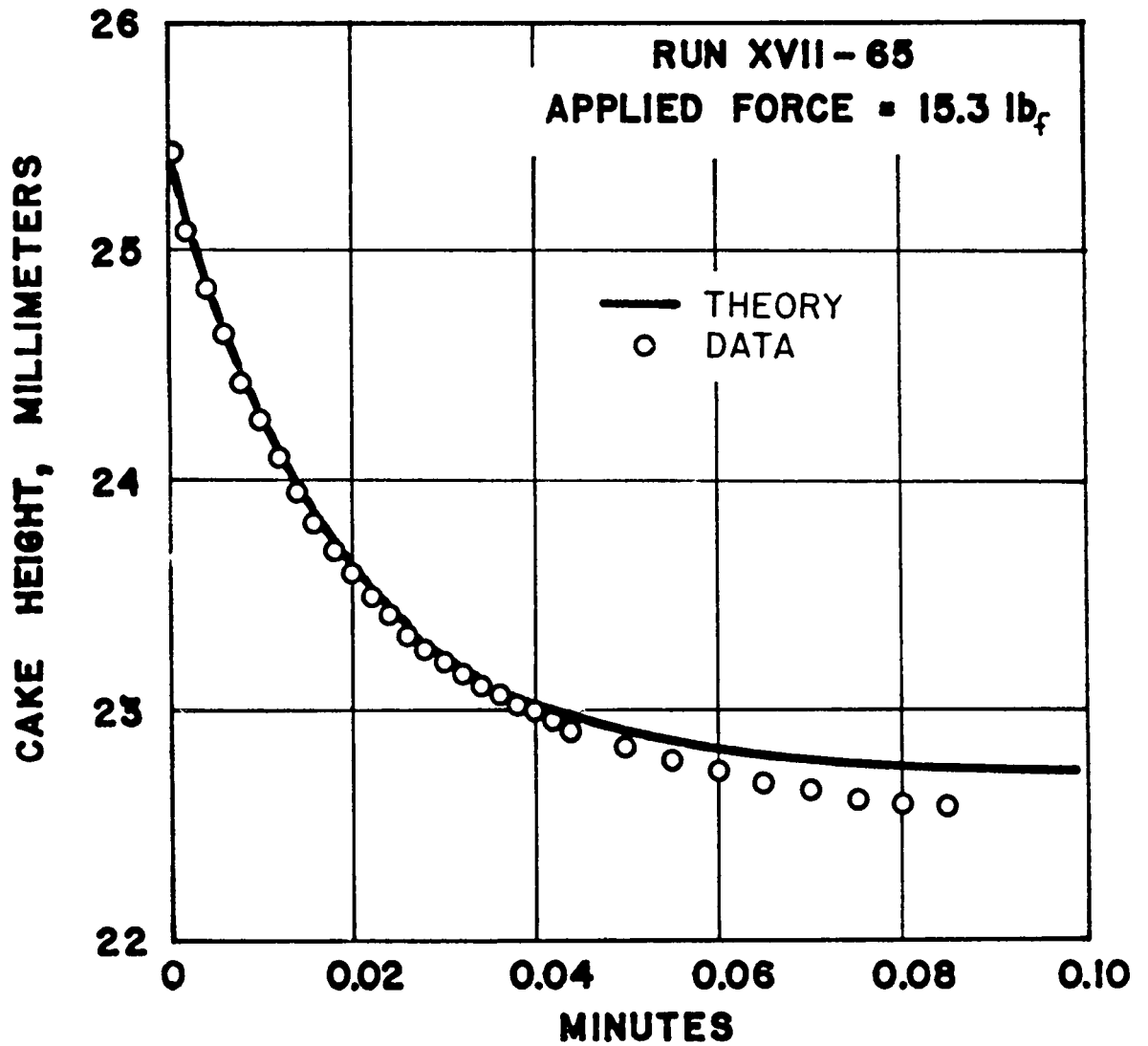


FIGURE IV-8 COMPARISON OF KELVIN MODEL TO RUN 65

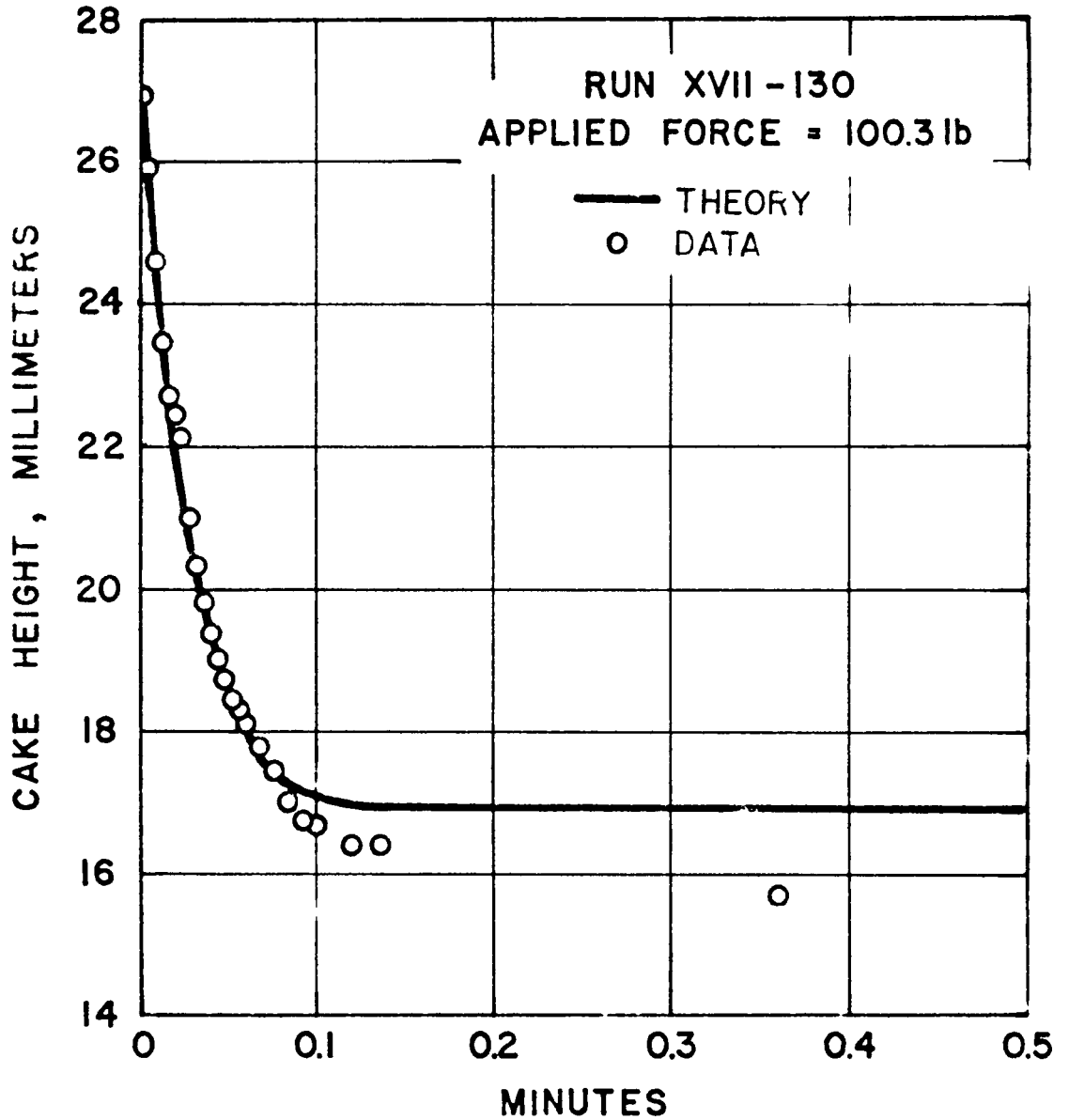


FIGURE IV-9 COMPARISON OF ALVIN 10 L TO RUN 130

made. The data were obtained from a similar run, XVII-63. The applied compressive force for this latter run was 15.3 pounds. The experimental results are reported in Appendix C. A comparison of the predicted results to the experimental results is shown in Figure IV-10. The points represent the experimental data and the solid line the predicted cake height. Again the agreement is good.

From the preceding analysis it may be assumed that the Kelvin model adequately predicts the primary compression of a filter cake. It is only the creep function which the model does not predict.

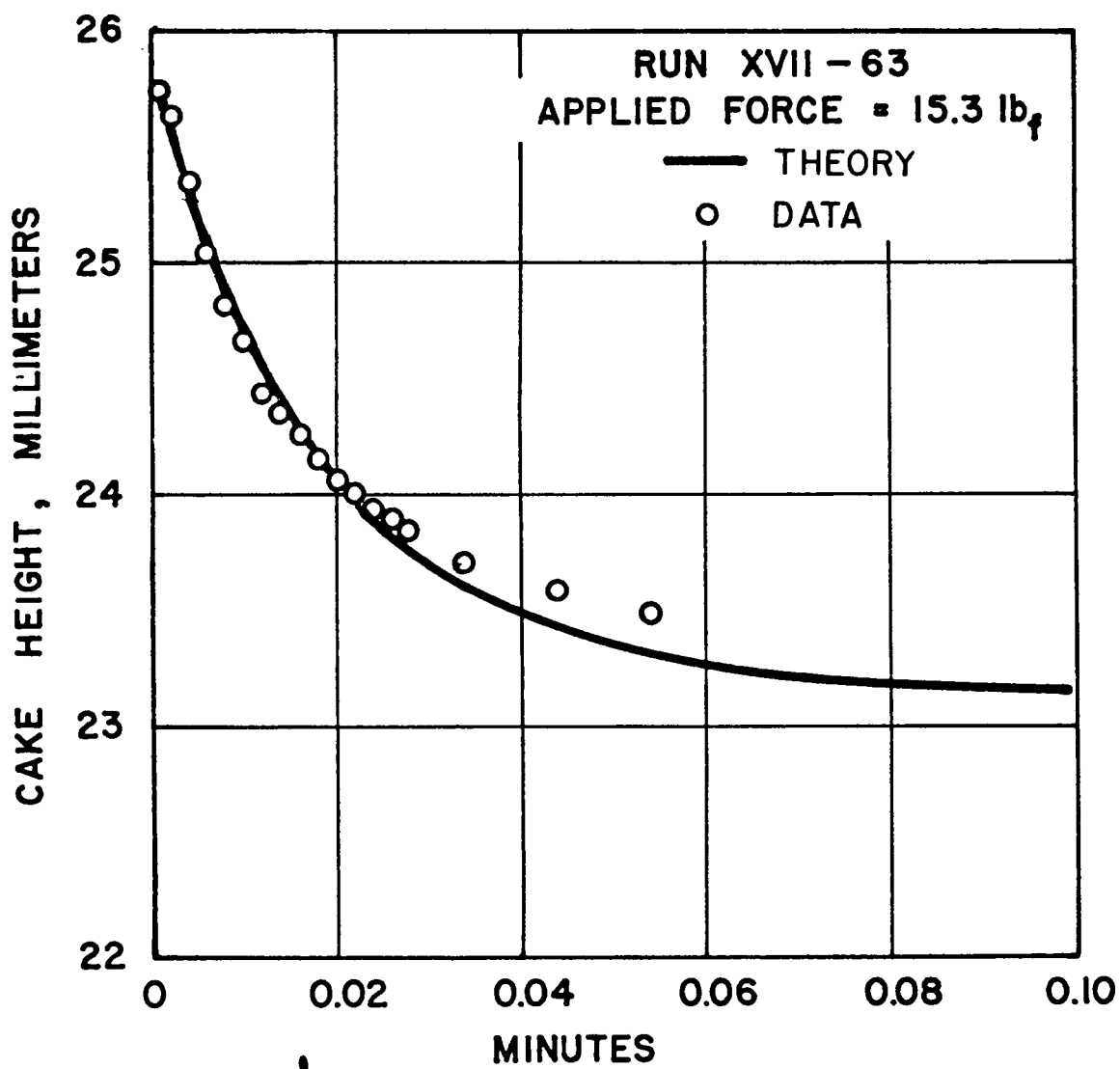


FIGURE IV-10 COMPARISON OF THE PREDICTED RESULTS TO THE RESULTS

CHAPTER V

SIDE-WALL FRICTION

IN COMPRESSION-PERMEABILITY TESTING

Important to filtration calculations are the values of porosity and specific cake resistance of a filter cake. These values can be obtained from a device known as a compression-permeability cell, in which a mechanical load is applied to a confined filter cake; and liquid is allowed to flow through the solids under relatively small liquid pressures. Permeability and porosity can be determined as a function of the applied pressure on the confined cake. Presently employed theory is based upon the assumption that specific cake resistance and porosity are functions of solids pressure alone.

Average values for porosity and specific cake resistance of a filter cake depend upon integration processes utilizing local or point values. The purpose of the compression-permeability cell is to provide a means for determining the point values which can be used to predict the relationship between porosity and solids pressure in a filter cake.

If the solids pressure produced by the mechanical load were uniform throughout the filter cake, then the average cell porosity and specific cake resistance could be used as

point values to describe the flow in a filtration process. However, an appreciable amount of friction has been found to exist between the filter cake and the wall of the compression-permeability cell. Thus, the cake is not uniformly compressed and only average values are obtained which must be corrected before being used in theoretical calculations. It is the purpose of this chapter to discuss side-wall friction and to derive a theory applicable for development of correction factors.

I. SIGNIFICANCE OF SIDE-WALL FRICTION

In compression-permeability cell testing it has been assumed (11) that the filter cake was uniformly compressed. However, because wall friction does exist, a portion of the force applied to the surface of the filter cake is transmitted to the wall causing a diminution of forces in subsequent layers of the filter cake. Thus, the cake is not uniformly compressed. Non-uniform compression of the filter cake causes a variation in porosity throughout the entire cake. Since the porosity depends upon the applied stress, which decreases from the top to the bottom of the cake, the porosity is greater at the bottom than at the top.

Utilizing experimental data, given later in this chapter, it will be demonstrated that side-wall friction does exist

in a compression-permeability cell. Wall friction is a function of the frictional contact area between side wall and confined solids which may be expressed in terms of the ratio of the area of the side wall of the flow area of the cake. Since the area ratio for a commercial filter is usually much smaller than the corresponding ratio for a compression-permeability cell, the wall effect for a commercial filter is probably negligible. However, in small tests filters of the bomb type having a diameter of one to four inches, side-wall friction may be an appreciable factor. The exact magnitude of the factor needs to be investigated experimentally.

II. PREVIOUS INVESTIGATORS

Few investigators have recognized that side-wall friction was significant. Grace (11) has reported data which show that the porosity of an extra thick cake within a compression-permeability cell was greater at the bottom than at the top of the cake. Although he did not emphasize it, side-wall friction must have been present and caused the porosity to vary.

Taylor (54) and Welch (70) recognized that side-wall friction was present in a consolidometer which is similar to a compression-permeability cell. Although these investigators differed in their conclusions as to the extent of the

side-wall friction, nevertheless, they did agree that friction was a function of the thickness-to-diameter ratio. For consolidation of soils these two authors did not consider a correction factor necessary.

Shirato (44) and Lu (31) have confirmed that side-wall friction is present in compression-permeability testing.

III. DEVELOPMENT OF THE THEORY

In order to establish a theory for side-wall friction, the forces acting at the interface of the filter cake and the wall of the compression-permeability cell must be determined.

The laws of statics, as expressed by Cauchy's (30) equations of equilibrium, were used by Biot (4), McNabb (32), McNamee (33), and Cryer (8) to study the forces existing within a mass of consolidating soil. The consolidating mass was of infinite extent, thus the effect of wall friction was not considered. The validity of using these laws of statics to describe the forces might be questioned. However, the results of their studies indicated that the use of these equations developed for equilibrium conditions were applicable.

Theories have been established for the effect of side-wall friction by Sower and Sower (47), Jenike (25), and Jaky (23). These theories were derived to determine the static pressure on the walls in storage silos and hoppers.

They too used the laws of statics as expressed by Cauchy's equation of equilibrium as:

$$\left. \begin{aligned} \frac{\partial p_z}{\partial z} + \frac{\partial \tau}{\partial y} &= \rho g \\ \frac{\partial p_y}{\partial y} + \frac{\partial \tau}{\partial z} &= 0 \end{aligned} \right\} \quad (V-1)$$

Thus from these two different approaches, of consolidating mass without friction, and side-wall friction without consolidation it is indicated that the equations of equilibrium can be utilized to describe side-wall friction in compression-permeability cell testing.

Taylor (54) in his studies of completely consolidated soil assumed that the side friction per unit of area at any height was proportional to the average vertical pressure at that height, as

$$p_y = K_o p_z \quad (V-2)$$

where K_o a physical characteristic of a given material is assumed to be constant. Sower and Sower (47) have reported K_o may have values ranging from 1.0 for soft clays to 0.4 for dense sand or gravels.

A schematic diagram of a layer filter cake within a compression-permeability cell is given in Figure V-1. The layer represented by this figure is z-distance from the lower drainage piston, D units in Diameter and dz units

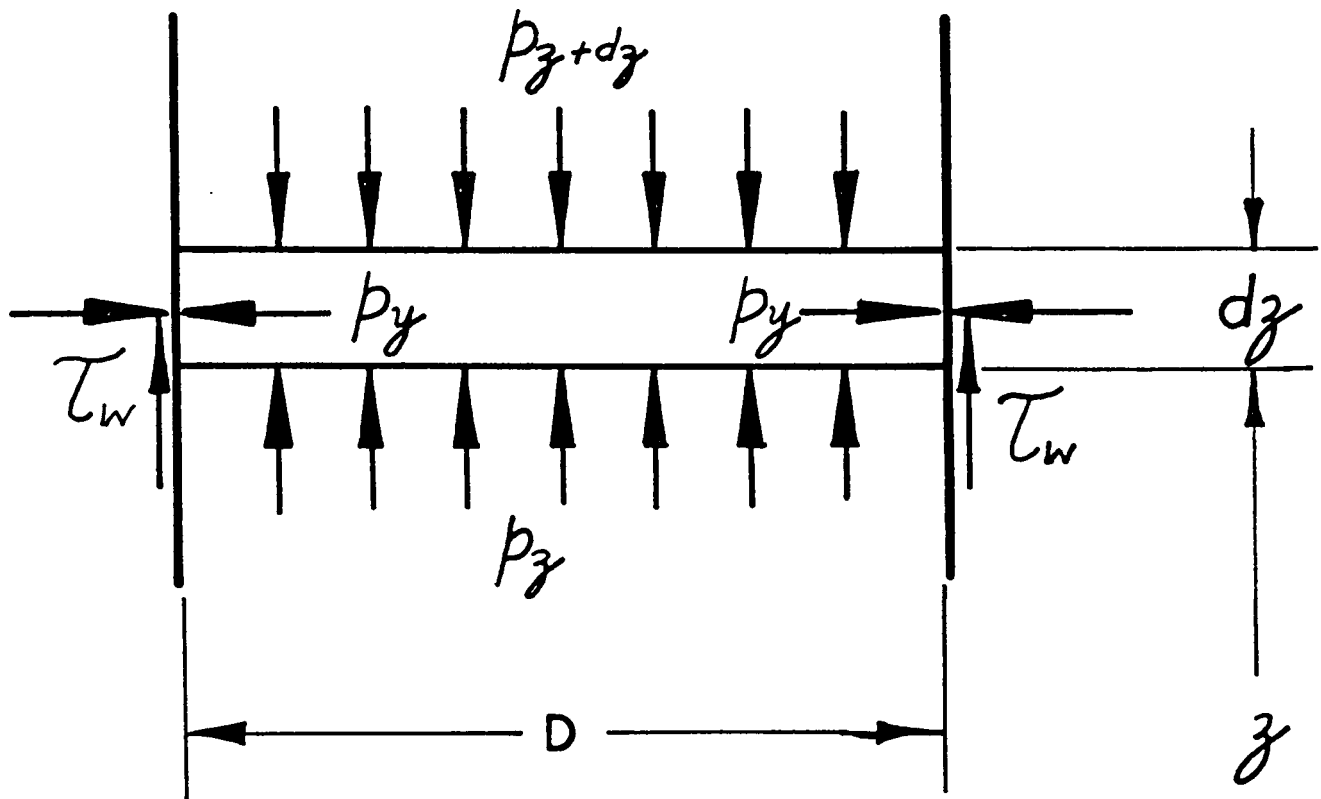


FIGURE V-1 SCHEMATIC DIAGRAM OF A LAYER
OF A FILTER CAKE

thick. The pressure applied is $p_{z+\Delta z}$ and that transmitted is p_z . The corresponding horizontal pressure developed is p_y which, at the wall surface, causes a shearing stress τ_w to be developed.

A simple force balance, assuming equilibrium, will yield

$$\frac{\pi D^2}{4} dp_z + \pi D \tau_w dz = \frac{\xi \rho}{\xi_c} \left(\frac{\pi D^2}{4} \right) dz \quad (V-3)$$

or

$$\frac{dp_z}{dz} + \frac{4}{D} \tau_w = \frac{\xi \rho}{\xi_c} \quad (V-4)$$

Then if p_z is known from empirical curves as

$$\tan \phi' = \frac{dp_z}{dz} \quad (V-5)$$

the wall frictional force becomes

$$\tau_w = \frac{D}{4} \left(\frac{\xi \rho}{\xi_c} - \tan \phi' \right) \quad (V-6)$$

By this means, a value for the coefficient of wall friction can be obtained as

$$\lambda_o = \frac{\tau_w}{p_y} = \frac{D}{4p_y} \left[\frac{\xi \rho}{\xi_c} - \tan \phi' \right] \quad (V-7)$$

Now examine more closely the state of stress with in the elementary prism. Consider the prism to be symmetric about the y -axis, also assume that the vertical pressure is uniformly distributed over the cross-sectional area as:

$$p_z = f(z) \quad (V-8)$$

Then from Cauchy's first equation of equilibrium the following is obtained:

$$\frac{\partial f(z)}{\partial z} = f'(z) = \frac{g\rho}{s_c} - \frac{\partial \tau}{\partial y} \quad (V-9)$$

or:

$$\tau = \left[\frac{g\rho}{s_c} - f'(z) \right] y + f_0(z) \quad (V-10)$$

Since $y=0$ is the symmetrical z -axis and it can be shown that $\tau=0$ along this axis, then $f_0(z)=0$ and

$$\tau = \left[\frac{g\rho}{s_c} - f'(z) \right] y \quad (V-11)$$

This means that the shearing stress, τ , is distributed linearly over the horizontal cross-section and thus at the wall will become:

$$\tau_w = \left[\frac{\rho g}{2} - f'(z) \right] \frac{D}{2} \quad (V-12)$$

Similarly the horizontal, normal stress, p_z , can be obtained from Cauchy's second equation of equilibrium as :

$$p_y = f'' \frac{y^2}{2} + g(z) \quad (V-13)$$

but, along the symmetrical axis, pure compression alone has been assumed, thus

$$g(z) = K_o p_z = K_o f(z) \quad (V-14)$$

and along the wall

$$p_y = K_o f(z) + f''(z) \frac{y^2}{2} \quad (V-15)$$

From the definition of the coefficient of wall friction, Equation (V-7), the following is obtained:

$$\lambda_o = \left(\frac{\tau}{p_y} \right)_{y=\frac{D}{2}} = \frac{\left[\frac{\rho g}{2} - f'(z) \right] \frac{D}{2}}{K_o f(z) + f''(z) \frac{D^2}{8}} \quad (V-16)$$

Upon rearrangement the following second order differential equation can be written:

$$f''(z)\frac{D^2}{8} + f'(z)\frac{D}{2\lambda_0} + f(z)K_0 = \frac{D\rho}{2\lambda_0} \quad (V-17)$$

A solution of this second order equation can be obtained by letting $\zeta = K_0 f(z) + \frac{D\rho}{2\lambda_0}$ which reduces Equation (V-17) to:

$$\zeta'' + \frac{4}{D\lambda_0}\zeta' + \frac{8K_0}{D^2}\zeta = 0 \quad (V-18)$$

The solution of this latter equation is

$$\zeta = c_1 e^{-\frac{2z\xi}{D\xi_1}} + c_2 e^{-\frac{2z\xi}{D\xi_2}} \quad (V-19)$$

where

$$\left. \begin{aligned} \xi_1 &= \frac{1}{\lambda_0} \left[1 + \sqrt{1 - 2K_0\lambda_0^2} \right] \\ \xi_2 &= \frac{1}{\lambda_0} \left[1 - \sqrt{1 - 2K_0\lambda_0^2} \right] \end{aligned} \right\} \quad (V-20)$$

or letting

$$f(z) = \frac{\zeta}{K_0} + \frac{D\rho}{2\lambda_0 K_0} \quad (V-21)$$

gives

$$f(z) = \frac{c_1}{K_0} e^{-\frac{2z\xi}{D\xi_1}} - \frac{c_2}{K_0} e^{-\frac{2z\xi}{D\xi_2}} - \frac{D\rho}{2\lambda_0 K_0} \quad (V-22)$$

Using this relationship, determine the ratio of the transmitted-to-applied force, $\frac{p_r}{p_a}$, as:

$$\frac{p_r}{p_a} = \frac{\frac{c_1}{K_0} e^{-\frac{2h\xi}{D}\xi_1} + \frac{c_2}{K_0} e^{-\frac{2h\xi}{D}\xi_2} + \frac{D\rho g}{2\lambda_0 K_0}}{\frac{c_1}{K_0} + \frac{c_2}{K_0} + \frac{D\rho g}{2\lambda_0 K_0}} \quad (V-23)$$

Upon division, this equation becomes:

$$\frac{p_r}{p_a} = e^{-\frac{2h\xi}{D}\xi_1} + \frac{c_2}{c_1} \left[e^{-\frac{2h\xi}{D}\xi_2} - e^{-\frac{2h\xi}{D}\xi_1} \right] + \left(\frac{c_2}{c_1} \right)^2 \left[\dots \right] + \dots$$

$$+ \frac{\frac{D\rho g}{2K_0} \left\{ 1 - e^{-\frac{2h\xi}{D}\xi_1} - \frac{c_2}{c_1} \left[e^{-\frac{2h\xi}{D}\xi_2} - e^{-\frac{2h\xi}{D}\xi_1} \right] + \dots \right\}}{\frac{c_1}{K_0} + \frac{c_2}{K_0} + \frac{D\rho g}{2K_0\lambda_0}} \quad (V-24)$$

Since the applied force is considerably larger in comparison to the force developed by the action of gravity on the density of the cake, the effect of the cake density, etc., can be neglected. Equation (V-24) reduces to :

$$\frac{p_r}{p_a} = e^{-\frac{2h\xi}{D}\xi_1} + \frac{c_2}{c_1 + c_2} \left[e^{-\frac{2h\xi}{D}\xi_2} + e^{-\frac{2h\xi}{D}\xi_1} \right] \quad (V-25)$$

Equation (V-25) can be converted to

$$\frac{p_r}{p_a} = e^{-\frac{2h\xi}{D\lambda_0}} \left\{ e^{-\frac{2h}{D}\sqrt{1-2K_0\lambda_0^2}\xi} + \frac{2c_2 \sinh \left[\frac{2h}{D\lambda_0}\sqrt{1-2K_0\lambda_0^2}\xi \right]}{(c_1 + c_2)} \right\} \quad (V-26)$$

To complete the solution, the values of C_1 and C_2 need to be evaluated. It has been fairly well established by Jamieson (24) and Jaky (23) as well as others, that the vertical pressure transmitted to the bottom approaches a limiting value as the height of the cake is increased, that is as the pressure is increased. This, in effect, gives one of two limiting values which can be used to evaluate the constants. As the cake thickness increases to a large value, say as $\frac{h}{D} \rightarrow 0$, then the ratio of transmitted-to-applied force approaches a finite limit; therefore,

$$\therefore C_2 = 0 \quad (V-27)$$

and thus

$$\frac{p_T}{p_A} = e^{-\frac{2h}{D\lambda} (1 + \sqrt{1 - 2K_0 \lambda_0})} \quad (V-28)$$

III. CORRECTION FACTORS FOR POROSITIES AND SPECIFIC CAKE RESISTANCES

Based upon published porosity versus pressure data, Tiller (60) has suggested that in the range up to 100 psi, the porosity of moderately compressible solids can be represented by the power function

$$\left. \begin{aligned} \epsilon_x &= \epsilon_0 p_s^{-\lambda} & p_s > p_1 \\ \epsilon_x &= \epsilon_i & p_s \leq p_1 \end{aligned} \right\} \quad (V-29)$$

No correction for wall effect were used in calculating ϵ_0 and λ from those published porosity-pressure data. Correction factors which may be applied to experimental porosity-pressure data will now be developed. It has been shown, in Equation (V-28) that the solids pressure is a function of the cake thickness and the applied pressure. Furthermore, the average porosity is defined as :

$$\epsilon_w = \frac{1}{L} \int_0^L \epsilon_z dz \quad (V-30)$$

Then the average porosity within such a cell can be obtained by the substitution of Equation (V-28) into Equation (V-29) and using this relationship for Equation (V-30); integration of this substituted expression between the limits of 0 and L will give, provided $p_s > p_1$:

$$\epsilon_w = \frac{\epsilon_0 p_s^{-\lambda} D \lambda_0}{2 \lambda L (1 + \sqrt{1 - 2K_0 \lambda_0^2})} \left[e^{\frac{2\lambda L}{D\lambda_0} (1 + \sqrt{1 - 2K_0 \lambda_0^2})} - 1 \right] \quad (V-31)$$

If the solids pressure were constant throughout the cake, as had been assumed in the past experiments, the porosity would be:

$$\epsilon_{\text{uniform}} = \epsilon_0 p_s^{-\lambda} \quad (V-32)$$

Thus, the correction factor would be:

$$\epsilon_{\text{uniform}} = \epsilon_w \left\{ \frac{\frac{2\lambda L}{D\lambda_0} \left[1 + \sqrt{1 - 2K_0\lambda_0^2} \right]}{\left[e^{\frac{2\lambda L}{D\lambda_0} \left(1 + \sqrt{1 - 2K_0\lambda_0^2} \right)} - 1 \right]} \right\} \quad (\text{V-33})$$

In a similar manner, the specific cake resistance may be corrected for the wall frictional effect. Tiller (60) represented the equilibrium point specific cake resistance of a moderately compressible solid as a power function of the solids pressure, in the range up to 100 psi, as:

$$\begin{aligned} \alpha_x &= \alpha_0 p_s^n & p_s > p_1 \\ \alpha_x &= \alpha_1 & p_s \leq p_1 \end{aligned} \quad (\text{V-34})$$

The average specific cake resistance has been defined as:

$$\alpha = \frac{1}{L} \int_0^L \alpha_x \, dz \quad (\text{V-35})$$

Then, in an identical procedure to that outlined for porosity, the correction factor for specific cake resistance within a compression-permeability cell would be, provided $p_s > p_1$

$$\alpha_{\text{uniform}} = \alpha_w \left\{ \frac{\frac{2nL}{D\lambda_0} \left[1 + \sqrt{1 - 2K_0\lambda_0^2} \right]}{\left[-e^{-\frac{2nL}{D} \left(1 - \sqrt{1 - 2K_0\lambda_0^2} \right)} \right]} \right\} \quad (\text{V-36})$$

In terms of the ratio of transmitted-to-applied pressures, Equations (V-33) and (V-36) can be transformed as

$$\epsilon_{\text{uniform}} = \epsilon_{aw} \left\{ \frac{\lambda \ln \frac{p_A}{p_T}}{\left(\frac{p_A}{p_T}\right)^\lambda - 1} \right\} \quad (\text{V-33a})$$

$$\alpha_{\text{uniform}} = \alpha_{aw} \left\{ \frac{n \ln \frac{p_A}{p_T}}{1 - \left(\frac{p_A}{p_T}\right)^n} \right\} \quad (\text{V-36a})$$

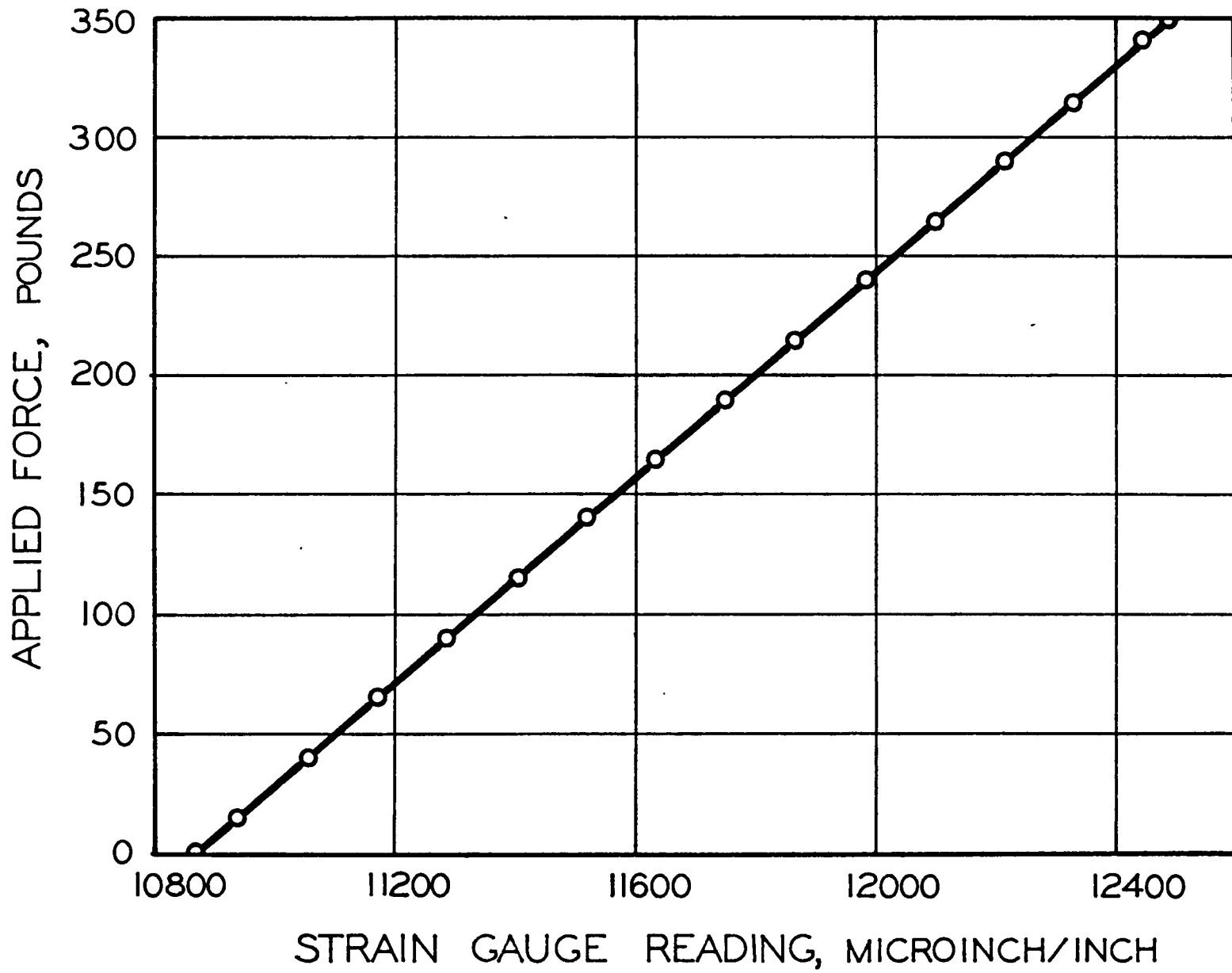
V. TESTING AND RESULTS

The magnitude of side-wall friction was determined using a modified compression-permeability cell. The cell consisted of a cylinder with an upper piston and a lower, free-floating base. The upper piston was made of mild, type 1040 steel which was given an 0.008 inch hard chromium plating after machining and then ground to 2.0225 inches o.d. Two different types of cylinders were used during this study. Originally a metallic cylinder was made of 316 type stainless steel with a bore measuring 2.0235 inches i.d. A "Teflon" lined, ordinary steel cylinder having the same internal diameter as the stainless steel cylinder was used for the latter tests. The lower free-floating, wall-effect filter base piston

was manufactured to have the same external diameter as the upper piston. The filter cake, which had been produced in the cylinder using a special caking piston, was compressed between the two movable pistons. The mechanical load applied to the top of the filter cake was the total of the weight of the compression piston plus cast steel weights as used in the experiments. The mechanical force transmitted through the cake was impressed on the wall-effect filter base piston, which was supported by an SR-4 strain gauge load transducer. The amount of force so received by the transducer was determined using an SR-4 strain gauge analyzer. Further details of the equipment may be found in Chapter VII.

As a part of each experiment and prior to the development of any cake within the compression-permeability cell cylinder, a calibration run was made. That run was performed for two purposes: first, to establish a calibration curve which related the SR-4 strain gauge readings, in microinches per inch, to the applied force, in pounds; and second, to determine the presence of any abnormal amounts of frictional drag on the piston-cylinder combination. Presence of the latter was indicated by a radical deviation from the established strain gauge reading-vs-force relationship. The results of a typical calibration run are shown in Figure V-2. In that figure the strain gauge reading is plotted versus

FIGURE V-2 TYPICAL CALIBRATION RUN



the force. Several factors may be illustrated by referring to this figure. Of primary importance is the existence of a straight line relationship between the gauge readings and the force. Any radical departure from this linear relationship indicated the presence of abnormal friction; and almost invariably the presence of some foreign substance on the cylinder or piston was detected.

Utilizing the experimental apparatus, side-wall friction measurements were made using three typical filter cake materials, namely super cel, solka floc, and talc. After the calibration procedure had been finished, a filter cake was produced in situ using the procedure described in Chapter VII. The appropriate mechanical load was applied via the compression piston to the top of the filter cakes. The mechanical force transmitted through the filter cake was measured using the load transducer and analyzer. After that measurement had been taken for a given applied load, an increment of load was added and the measurement repeated until the final load was reached.

The results of the experiments indicated that side-wall friction was present in both conventional and "Teflon" lined cylinders. The effect of this wall friction can be seen from a plot of the transmitted versus applied force. Typical of these plots are those for a $3/4$, $1\frac{1}{2}$, and 3 inch cakes

of super cel, as given in Figure V-3. A straight line intercepting the origin can be drawn through the experimental points. The significance of these plots is as follows: first, the straight line relationship shows that the transmitted force is a linear function of the applied force; second, the fact that the straight line can be drawn through the origin, indicates the absence of any abnormal frictional effects during the tests. The line is of the form

$$p_t = \text{slope} (p_s) \quad (V-37)$$

The slopes for all lines were less than unity; thus, it can be concluded that a diminution of force occurred, or in other words side-wall friction was detectable. Finally, slopes for the thicker cakes were less than that for thinner ones indicating that side-wall friction increased with cake thickness.

The ratio of the transmitted force divided by the applied force has been shown by Equation (V-28) to be a semi-logarithmic function of the thickness-to-diameter ratio, L/D . The pressure ratio, p_t/p_a , can be determined from plots like those given in Figure V-3. In order to determine the correctness of Equation (V-28), the logarithmic pressure ratios may be plotted as a function of the thickness-to-diameter ratios

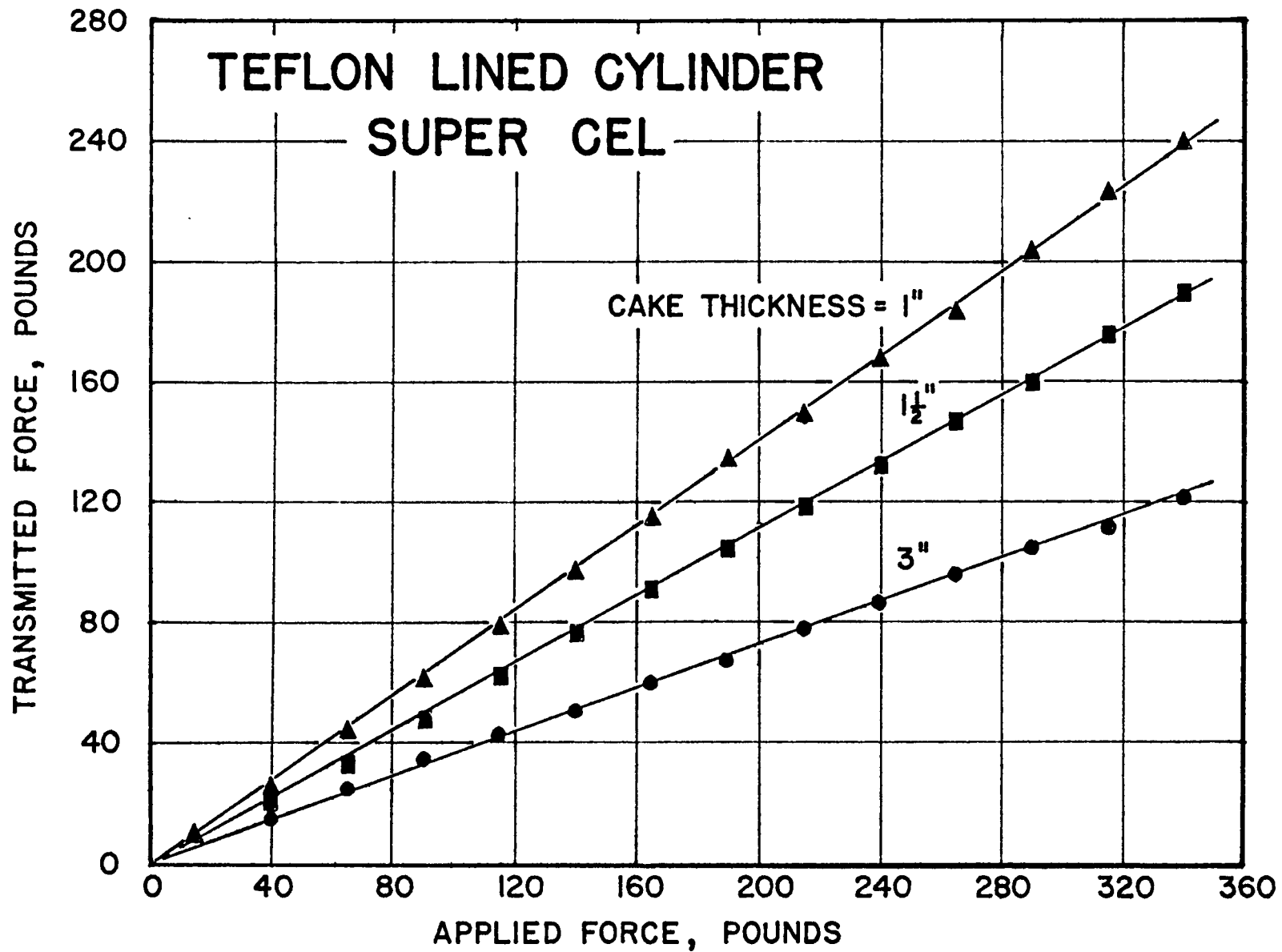


FIGURE V-3

as has been done in Figure V-4. The slopes of those curves represent values of $\frac{1}{\lambda_0} \left(1 - \sqrt{1 - 2K_0 \lambda_0^2} \right)$ for the repective filter cake substances and cylinder lining materials. Values of $\frac{1}{\lambda_0} \left(1 - \sqrt{1 - 2K_0 \lambda_0^2} \right)$ as experimentally determined for super cel, solka floc, and talc are given in Table I.

Earlier runs were made with the stainless steel cylinder and filter cakes of super cel. The results of these runs are also shown in Figure V-4. From this figure it is quite evident that the material of the cylinder lining also effects the slope of the semi-logarithmic plot and hence the value of $\frac{1}{\lambda_0} \left(1 - \sqrt{1 - 2K_0 \lambda_0^2} \right)$. This would be expected since the coefficient of wall friction, λ_0 , would not be the same for the cake-to-steel interface as it would be for the cake-to-"Teflon" interface.

Using the above method, values for K_0 could be calculated, provided the coefficient of wall friction was known. Conversely, the coefficient of wall friction could be determined experimentally for a given compression-permeability cell cylinder lining, if a value for K_0 were known.

The values for $\frac{1}{\lambda} \left(1 - \sqrt{1 - 2K_0 \lambda^2} \right)$ as found above, together with the pressure exponents for the porosity and the specific cake resistance as reported by Tiller (60), permits calculation of correction factors for porosity and cake resistance as given by Equations (V-33) and (V-36),

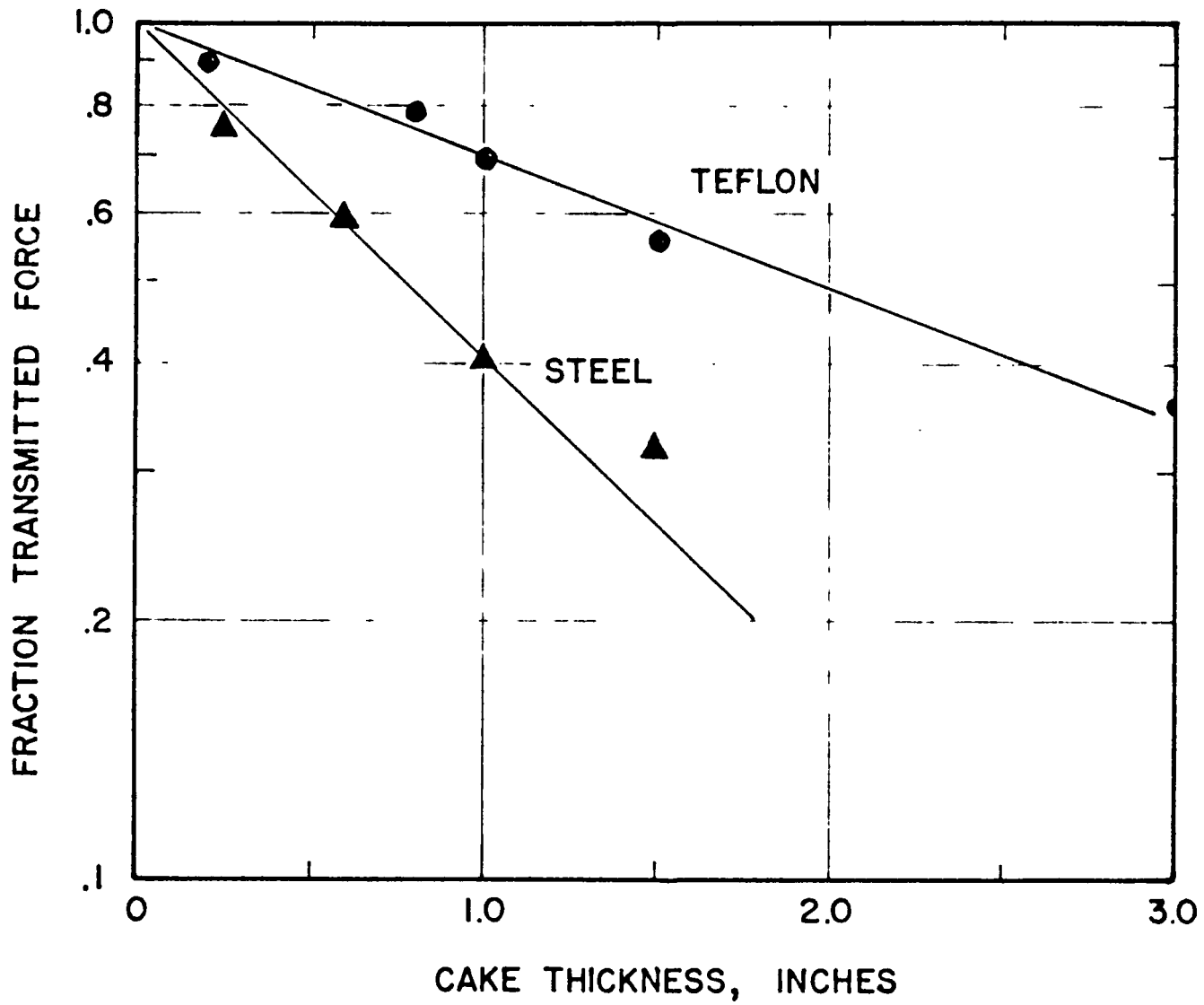


FIGURE V-4 COMPARISON OF STEEL AND TEFLON LINED CYLINDERS

TABLE I

CORRECTION FACTORS FOR SIDE-WALL FRICTION

<u>Substance</u>	$\frac{1}{\lambda_0} \left(1 - \sqrt{1 - 2K_0 \lambda_0} \right)$ for "Teflon" Cylinder	<u>Pressure Exponents</u>		<u>Correction Factors (1" cake)</u>	
		<u>n</u>	<u>λ</u>	<u>Porosity</u>	<u>Resistance</u>
SUPER CEL	0.360	0.137	0.0104	0.998	1.022
SOLKA FLOC	0.284	2.076	0.0532	0.992	1.291
TALC	0.216	0.506	0.054	0.989	1.112

respectively. These corrections are also reported in Table 1. Although correction for porosity amounts to only one to two percent, the correction factor for cake resistance varies between two and twenty-nine per cent. It is evident that this variation in cake resistance warrants further investigation.

CHAPTER VI

SPECIFIC CAKE RESISTANCE VERSUS TIME

The average filtration resistance is generally defined by the Ruth equation. This equation is a modification of the Sperry equation and mathematically results from equating the flow rate through a filter cake to the pressure driving potential divided by a resistance term. Ruth's equation (38) can be represented in the form:*

$$q_1 = \frac{s_c \rho}{\mu (\alpha_R \omega + R_m)} \quad (\text{VI-1})$$

The resistance to flow is shown in this equation to be separated into parts. The first is the cake resistance which equals the product of a resistance coefficient, α_R , and the mass of the porous solid material making up the filter cake. The second part of this resistance to flow is the resistance of the supporting medium, R_m . Equation (VI-1) is an empirical differential equation in which α_R is primarily a function of the pressure drop across the cake.

* In this equation, q is assumed constant. Tiller and Shirato (64) have derived a new definition for the cake filtration resistance in terms of a factor J which depends upon slurry concentration as well as applied pressure.

Whereas the average filtration, α_R , has been defined by Equation (VI-1) the local filtration resistance, α_x , is defined by Tiller (59) as

$$g_c \frac{dp_x}{dw_x} = -g_c \frac{dp_s}{dw_x} = \mu \alpha_x q_x \quad (\text{VI-2})$$

The relationship between α_R and α_x has been shown, in Equation (III-57) to be

$$\alpha_R = \frac{p - p_1}{\int_0^{p-p_1} \frac{dp_s}{\alpha_x}} \quad (\text{VI-3})$$

On the basis of previous experimental data, it has been assumed that α_x has been a function of the solids pressure p_s alone. In turn, the solids pressure is assumed to be related to the hydraulic pressure, p_x , as shown in Equation (III-9).

The values of α_x previously reported in the literature were obtained from a compression-permeability cell or indirectly calculated from average values (59). These values for α_x were used to calculate average α_R based upon the fundamental postulate that α_x has identical values in a cake and a permeability cell when $p - p_x$ in the cake equals the solids pressure in the cell. For moderately compressible materials up to 100 p.s.i., Tiller (60) and Shirato and Okamura (42) have indicated that the point filtration resistance

can be related empirically to the compressive pressure by:

$$\left. \begin{aligned} \alpha_x &= \alpha_o p_s^n & p_s > p_i \\ \alpha_x &= \alpha_i & p_s \leq p_i \end{aligned} \right\} \quad (\text{VI-4}).$$

where it has been assumed that α_x approached a limiting value α_i at some low pressure p_i . Lu (31) has recently measured the filtration resistance in the low pressure region. The results of his experiments agreed fairly well with Tiller's postulate, that α_x becomes constant and equal to α_i in the lower pressure region.

I. EXPERIMENTAL STUDIES OF SPECIFIC CAKE RESISTANCE

During an earlier study of the effect time and pressure has on porosity, few values for cake resistance were obtained. As reported in Chapter IV, an analysis of the porosity data of the earlier study indicated that equilibrium had not been attained during the study. Thus, it became necessary to make an additional study of the effect time has on specific cake resistance as well as porosity.

For this second series of experiments, the modified compression-permeability cell, as described in Chapter VII, was used. Filter cakes of highly compressible Solka Floc (alpha cellulose) were made in situ using the special caking piston. A total of six runs were made during this series.

The runs consisted of : preparing the filter cake; applying a single, constant loading of either 25.3, 50.3, 75.3, or 100.3 pounds force to the compression piston; and obtaining and recording periodic readings of cake height, elapsed time and filtrate volume. These runs lasted three hours to several days. Additional details of the experimental procedure used are given in Chapter VII.

The data obtained during the experiments were used to calculate the average porosity and specific cake resistance according to the following formulae

$$\epsilon = 1 - \frac{W}{\rho_s L A} \quad (\text{VI-5})$$

$$\alpha = \frac{\epsilon_c \Delta P_h A}{\mu \left(\frac{\Delta v}{\Delta \theta} \right) W} \quad (\text{VI-6})$$

The results of these calculations are listed in Appendix D.

II. RESULTS AND DISCUSSIONS

The calculated values obtained for the specific cake resistance are plotted in Figure VI-1. This figure presents the values of specific cake resistance as a function of time, in seconds, plotted on log-log scales. Since the previously reported values of cake resistance were obtained during studies

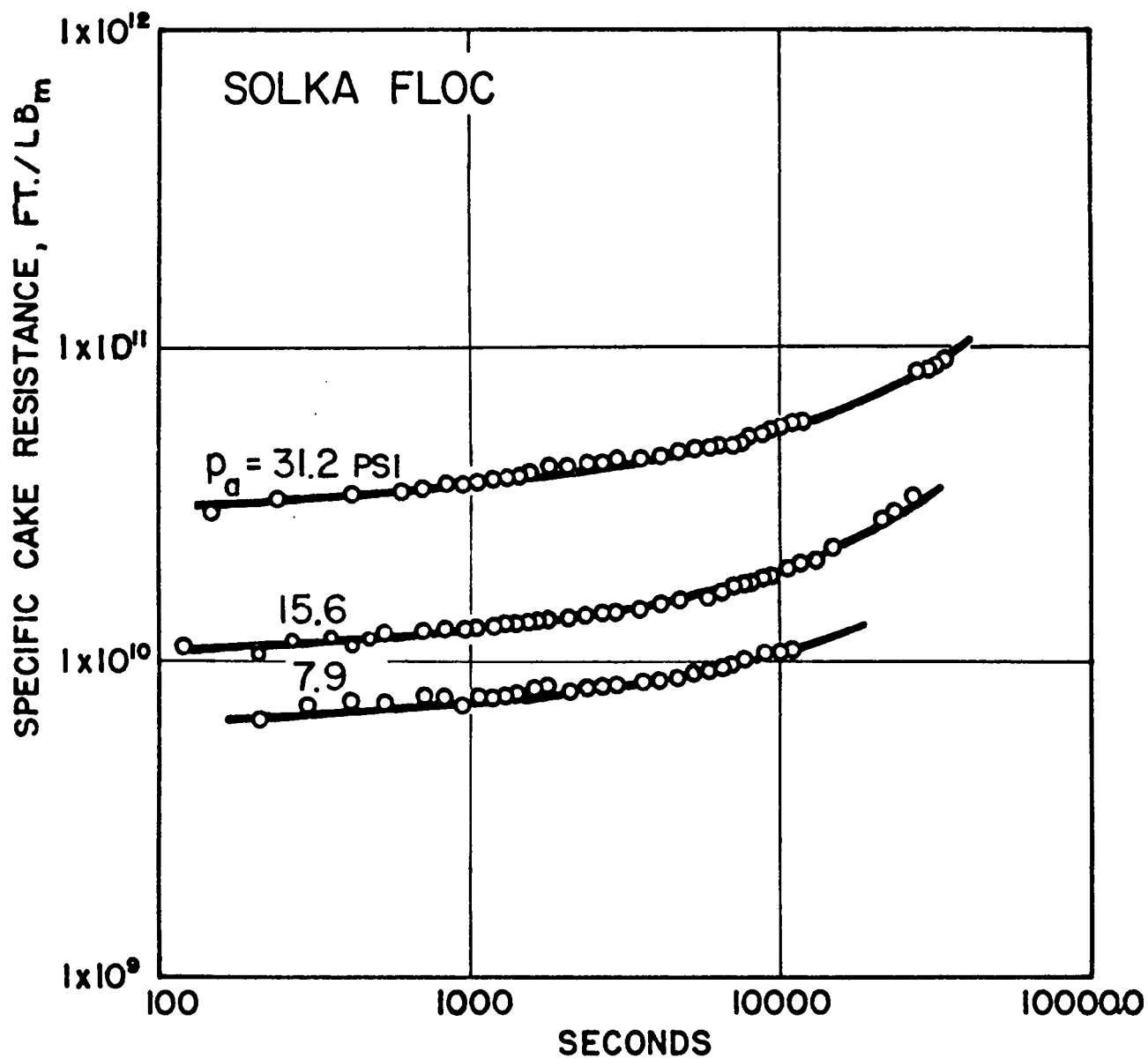


FIGURE VI-1 SPECIFIC CAKE RESISTANCE VERSUS TIME

varying only the applied pressure, a direct comparison of the present experimental values to those previously reported is not possible. However, if it could be assumed that the literature values were obtained after the compression-permeability cell had been loaded for 10 minutes, then the values of the present investigation at the end of 10 minutes might be compared to those of the literature. (This assumption would require an additional investigation.) Such a plot of specific cake resistance versus pressure is presented as a log-log plot in Figure VI-2. Referring to the latter figure it will be noted that these results agree fairly well with the postulated power function relation of Tiller's (60).

Three conclusions can be made from this study of the resistance of a compression-permeability cell cake. First, by referring to Figure VI-1 it is evident that under constant applied pressure, the specific cake resistance, α , is a function of time. Moreover, the specific cake resistance at a given time is a function of the applied compressive pressure as shown in Figure VI-2. Thus it might appear, for a compression-permeability cell, that the specific cake resistance is a function of both time and solids compressive pressure.

With regards to the function of time, as shown in Figure VI-1, it would appear that the values for cake resistance must approach a low, but finite value, greater than zero.

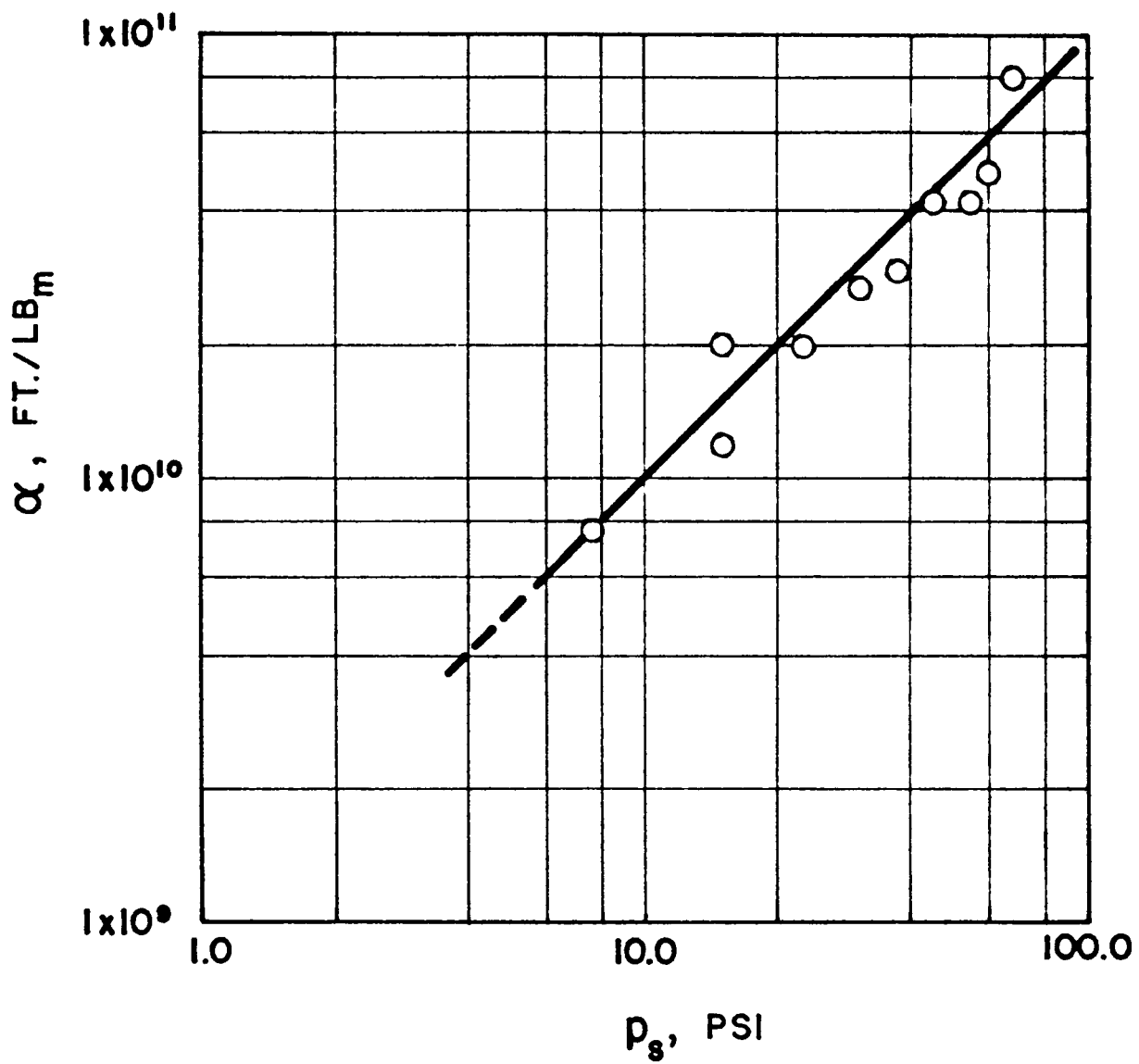


FIGURE 1- S GIPIN AND DISTANCE FROM PRESSURE

Certain unpublished data by Lu indicate this decrease in cake resistance at short times is valid. Furthermore, according to Ruth's equation the cake resistance value must not approach zero, because the rate of filtrate flow, q , would approach an exceedingly large value as α_x approached zero, which is not logical since

$$\lim_{\alpha_x \rightarrow 0} \{q\} = \lim_{\alpha_x \rightarrow 0} \left\{ \frac{\epsilon_c \frac{d\sigma_x}{dx}}{\mu \alpha_x w} \right\} \rightarrow \infty \quad (\text{VI-7})$$

Finally, it would appear that the specific cake resistance would increase without limit as time increases. Evidence of this time effect might be postulated from an examination of the decrease in permeability of sediments deposited in recent geological times. Since it has been established that permeability and cake resistance are reciprocally related, this decrease in permeability of sediment would indicate a corresponding increase in the resistance of sediments. Thus an increase in resistance with time is definitely indicated by the above analogy.

It is evident from the results of this study that time effects the specific cake resistance of a compression-permeability cell cake. Whether this phenomena exists in a filtration cake will require additional studies designed to separate this effect from others in a filtration process.

Furthermore, even if this phenomenon did exist and the values for the specific cake resistance were known as functions of time and pressure, it would still be necessary to determine the path by which the specific cake resistance were to progress from α_x at a given pressure and time to a new pressure p_s and time θ' . Thus, as with porosity, there exist two time scales, θ and θ' . A distinction between these two time scales can be made clearer by referring to Figure VI-3.

In this figure, α_x is presented as an arithmetic plot versus θ . Two isobaric values of α_x are presented by the lines labeled $p_{s,\theta+\Delta\theta}$ and $p_{s,\theta}$. It may be assumed that the filtration process has been continuing for sufficient length of time so that the value of α_x is $\alpha_{x,\theta}$. The corresponding pressure is $p_{s,\theta}$. In an increment of time later the solids compressive pressure, $p_{s,\theta}$, has increased to $p_{s,\theta+\Delta\theta}$. The instantaneous value of the cake resistance on this new isobaric line is related to the corresponding value θ' , as shown be the coordinates of the intersection of the upper isobar and the previous value of α_x . During the subsequent interval of time $\Delta\theta$, the value of α_x rises along the upper isobaric line to the corresponding intersection of $\theta'+\Delta\theta$, and thus gives rise to a new value for α_x , namely $\alpha_{x,\theta'+\Delta\theta}$. Similarly, the values for other portions of the cake will be adjusted in terms of the corresponding

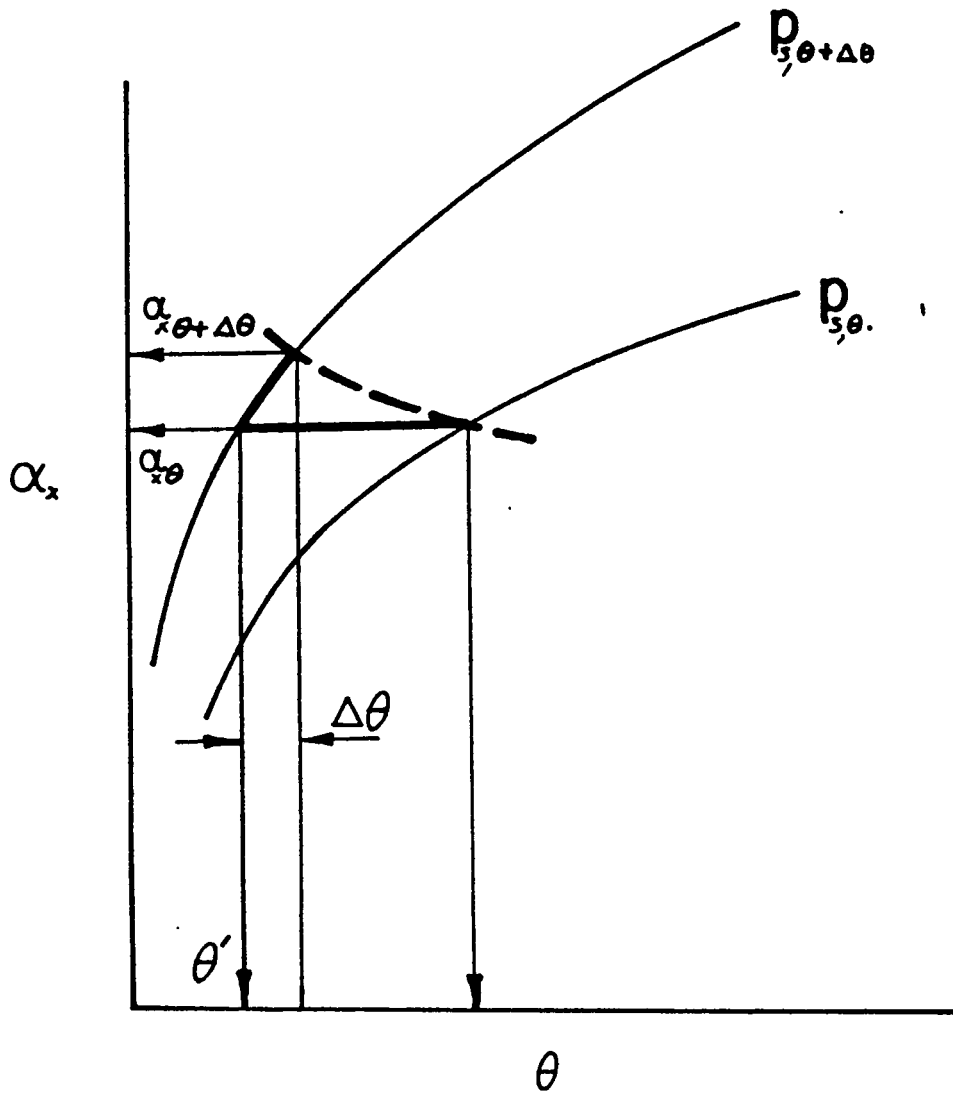


FIGURE VI-5, VARIATION OF α WITH TIME
AND PRESSURE

equivalent values for θ 's.

The exact process whereby the value of α_c progresses from one solids compressive pressure and time to a new time and pressure will have to be established during an actual filtration process. Any conclusions based solely on compression-permeability cell results would have to be modified because the two time scales θ and θ' are equal for the compression-permeability cell.

CHAPTER VII

EQUIPMENT AND PROCEDURE

An experimental study was made to determine the actual behavior of a filter cake in a compression-permeability cell. These experiments measured the variation in porosity, specific cake resistance, and side-wall friction with time and under various pressure loadings. The cake materials, the equipment, and the testing procedure used for these experiments are described in this chapter.

I. MATERIALS

The three materials tested during this work were Solka Flocc, Super Cel, and Talc C. These materials are described as follows: (1) Solka Flocc, a highly compressible alpha cellulose made by Brown and Company; (2) Super-Cel, a fine grade of diatomaceous earth refined by Johns-Mansville and Company; and (3) Talc, a finely powdered, hydrated magnesium silicate prepared by Millwhite. The physical properties of these materials are presented in Table II. Since it was thought that these materials might vary slightly from purchased batch to batch, sufficient quantities of a single batch of each of these substances was set aside for these tests.

TABLE II

PHYSICAL PROPERTIES OF THE MATERIALS

	<u>TALC</u>	<u>SUPER-CEL</u>	<u>SOLKA FLOC</u>
Generic Name	Magnesium Silicate	Diatomaceous Earth	α -Cellulose
Density	2.67	1.997	1.535
Average Particle size, microns	2 - 3	2 - 3	17
Moisture Content	1%	1%	5% max.

Pure distilled water was used for all experiments, whether in the preparation of the slurries or in performing the permeability tests.

II. EQUIPMENT

Compression-permeability Cell

The standard compression-permeability cell, as described by Grace, (11), Kottwitz (28), and Ruth (37), was modified for this study. These modifications consisted of a caking piston, a wall effect piston base, and a different type of cylinder lining.

Prior to this study, it had been the experimental procedure to place a wet cake or pour a thickened slurry of the test material into the cell. A saturated cake was then produced in the bottom of the cell by applying a slight vacuum of 1 inch of mercury to the drainage area. By this procedure, it was entirely possible to introduce uneven porosity distribution into the filter cake prior to compression. To prevent this, a caking piston was designed. This piston was a separate device which was used for preparing an uniform filter cake, in situ, from a well mixed slurry. This caking piston is shown in Figure VII-1. Prefilt slurry was introduced into the piston by means of the left hand stainless steel tubing. The slurry was given a swirling motion by the crook in this tubing at the bottom of the piston.

CAKING PISTON

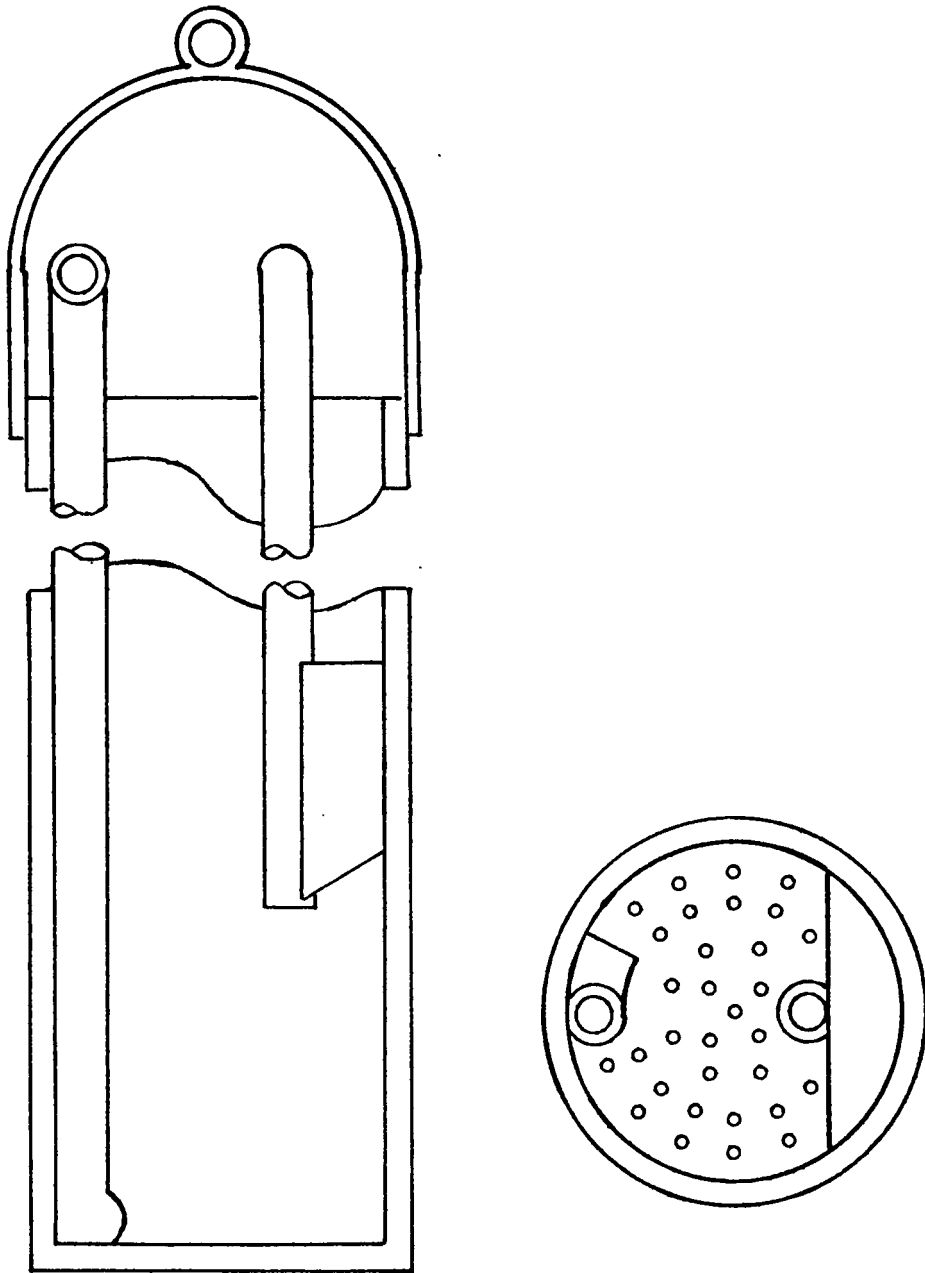


FIGURE VII-1

The circulating slurry then overflowed the overflow wiper and returned to the prefilter slurry storage vessel by means of the right hand tubing. The portion of this circulating slurry used to form the filter cake passed through a series of 1/16 inch holes in the bottom of the caking piston.

When a cake of the desired thickness had been produced, the prefilter circulation was stopped and the caking piston gently lowered to rest lightly on the filtered cake. The excess slurry standing in the caking piston was then removed by suction.

In order to determine whether the force exerted on the filter cake was transmitted, undiminished, through the filter cake to the surface of the filter septum, a wall-effect filter base piston was used. Previously, the lower drainage base had been an integral part of the cell proper. By the use of the wall effect filter base piston and an SR-4 strain gauge transducer, it was possible to measure the force transmitted through the cake independent of any force transmitted to the wall. It was by means of the above described change in the design of the compression-permeability cell that the presence and measurement of side wall friction was possible. The mechanical design of this piston is shown in Figure VII-2. The piston was made of mild steel which was given an 0.008 inch hard chromium plating and then ground to 2.0225

WALL EFFECT FILTER BASE

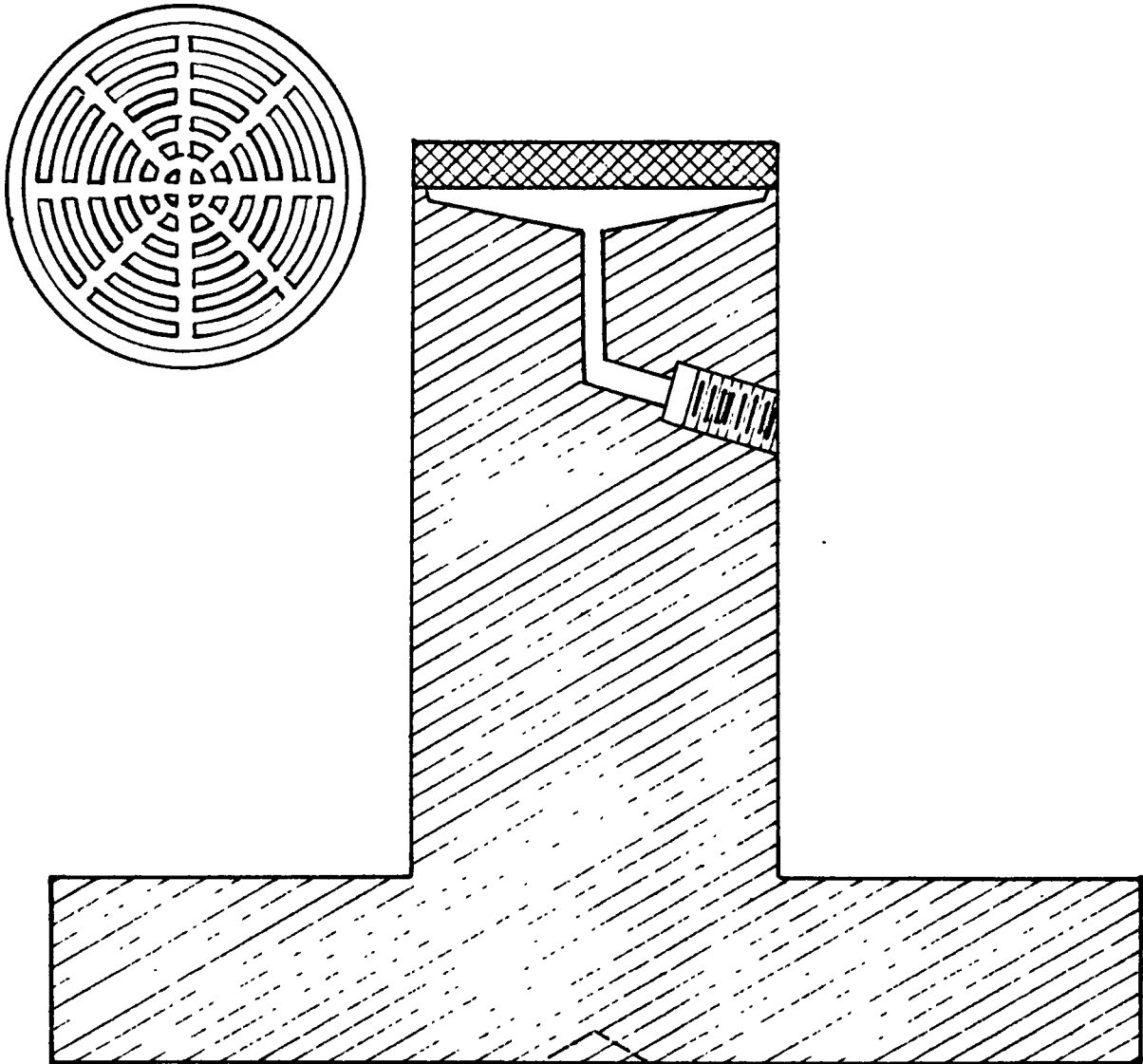


FIGURE VII-2 FREE-FLOATING PISTON

inches o.d. The porous drainage disk was made of grade C porosity stainless steel porous metal obtained from the Micro-Metallic Corporation.

The usual compression-permeability cell cylinder is made of 316 type stainless steel or similar metal. For the early part of the study, a metallic cylinder was made of stainless steel with a bore measuring 2.0235 inches i.d. To fit within this cylinder and to permit the compression of the cake, a compression piston was made of mild steel tubing which was given a 0.008 inches of hard chromium plating and was then ground to 2.0225 inches o.d. See Figure VII-3 for further details of this piston and steel cylinder. Preliminary tests with the stainless steel cylinder indicated that a appreciable amount of friction existed between the compression-permeability cell cake and the wall of the cylinder. It was thought that this friction would be greatly diminished by the use of a cylinder lined with a material having a lower coefficient of friction. Thus, a "Teflon" lined cylinder was manufactured to have the same internal diameter as the stainless steel cylinder. The remaining tests were made with this "Teflon" lined cylinder.

Three additional pieces of equipment were used in the testing of the filter cakes. A supporting framework was built to support the cylinder and lower wall-effect piston

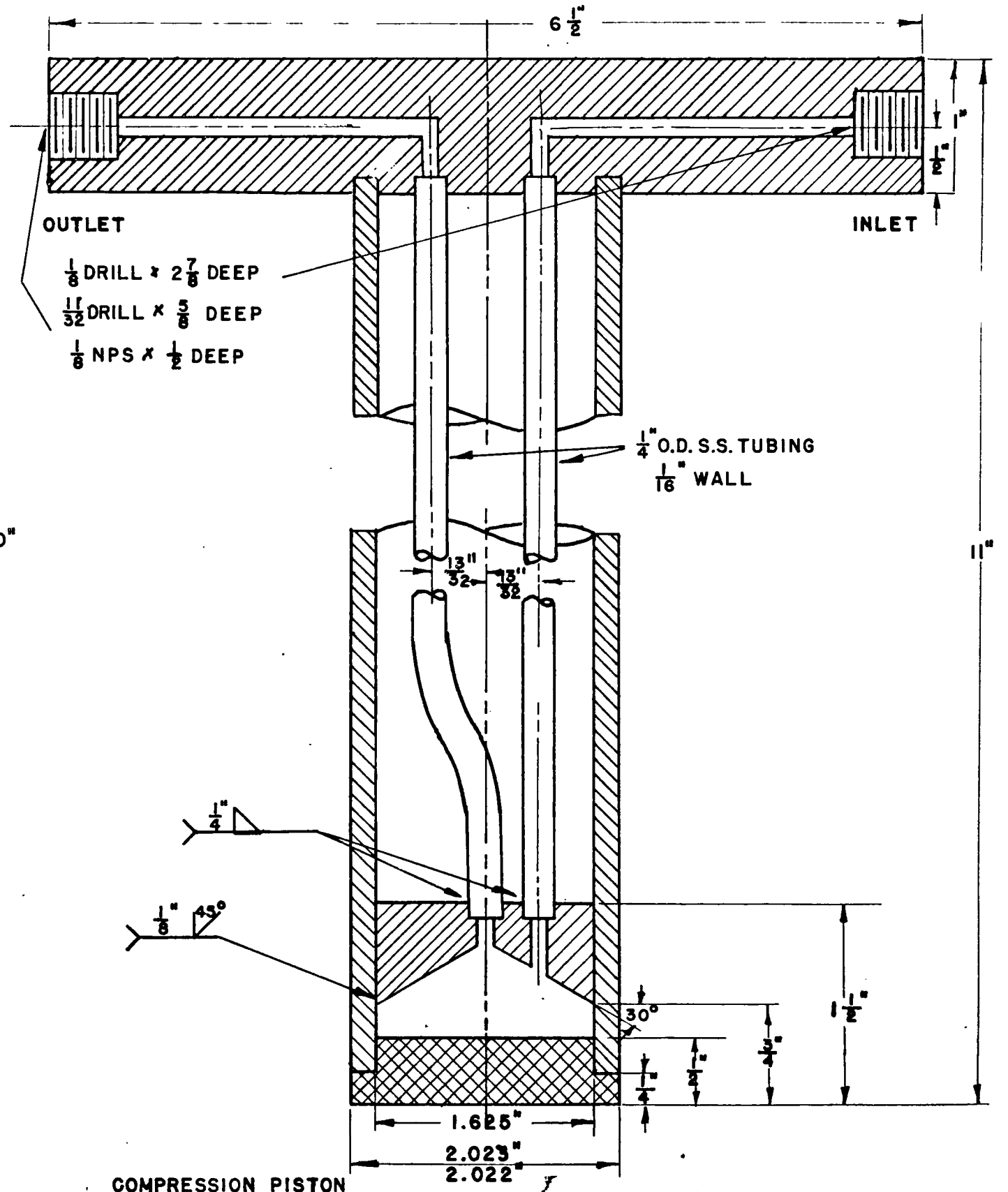
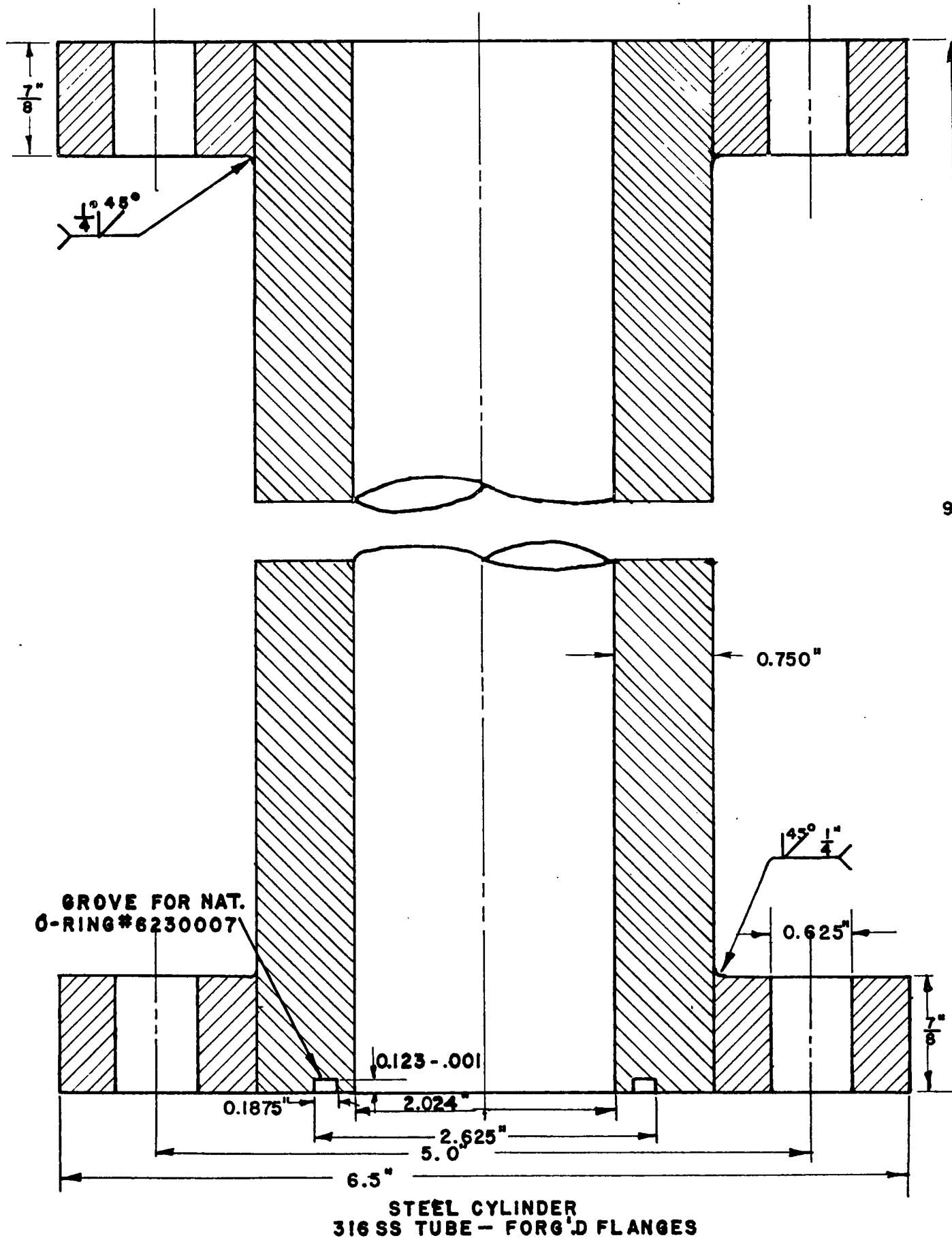


FIGURE VII-3

COMPRESSION-PERMEABILITY CELL

CYLINDER & PISTON

SCALE - FULL

independently of each other. During the permeability testing, a Marionette bottle was used to supply a constant head source of distilled water. These two items are shown in Figure VII-4. During the preparation of the filter cake, a pump and a slurry mixing tank were used with the caking piston. These items may be seen in Figure VII-5.

Measuring Equipment

During each compression-permeability cell run, cake thickness, transmitted force, and volume of filtrate were measured by the use of several instruments. These devices were: calipers, micrometers, force transducers, burettes, dial indicators, strain gauge analyzer, and a movie camera.

The thickness of the filter cake inside the compression-permeability cell was measured in the following manner. First, the final cake thickness was determined by measuring the height of the piston above the upper flange when the cake had reached its final compressed thickness and subtracting from this reading the initial height of the piston. This latter height was determined before the filter cake was made inside the cylinder. These measurements were obtained using inside calipers and a micrometer. Secondly, the intermediate cake thicknesses were determined by noting the changes in cake height using a Federal Dial Indicator

TEST CELL SYSTEM

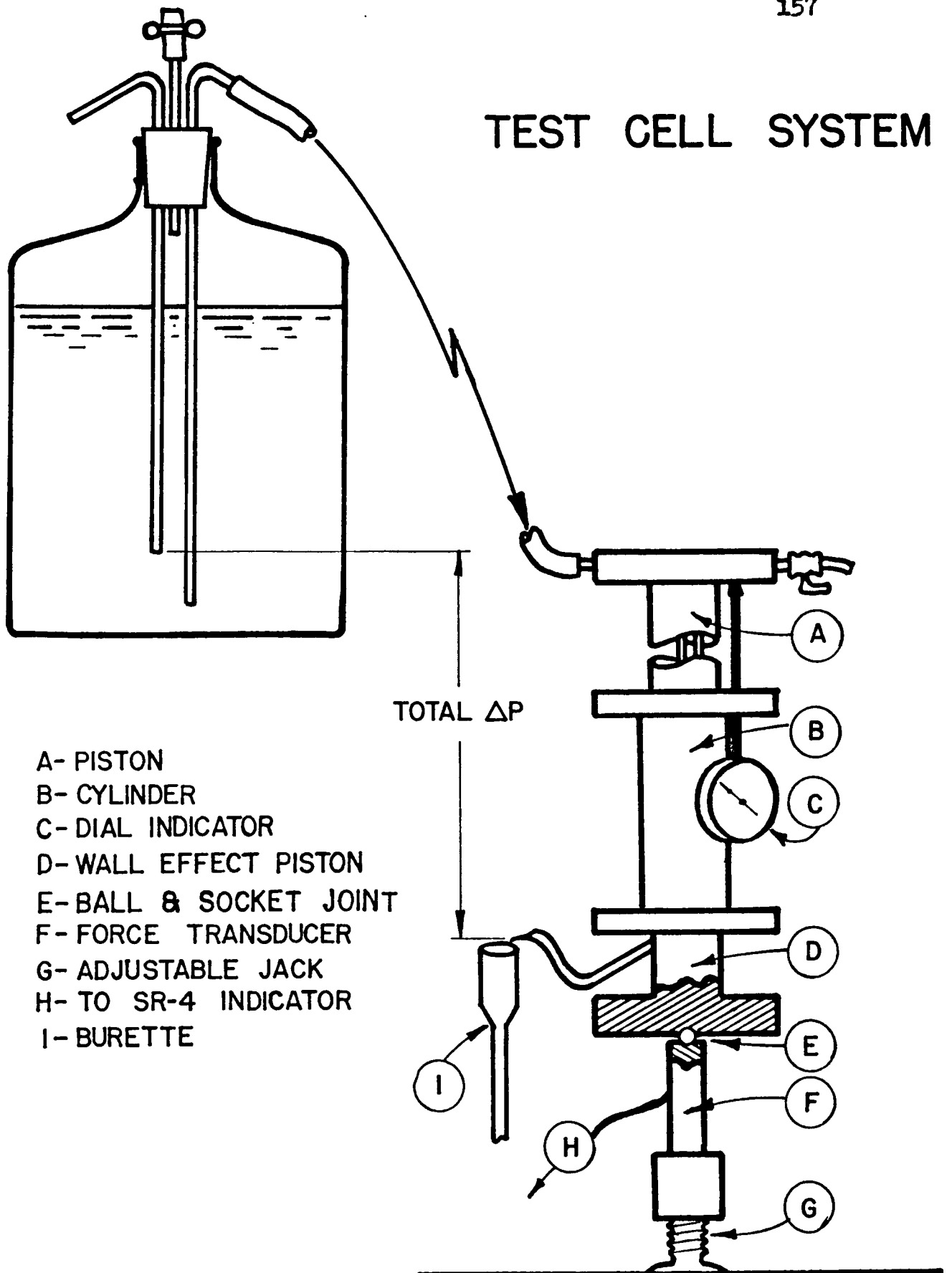


FIGURE VII-4

CAKING SYSTEM

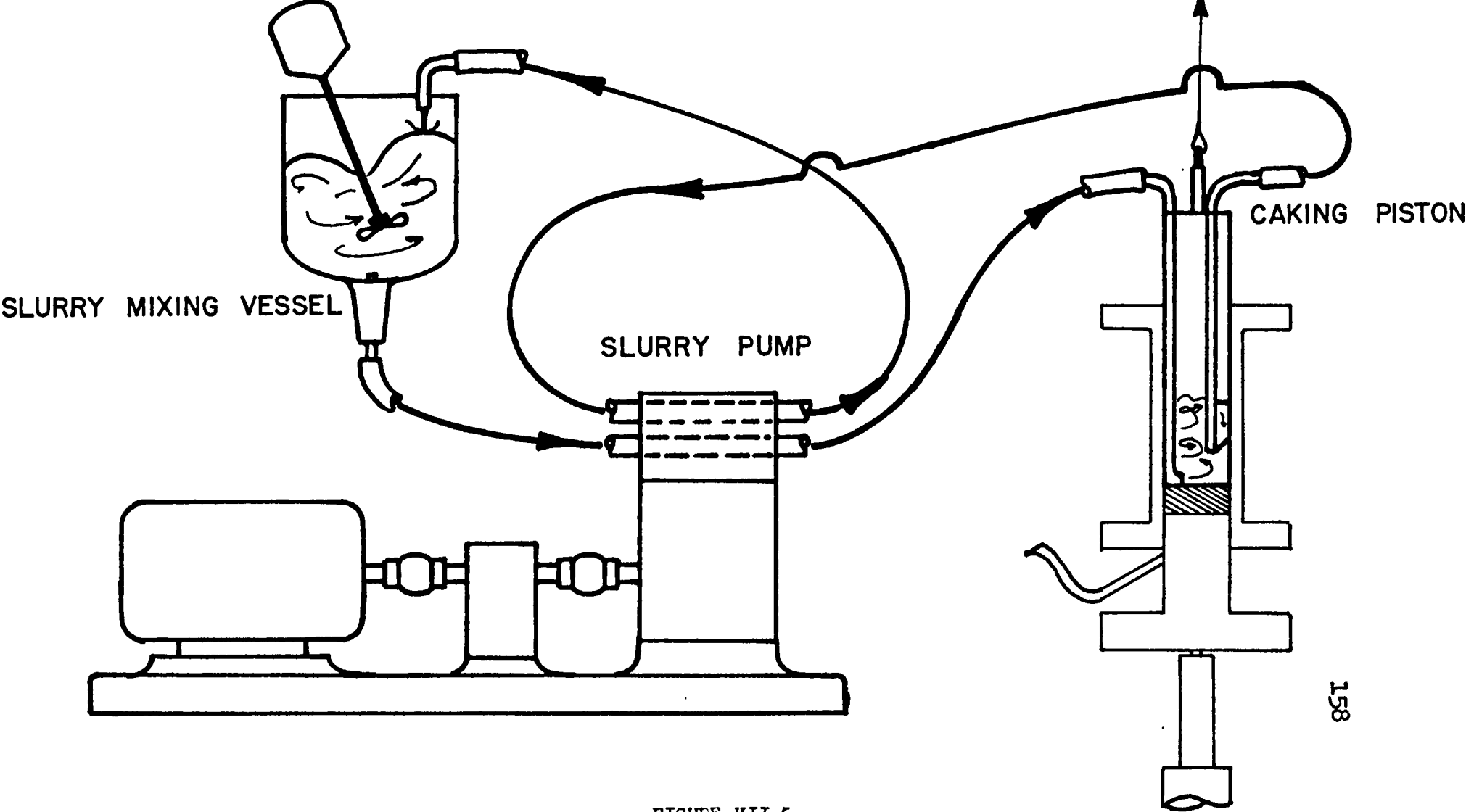


FIGURE VII-5

gauge which was graduated to 0.01 millimeters and had an over-all range of 25.4 millimeters. The absolute value of intermediate thickness was thus determined by adding to the final cake thickness the difference between the instantaneous dial readings and the final dial reading.

During the earlier portion of each run, the cake thickness changed so rapidly that it was impossible to read the dial indicator. To aid in reading these changes, a movie camera recording was made of the movement of the dial indicator needle. A Pillar Bolex 16 mm movie camera, provided with a special motor drive, was used which allowed pictures to be taken every 0.001 minutes. Most of these runs lasted two minutes or more during which time the first six seconds of data were recorded using the camera. However, whenever the entire run lasted six seconds, the camera was used to record the SR-4 strain gauge readings as well.

The total volume of the filtrate was collected throughout a compression-permeability cell run. The amount collected during a given period of time was measured using a precision burette. These measured volumes were used to calculate the cake resistance.

A force transducer was used to measure the transmitted force. This transducer was machined from brass. Four SR-4 strain gauges, connected in a wheatstone bridge, were cemented to the transducer which had been machined to be 0.250

inches o.d. at its narrowest point. Two of these gauges were placed parallel to the principle fiber of the brass and on opposite sides of the narrow column. The other two were placed at right angles to the fiber and 90° from the previous two. Thus, the assemblage was a rosette pattern.

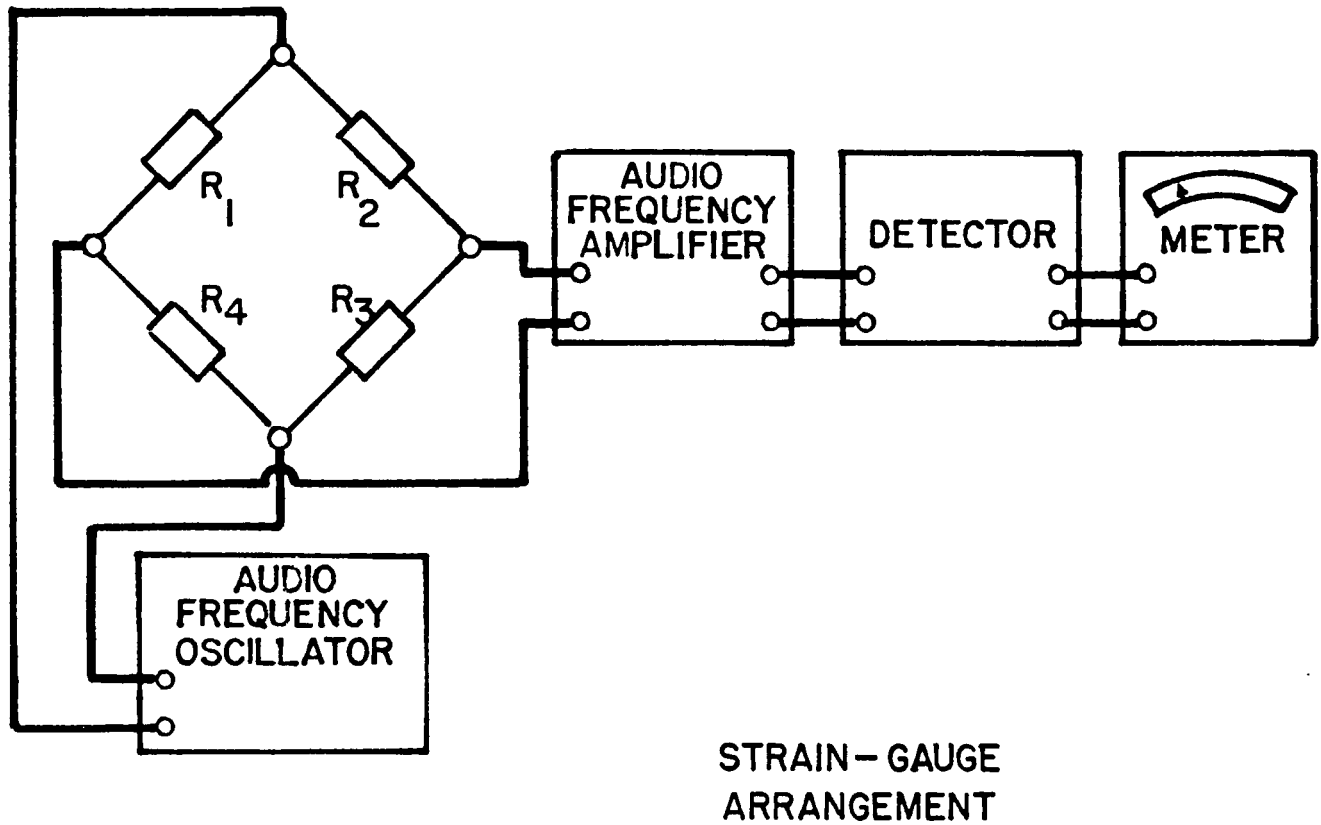
A Baldwin-Lima-Hamilton SR-4 strain indicator was used to determine the transmitted load applied to the force transducer. The circuitry of this indicator is typical of commercial amplifier-indicator systems, a functional block diagram of which is shown in Figure VII-6. Across two legs of the wheatstone-bridge is imposed the output of an audio frequency oscillator, as shown in the diagram. An audio frequency amplifier is driven by the signal taken from the wheatstone bridge, and hence, the change in resistance due to the load imposed on the transducer.

A few runs were made to determine the speed with which these transmitted forces were developed. For these runs the load cell was connected to a Model 152 Sanborn Recorder.

III. TESTING PROCEDURE

Prior to each experiment a calibration run was made to establish the stress-force relationship of the system. The cylinder was placed in the supporting framework. The lower cylinder was raised into position, supported by the force transducer which rests on the base of the framework.

BLOCK DIAGRAM OF STRAIN-GAUGE INDICATOR



STRAIN-GAUGE ARRANGEMENT

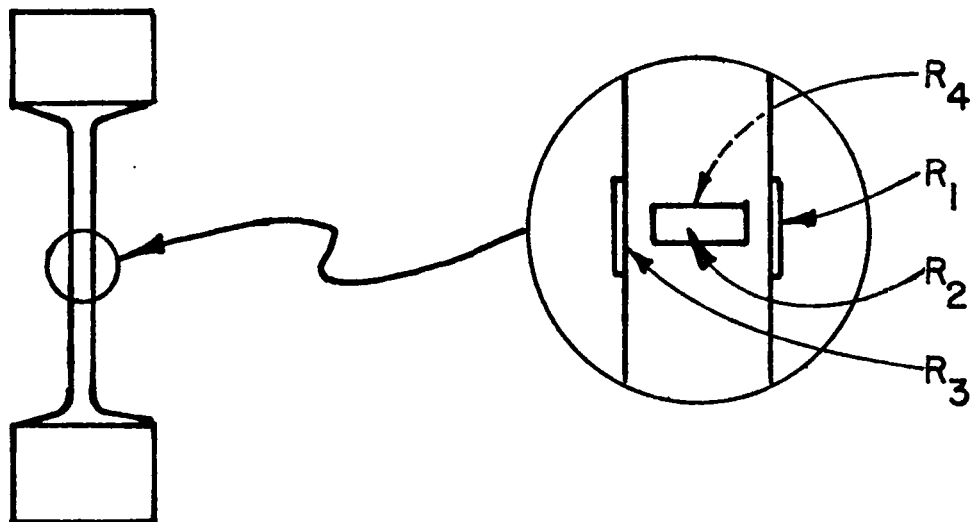


FIGURE VII-6

Two Whatman No.4 filter paper, grade disks were placed on top of the lower piston and a strain gauge reading was taken. This initial reading was considered as the zero reading for the calibration run.

Next, the upper piston was lowered to rest on the lower piston and the dial indicator was affixed to the side of the cylinder so that the dial indicator's anvil was depressed and forced down by the upper piston. A strain gauge reading and a dial reading was taken with this weight in place. Then additional weights, either 25 or 10 pounds each, were placed on top of the upper piston until a total of 335 pounds was reached. Strain gauge and dial readings were taken for each addition of weight. Since the upper piston weighed 15.30 pounds, the total weight was 350.3 pounds. This made the pressure exerted on the lower piston equal to 109.45 psi (the piston area was 3.2135 square inches). A plot of these strain gauge readings versus applied load was then made. The slope of this plot was then calculated in dimensions of micro-inches / (pound).

Before removing the additional weights, the height between the upper flange and the lower surface of the piston was measured using inside calipers and a micrometer. This measurement was called the initial height of the piston.

After the calibration run, the weights and the upper

piston were removed and a filter cake was prepared in situ within the confines of the lower piston-cylinder combination. The detailed description of this step has been given previously in the section of this chapter concerned with the equipment. The filtration was stopped when the desired initial cake thickness had been reached.

Again, an initial reading was taken with the SR-4 strain gauge indicator. The difference between this reading and the initial reading taken during the calibration run never differed more than 1 Or 2 micro-inches which was equivalent to a difference of $\frac{1}{4}$ to $\frac{1}{2}$ pounds. This difference was considered to be within the accuracy that could be read with the indicating dial of the analyser.

The actual runs consisted of placing weights upon this filter cake and observing the effect in terms of transmitted force, the compression of the cake, and periodically measuring the volume of the filtrate collected. These results were translated into transmitted force, porosity and cake resistance. The data so obtained from these runs are given in Appendix D.

CHAPTER VIII

DISCUSSIONS AND CONCLUSIONS

Equations for rotary drum filtration have been established which account for the variation in flow rates (superficial velocity) within the cake. In the derivation of those equations, the movement of the solids and the filtrate toward the medium as reported by Shirato and co-workers (44) was included. For moderately compressible materials, the general expression for q_x/q_1 and q_x/q_1 were derived as

$$\frac{q_x}{q_1} = 1 - \left[1 - \frac{q_1}{q_1} \right] \left(\frac{x}{L} \right) \left\{ \frac{\epsilon_x - \epsilon_{aw,x} + \lambda \epsilon_{aw,x} \frac{d \ln p}{d \ln L}}{\epsilon_x - \epsilon_{aw} - L \frac{d \epsilon_{aw}}{d L}} \right\} \quad (\text{VIII-1})$$

$$\frac{q_1}{q_1} = \frac{1 - m_1 s}{1 - m s} \left\{ 1 - \frac{(1 - m_1) s}{1 - m_1 s} \left[\frac{\epsilon_x - \epsilon_{aw} - L \frac{d \epsilon_{aw}}{d L}}{1 - \epsilon_{aw} \left(L - \frac{L s (1 - m)}{(1 - m s) \epsilon_w} \right) \frac{d \epsilon_{aw}}{d L}} \right] \right\} \quad (\text{VIII-2})$$

A numerical calculation procedure to solve these equations was programmed for a digital computer. The results computed were used for several purposes. First, they were compared with those obtained using the equations suggested by Ruth and Kempe (39) and those of Cooper (7).

From the comparison it is evident that in general the results of the three methods are in agreement; however, the filtrate rate predicted using the above equations are higher than the other two. This is due to the approximation used in solving the flow of the latter methods. Second, the computer results indicated that a fair degree of error would result if values for R_m and α were determined from experimental data using the Ruth and Kempe (39) rotary drum filtration equation. Lastly, the effect of changes in operating variables were investigated. It was shown that greater tonnage production could be attained by increasing the concentration of the solids in the slurry feed. Also, the filtration rate was increased by using higher vacuum. Furthermore, greater filtration rates will result from larger drum submergences. The effect of rotational speed upon the filtration rate is not the same for all pressure levels. It was found to be greater for a higher vacuum than for a lower vacuum.

The variation of porosity with pressure and time was experimentally determined using a compression-permeability cell. It was found that the porosity decreased with time sharply at first and then a gradual creep was evidenced. The porosity was empirically fitted to several rheological models. Good agreement was found for the Kelvin model in

describing the primary compression. Tiller's observation concerning the creep function in a compression-permeability cell has been confirmed experimentally; however, this effect has not been investigated in a filtration process.

Side-wall friction was found to be present in both conventional and "Teflon" lined compression-permeability cells. A simplified equation was derived and tested which describe the frictional effect in terms of the thickness-to-diameter ratio for the cake, the properties of the cake material, and the coefficient of friction of the cake and the cell lining. Correction factors were derived which correct the porosity and specific cake resistance measurements for the side-wall frictional effect. Although the correction factor for the porosity is not usually large, a measurable error would be caused if this effect were neglected. The correction for the specific cake resistance is considerably larger and normally should not be neglected.

CHAPTER IX

RECOMMENDATIONS FOR FUTURE WORK

As a means of obtaining a better understanding of filtration, the following areas for future research are recommended.

1. Study the effect that compression-permeability cell cake thickness-to-diameter ratio has upon wall friction, cake porosity, and specific cake resistance. This study should include different diameters of the compression-permeability cell as well as different materials for the lining of the cell.
2. Investigate the effect of wall friction on correlation of laboratory data with commercial results.
3. Determine the effect of time on specific cake resistance under zero compressive pressure. Also, devise a means for experimentally determining the specific cake resistance at zero time under a given compressive pressure.
4. Study the area of contact between cake particles in relation to intergranular pressures.
5. Develop methods for calculating internal flow rate variation in variable pressure filtration

under conditions of non-equilibrium porosities and specific cake resistances.

6. Develop a compression-permeability cell which will permit the measurement of the distribution of lateral pressures during compression tests. Such measurements will permit a better understanding of the forces active during compression.
7. Determine whether the creep function is present during an actual filtration process.
8. Using the Kelvin model, set up a differential model to be fed into the filtration theory.

NOMENCLATURE

Roman

- A cross sectional area, ft^2
- B constant defined in Equation (III-40), dimensionless
- B' Dashpot constant defined in Equation (IV-6), $(\text{lb}_f\text{-sec})/\text{ft}$.
- C₁ constant of integration defined in Equation (V-19), dimensionless
- C₂ constant of integration defined in Equation (V-19), dimensionless
- D diameter, ft.
- e base of Napierian logarithms 2.71828....., dimensionless
- F force, lb_f
- F_s solids compressive force, lb_f
- F_w friction at wall, lb_f
- g local gravitational constant, ft/sec^2
- g_c conversion factor, $(\text{lb}_m\text{-ft})/(\text{lb}_f\text{-sec}^2)$
- J_T correction factor for filtration resistance, ratio of average flow ratio to rate at medium, q_{av}/q_1 , dimensionless
- k Kozeny-Carman's coefficient of permeability as given in Equation (II-3), lb_m/ft^3
- K Darcy's coefficient of permeability, defined in Equation (II-3), ft^2
- K' elastic constant defined in Equation (IV-5), lb_f/ft .
- K_o lateral pressure coefficient, ratio between lateral and vertical pressures defined in Equation (V-2), dimensionless

- L cake thickness, ft.
- m ratio of mass of wet to mass of dry cake, dimensionless
- m_i value of m in the infinitesimal surface layer of cake, dimensionless
- n compressibility coefficient for specific resistance, dimensions meaningless
- N rotational speed of drum, r.p.m.
- p applied filtration pressure, lb_f/ft^2
- p_h hydrostatic pressure exerted by slurry, lb_f/ft^2
- p_i the solids pressure below which cake is assumed to have constant properties, lb_f/ft^2
- p_s solids compressive pressure at distance x from medium, also total compressive pressure, lb_f/ft^2
- p_t transmitted pressure at the bottom of a compression-permeability cell, lb_f/ft^2
- p_v vacuum applied, lb_f/ft^2
- p_x hydraulic pressure at a distance x from medium, lb_f/ft^2
- p_z vertical solids pressure developed in a compression-permeability cell, lb_f/ft^2
- Δp_c pressure drop across cake as defined in Equation (III-6), lb_f/ft^2
- p_1 pressure at interface of medium and cake, lb_f/ft^2
- q_f filtrate flow rate as defined in Equation (III-69), ft^3/sec .
- q_i value of q_x in infinitesimal surface layer cake, $\text{ft}^3/(\text{ft}^2\text{-sec})$
- q_x rate of liquid flow at distance x from medium, $\text{ft}^3/(\text{ft}^2\text{-sec})$
- q_1 value of q_x at interface of medium and cake, $\text{ft}^3/(\text{ft}^2\text{-sec})$
- q_{av} average value for q_x , $\text{ft}^3/(\text{ft}^2\text{-sec})$

r_1	value of r in infinitesimal surface layer of cake, $\text{ft}^3/(\text{ft}^2\text{-sec})$
r_0	apparent rate of solid flow approaching cake surface, $\text{ft}^3/(\text{ft}^2\text{-sec})$
r_x	apparent rate of migration of solids at distance x from medium, $\text{ft}^3/(\text{ft}^2\text{-sec})$
R	radius of filter drum, ft.
R_m	medium resistance, $1/\text{ft}$.
s	mass fraction of solids in the slurry, dimensionless
S_0	specific surface area, ft^2/lb_m
v	volume of filtrate, ft^3/lb_m
w	total mass of solids per unit area, lb_m/ft^2
w_f	tonnage capacity of filter as defined in Equation (III-84) $\text{tons}/(\text{sec-ft})$
w_x	mass of solids per unit area in distance x from medium, lb_m/ft^2
x	distance from the medium, ft.
z	distance from drainage base of a compression-permeability cell, ft.
Z	electrical impedance, ohms
V'	voltage

Greek

α	average specific resistance, ft/lb_m
α_R	Ruth's average value for α uncorrected for variation of flow rate, ft/lb_m
α_T	True average specific resistance, ft/lb_m

- α_x value of specific resistance at distance x from medium where solid compressive pressure is p_s , ft/lb_m
- α_0 constant in Equation (III-43) where p_s is in lb_f/ft^2 , dimensions meaningless
- α_i value of α_x when $p_s \equiv p_1$, dimension meaningless
- β exponent in Equation (III-40), dimensions meaningless
- ϵ porosity, dimensionless
- ϵ_i porosity in the infinitesimal surface layer, dimensionless
- ϵ_{ps} porosity function defined in Equation (III-7b), dimensionless
- ϵ_x porosity at distance x from medium, dimensionless
- ϵ_0 constant in Equation (III-7b), dimensionless
- ϵ_1 porosity in layer adjacent to medium, dimensionless
- ϵ_{av} average porosity, dimensionless
- ϵ_{avx} average porosity for the portion of cake between medium and distance x , dimensionless
- $\epsilon_{x/L}$ porosity function defined in Equation (III-7b), dimensionless
- θ time, sec.
- ζ transformed variable found in Equation V-18, dimensionless
- λ exponent in Equation (III-7b), dimensions meaningless
- λ_0 coefficient of wall friction defined in Equation (V-16), dimensionless
- μ viscosity, $\text{lb}_m/(\text{ft} \cdot \text{sec})$
- ξ root of Equation (V-18), dimensionless
- ρ density of liquid, lb_m/ft^3

- ρ_f density of slurry, lb_m/ft^3
- ρ_s density of solids, lb_m/ft^3
- T wall frictional force defined in Equation (V-6), lb_f/ft^2
- ϕ variable angle, radians
- ϕ_0 one-half of angle of submergence, radians
- ϕ' angle of internal friction of cake particles defined in Equation (V-5), dimensions meaningless
- ω angular velocity of drum, radians/sec.

BIBLIOGRAPHY

1. Almy, C. and W. K. Lewis, *Ind. Eng. Chem.*, 4, 528 (1912).
2. Baker, F. P., *Ind. Eng. Chem.*, 13, 610 (1921).
3. Bell, G. R. and F. B. Hutto, *Chem. Eng. Progr.*, 55, (1959).
4. Biot, Maurice A., *Appl. Phys.*, 26, 182 (1955).
5. Brandt, H. L. and B. M. Johnson, *A.I.Ch.E. Journal*, 9, 771 (1963).
6. Carman, P. C., *Trans. Inst. Chem. Engrs. (London)*, 16, 168 (1938).
7. Cooper, Harrison R., M.S. thesis, University of Houston, Houston, Texas (1958).
8. Cryer, C. W., *Quart. J. Mech. and Appl. Math.*, 16,
9. Darcy, H. P., "Les Fontaines Publiques de la Ville de Dijon," Victor Dalmont, Paris, France (1856).
10. Famularo, J. and J. Happel, *A.I.Ch.E. Journal*, 11, 981 (1965).
11. Grace, H. P., *Chem. Eng. Progr.*, 49, 303 (1953).
12. Grace, H. P., *Chem. Eng. Progr.*, 49, 367 (1953).
13. Grace, H. P., *Chem. Eng. Progr.*, 49, 427 (1953).
14. Graton, L. C. and H. J. Fraser, *J. Geol.*, 43, 785 (1935).
15. Hagen, G., *Pogg. Ann.*, 46, 423 (1839).
16. Happel, J., *A.I.Ch.E. Journal*, 4, 197 (1958).
17. Happel, J. and Howard Brenner, "Low Reynolds Number Hydrodynamics with Special Application to Particulate Media," Prentice-Hall, Englewood Cliffs, N. J. (1965).
18. Hatchek, E. J., *J. Soc. Chem. Ind.*, 27, 538 (1909).
19. Hutto, F. B., *Chem. Eng. Progr.*, 49, (1953).

20. Ingmanson, W. L., Chem. Eng. Progr., 53, 328 (1957).
21. Isaakyan, S. M. and A. M. Gasparyan, Interna. Chem. Eng., 6, 74 (1966).
22. Jaeger, J. C., "Elasticity, Fracture, and Flow," John Wiley and Sons, New York (1962).
23. Jaky, J., Proceedings of the Second International Conference on Soil Mechanics and Foundation Engineering, 1, 103 (1948).
24. Jamieson, S., Eng. News, 51, 236 (1904).
25. Janike, Andrew W., "Storage and Flow of Solids," Bullentin No. 123, Utah Engineering Experimental Station, University of Utah, Salt Lake City (1964).
26. Kantorovich, L. V. and V. I. Krylov, "Approximate Methods of Higher Analysis," P. Noordhoff Ltd., Groningen, The Netherlands (1958).
27. King, F. H., U. S. Geo. Survey, 19th Annual Report Part II, 1 (1897-98).
28. Kottwitz, F. A., Ph. D. thesis, Iowa State University, Ames, Iowa (1957).
29. Kozeny, J., Sitzber. Akad. Wiss. Wien. Abh. IIa, 136, 271 (1927).
30. Love, A. E. H., "A Treatise on the Mathematical Theory of Elasticity," Fourth Edition, Cambridge University Press, Cambridge (1927).
31. Lu, Wei-Ming, M. S. thesis, University of Houston, Houston, Texas (1964).
32. McNabb, A., Quart. Appl. Math., 17, 337 (1960).
33. McNamee, John, Quart. J. Mech. and Appl. Math., 13, 98 (1960).
34. Mondria, H., Appl. Sci. Research, A2, 165 (1950).
35. Poiseuille, J. L., Compt. Rend., 15, 1167 (1842).
36. Prager, W. and Philip Hodge, "Theory of Perfectly Plastic Solids," John Wiley and Sons, New York (1951).

37. Ruth, B. F., Ind. Eng. Chem., 27, 708 (1935).
38. Ruth, B. F., Ind. Eng. Chem., 38, 564 (1946).
39. Ruth, B. F. and L. L. Kempe, Trans. Am. Inst. Chem. Engrs., 33, 34 (1937).
40. Scheidegger, A. E., "The Physics of Flow Through Porous Media," The Macmillan Company, New York (1960).
41. Schepman, B. A., B. Martin, and D. A. Dahlstrom, Chem. Eng. Progr., 52, 423 (1956).
42. Shirato, Mompei and Sakio Okamura, Chem. Eng. (Japan), 19, 104 (1955).
43. Shirato, Mompei and M. Sambuichi, Chem. Eng. (Japan), 27, 476 (1963).
44. Shirato, Mompei, Hiroo Kato, M. Sambuichi, and T. Aragaki, "Analysis For Internal Flow Mechanism Through Constant Pressure Filter Cake," submitted to A.I.Ch.E. Journal for publication.
45. Slichter, C. S., U. S. Geo. Survey, 19th Annual Report, (Part II, 295 (1897-98)).
46. Sjenitzer, F., Trans. Inst. Chem. Engrs. (London), 33, 289 (1955).
47. Sowers, G. B. and G. F. Sowers, "Introduction Soil Mechanics and Foundations," The Macmillan Co., New York (1951).
48. Snyder, L. J. and W. E. Stewart, A. I. Ch. E. Pre-print No. 43b, presented at the 55th National Meeting, Houston, Texas (1965).
49. Sperry, D. R., Chem., 15, 198 (1916).
50. Sperry, D. R., Ind. Eng. Chem., 13, 986 (1921).
51. Sperry, D. R., Ind. Eng. Chem., 20, 892 (1928).
52. Sperry, D. R., Ind. Eng. Chem., 36, 323 (1944).
53. Taylor, D. W., J. Math. Phys., 19, 167 (1940).
54. Taylor, D. W., "Research on Consolidation of Clays," Dept. of Civil and Sanitary Engineering, Massachusetts

- Institute of Technology, Cambridge (1942).
55. Taylor, D. W., "Fundamentals of Soil Mechanics," John Wiley and Sons, Inc., New York (1948).
 56. Terzaghi, Karl, "Theoretical Soil Mechanics," John Wiley and Sons, Inc., New York (1943).
 57. Tiller, F. M., Chem. Eng. Progr., 49, 467 (1953).
 58. Tiller, F. M., Chem. Eng. Progr., 51, 282 (1955).
 59. Tiller, F. M., A.I.Ch.E. Journal, 4, 170 (1958).
 60. Tiller, F. M., Lecture Notes (1962).
 61. Tiller, F. M., and Harrison R. Cooper, A.I.Ch.E. Journal, 6, 595 (1960).
 62. Tiller, F. M., and Harrison R. Cooper, A.I.Ch.E. Journal, 8, 445 (1962).
 63. Tiller, F. M. and C. J. Huang, Ind. Eng. Chem., 53, 529 (1961).
 64. Tiller, F. M. and M. Shirato, A.I.Ch.E. Journal, 10, 61 (1964).
 65. Tiller, F. M. and M. Shirato, Chem. Eng. (Japan), 26, 918 (1962).
 66. Timoshenko, S. and J. M. Goodier, "Theory of Elasticity," McGraw-Hill Book Co., New York (1951).
 67. Toro, Liberto, M.S. thesis, University of Houston, Houston, Texas (1965).
 68. Underwood, A. J. V., Trans. Inst. Chem. Eng. (London), 4, 19 (1926).
 69. Underwood, A. J. V., Soc. Chem. Ind., 47, 325T (1928).
 70. Welch, Robert C., M.S. thesis, University of Texas, Austin, Texas (1960).

APPENDIX

APPENDIX A

COMPUTER PROGRAM FOR ROTARY DRUM FILTRATION

DATA USED IN CALCULATIONS

NOMENCLATURE USED IN PROGRAM

\$COMPILE MAD,EXECUTE,PRINT OBJECT,DUMP

D (01 OCT 1965 VERSION) PROGRAM LISTING

.....ROTARY FILTRATION ----- 12/03/65 -----.....

DIMENSION EPS(40),EPC(40),EPSAV(40),PS(40),PSC(40),PSE(40),
 1 QBYW(40),QXQ1(40),SARE(40),XGL(40)
 INTEGER K,TAB,TAB1,COUNT
 GC=32.174
 PI=3.1415926536
 PRINT COMMENT \$1\$
 READ AND PRINT DATA

START

THIS READS IN THE FOLLOWING DATA

EPSI = POROSITY IN THE SURFACE LAYER OF THE CAKE
 EPS0 = POROSITY AT 1.0 PSIA
 RAMDA = POROSITY EXPONENT
 PSUBI = MINIMUM COMPRESSIVE PRESSURE, LB.F/SQ.IN.
 ALFA0 = SPECIFIC FILTRATION RESISTANCE AT 1.0 PSIA
 ENYA = SPECIFIC FILTRATION RESISTANCE EXPONENT
 RH0L = DENSITY OF LIQUID, LB.M/CU.FT.
 RH0S = TRUE DENSITY OF SOLIDS, LB.M/CU.FT.
 MU = VISCOSITY OF LIQUID, LB.M/(FT.-SEC.)
 BETA = POROSITY-PRESSURE EXPONENT
 DRUMR = DRUM RADIUS, FEET
 OMEGA = ANGULAR VELOCITY, R.P.M.
 SUBMR = DRUM SUBMERGENCE, DEGREES
 VACU = VACUUM, INCHES MERCURY AT 32 F
 RMEDM = MEDIUM RESISTANCE, 1/FEET
 S = WEIGHT FRACTION SOLIDS IN SLURRY, DIMENSIONLESS
 INCR = INCREMENTS OF TIME, DIMENSIONLESS

AA=ENYA+BETA

AB=1.-AA

AC=1./AB

AD=-RAMDA/AB

AE=1.-ENYA

EPS(40)=EPSI

PVACU=70.727*VACU

FSUBI=144.*PSUBI

BFF=BEE/(144.*P.BETA)

ALFFA0=ALFA0/(144.*P.ENYA)

MIRAT0=1.0+RH0L*EPSI/(RH0S*(1.-EPSI))

PHI0=PI*SUBMR/360.

RH0F=1./(S/RH0S+(1.-S)/RH0L)

OMEGAS=2.*PI*OMEGA/60.

ENDTIM=2.*PHI0/OMEGAS

DELTHE=ENDTIM/INCR

W=INVER DELTHE.G.1.0, DELTHE=1.0

THETA=0.0

Q1=3C*PVACU/(MU*RMEDM)

WCAKE=0.0

PRESS0=0.0

Q10LC=Q1

STUART

THETA=THETA+DELTHE

```

WHENEVER THETA.G.ENDTIM,TRANSFER TO START
PHI=PI*THETA*OMEGA/30.
PRESST=PVACU+RHOF*DRUMR*(COS.(PHIO-PHI)-COS.(PHIO))
PRESS1=MU*Q1*RMEDM/GC
PRESS=PRESST-PRESS1
PSIA=PRESST/144.
WHENEVER PRESS.G.(0.5*PRESST),DELTHE=ENDTIM/INCR
PSI=PRESS/144.
PS(40)=0.0
X0L(40)=1.0
EPRESS=EPS0*PSI.P.(-RAMDA)
THROUGH UN0,F0R K=0,1,K.G.39
    X0L(K)=K/40.
    EPS(K)=EPRESS*(1.-X0L(K)).P.AD
    WHENEVER EPS(K).G.EPSI,EPS(K)=EPSI
UN0    PS(K)=PSI*(1.-X0L(K)).P.AC
L00P1  TAB1=0
    SUM=0.0
    THROUGH D0S,F0R K=2,2,K.G.40
        SUM=SUM+(EPS(K-2)+EPS(K)+4.*EPS(K-1))/120.
D0S    EPSAV(K)=SUM/X0L(K)
    EPSAV(0)=EPS(0)
    EPSAVG=EPSAV(40)
    THROUGH TRES,F0R K=1,2,K.G.39
TRES    EPSAV(K)=(EPSAV(K+1)+EPSAV(K-1))/2.
    MRATIO=1.+RH0L*EPSAVG/(RH0S*(1.-EPSAVG))
    AF=S*(MRATIO-1.)/(EPSAVG*(1.-MRATIO*S))
    QIQ1=EPSI*(EPSI-EPSAVG)*AF/(1.-EPSI)+(1.-MIRAT0*S)/(1.-MRATIO
1      *S)
    THROUGH QUATR0,F0R K=0,1,K.G.40
        QXQ1(K)=1.-AF*(EPS(K)-EPSAV(K))*X0L(K)
QUATR0  WHENEVER EPS(K).E.EPSI, QXQ1(K)=QIQ1
    THROUGH CINC0,F0R K=0,1,K.G.40
CINC0   PSE(K)=(QXQ1(K)-EPS(K))*PS(K).P.ENYA
    SUM=0.0
    THROUGH SEITE,F0R K=2,2,K.G.40
        SUM=SUM+(PSE(K-2)+PSE(K)+4.*PSE(K-1))/120.
SEITE   SARE(K)=SUM
    C0UNT=0
    THROUGH 0CH0,F0R K=0,2,K.G.40
        PSC(K)=PSI*(1.-SARE(K)/SUM)
        EPC(K)=EPS0*PSC(K).P.(-RAMDA)
        WHENEVER PSC(K).LE.PSUBI, EPC(K)=EPSI
        DELTA=EPC(K)/EPS(K)
0CH0    WHENEVER DELTA.G.1.01.0R.DELTA.L.0.99, C0UNT = C0UNT+1
    WHENEVER TAB1.G.6, TRANSFER TO C0LLEN
    WHENEVER C0UNT.G.5
        THROUGH NUEVE,F0R K=1,2,K.G.39
            EPC(K)=(EPC(K+1)+EPC(K-1))/2.
        THROUGH DIEZ,F0R K=0,1,K.G.40
            PS(K)=PSC(K)
DIEZ    EPS(K)=EPC(K)
        TAB1=TAB1+1
        TRANSFER TO L00P1
    OTHERWISE
    END OF C0NDITIONAL
C0LLEN  THROUGH 0NCE,F0R K=0,1,K.G.40
0NCE    QBYW(K)=QXQ1(K)*(1.-EPS(K))/(1.-EPSAVG)
    JAY=0.
    THROUGH D0CE,F0R K=2,2,K.G.40

```

```

DOCE      JAY=JAY+(QBYW(K-2)+QBYW(K)+4.*QBYW(K-1))/120.
          PRINT FORMAT NAME
          VECTOR VALUES NAME =$1HO,S10,28HC0NSTANT PRESSURE FILTRATION
1 /*$
          PRINT RESULTS PSIA,Q1,PSI,QIQ1,MRATIO,MIRAT0,JAY,TAB1
          TAB=0
          BA=PRESS.P.AB-AA*FSUBI.P.AB
          BB=PRESS.P.AE - ENYA*FSUBI.P.AE
JACKIE    WHENEVER TAB.G.6, TRANSFER TO SONDRRA
          TAB1=0
HAYNES    DELWC=Q1*DELTHE*S*RH0L/(1.-MRATIO*S)
          WCAKE0=WCAKE+DELWC
          DEN0M=JAY*MU*RH0S*ALFFA0*BFF*Q1
          LCAKE=GC*BA/(DEN0M*AB)
          WHENEVER PSI.LE.PSUBI
            ALPHA=ALFFA0*FSUBI.P.ENYA
          OTHERWISE
            ALPHA=ALFFA0*AE*PRESS/BB
          END OF CONDITIONAL
          DLDP=GC*(PRESS.P.AA)/DEN0M-LCAKE
          DEAVDP=BFF*AB*(PRESS.P.ENYA)*(1.-(1.-EPSAVG)*(PRESS.P.(-BETA)
1          )/BFF)/BA
          DQ1DP=(Q1-Q10LD)/(PRESS-PRESS0)
          DLDP=GC*(PRESS.P.(-AA))/DEN0M-LCAKE*DQ1DP/Q1
          DEAVDL=DEAVDP/DLDP
          QIXQ1=((1.0-MIRAT0*S)/(1.0-MRATIO*S))*(1.0-((1.-MIRAT0)*S/
1          (1.-MIRAT0*S))*(EPSI-EPSAVG-LCAKE*DEAVDL)/(1.-EPSAVG
2          -(LCAKE-LCAKE*S*(1.-MRATIO)/(EPSAVG*(1.-MRATIO*S)))*
3          DEAVDL))
          THROUGH EIN,F0R K=0,1,K.G.40
          WHENEVER EPS(K).E.EPSI
            QXQ1(K)=QIXQ1
          OTHERWISE
            QXQ1(K)=1.0-(1.-QIXQ1)*(EPS(K)-EPSAV(K)+RAMDA*EPS(K)*
1          DLDP)/(EPSI-EPSAVG-LCAKE*DEAVDL)*X0L(K)
          END OF CONDITIONAL
          QBYW(K)=QXQ1(K)*(1.-EPS(K))/(1.-EPSAVG)
          JBIRD=0.0
          THROUGH ZWEI,F0R K=2,2,K.G.40
ZWEI      JBIRD=JBIRD+(QBYW(K-2)-QBYW(K)+4.*QBYW(K-1))/120.
          DIFF=.ABS.((JAY-JBIRD)/JBIRD)
          JAY=JBIRD
          WHENEVER DIFF.L.0.005.0R.TAB1.G.10, TRANSFER TO TILLER
          TAB1=TAB1+1
          Q1=GC*PRESST/(MU*(JAY*ALPHA*RH0S*(1.-EPSAVG)*LCAKE+RMEDM))
          TRANSFER TO HAYNES
TILLER    THROUGH DREI,F0R K=0,1,K.G.40
DREI      PSE(K)=(QXQ1(K)-EPS(K))*PS(K).P.ENYA
          SUM=0.0
          THROUGH VIER,F0R K=2,2,K.G.40
          SUM=SUM+(PSE(K-2)+PSE(K)+4.*PSE(K-1))/120.
VIER      SARE(K)=SUM
          COUNT=0
          THROUGH FUMP,F0R K=0,2,K.G.40
          PSC(K)=PSI*(1.-SARE(K)/SUM)
          WHENEVER PSC(K).LE.PSUBI
            EPC(K)=EPSI
          OTHERWISE
            EPC(K)=EPS0*PSC(K).P.(-RAMDA)
          END OF CONDITIONAL

```

```

          DELTA=EPC(K)/EPS(K)
FUMP      WHENEVER DELTA.G.1.01.0R.DELTA.L,0.99,COUNT=COUNT+1
          WHENEVER COUNT.G.7
          THROUGH SECHS, FOR K=1,2,K.G.39
SECHS     EPC(K)=(EPC(K+1)+EPC(K-1))/2.
          THROUGH SIEBEN, FOR K=0,1,K.G.40
          PS(K)=PSC(K)
SIEBEN    EPS(K)=EPC(K)
          SUM=0.0
          THROUGH ACHT, FOR K=2,2,K.G.40
          SUM= SUM+(EPS(K-2)+EPS(K)+4.*EPS(K-1))/120.
ACHT      EPSAV(K)=SUM/X0L(K)
          THROUGH NEUN, FOR K=1,2,K.G.39
NEUN     EPSAV(K)=(EPSAV(K+1)+EPSAV(K-1))/2.
          EPSAVG=EPSAV(40)
          MRATIO=1.+RH0L*EPSAVG/(RH0S*(1.-EPSAVG))
          TAB=TAB+1
          Q1=GC*PRESST/(MU*(JAY*ALPHA*RH0S*(1.-EPSAVG)*LCAKE
1         +RMEDM))
          TRANSFER TO JACKIE
          OTHERWISE
          END OF CONDITIONAL
SONDRA    PRINT COMMENT $ ROTARY DRUM FILTRATION $
          PRINT RESULTS THETA,PRESS,LCAKE,JAY
          PRINT RESULTS DEAVDL,ALPHA,Q1,DVDL,MRATIO,QIXQ1,EPSAVG,TAB
          WCAKE=WCAKE0
          PRINT RESULTS TAB1,WCAKE
          Q1=GC*PRESST/(MU*(JAY*ALPHA*WCAKE+RMEDM))
          PRESS0=PRESS
          Q10LD=Q1
          TRANSFER TO STUART
          END OF PROGRAM

```

THE FOLLOWING NAMES HAVE OCCURRED ONLY ONCE IN THIS PROGRAM.
 COMPILATION WILL CONTINUE.

ALFA0	*016
BEE	*015
DRUMR	*032
DVDL	*166
SUBMR	*018
VACU	*013

TABLE III

DATA USED IN ROTARY
DRUM FILTRATION PROGRAM

The nomenclature used in the rotary drum filtration program may be found by referring to the program given in this appendix. The constants used for talc, supercel, and Hong Kong pink kaolin are listed below.

	Talc	Super Cel	Hong Kong Pink Kaolin
EPSI k_{si}	0.903	0.896	0.72
EPSO G_0	0.860	0.875	0.695
RAMDA k_c	0.054	0.0104	0.0586
PSUBI	0.4	0.1	0.6
ALFAO α_0	8.66×10^{10}	3.22	1.01
ENYA m	0.506	0.137	0.332
RHOL μ_L	62.4	62.4	62.4
RHOS ρ_s	166.8	124.6	166.
MU μ	0.001	0.001	0.001
BETA	0.203	0.0442	0.095
RMEDM	2.00×10^{10}	2.00×10^{10}	2.00×10^{10}

APPENDIX B

RUTH PROGRAM FOR ROTARY DRUM FILTRATION
PROGRAM FOR DETERMINING THE COEFFICIENTS FROM
CONSTANT PRESSURE DATA
GAUSSIAN ELIMINATION FOR CURVEFIT
RESULTS FROM CALCULATIONS

\$COMPILE MAD, EXECUTE, PRINT OBJECT, DUMP

D (01 OCT 1965 VERSION) PROGRAM LISTING

..... RUTH PROGRAM FOR ROTARY DRUM FILTRATION WITH CORREC-
TION FOR HYDROSTATIC PRESSURE OF SLURRY

DIMENSION THETA(20), V(20), PHI(20), A(10), B(10)

INTEGER I, INCR

PI=3.1415926536

START PRINT COMMENT \$1\$

READ AND PRINT DATA

THIS READS IN THE FOLLOWING DATA

RH0L = DENSITY OF LIQUID, LB.M/CU.FT.

RH0S = TRUE DENSITY OF SOLIDS LB.M/CU.FT.

MU = VISCOSITY OF LIQUID LB.M/(FT.-SEC.)

VACU = VACUUM, INCHES MERCURY AT 32 F

DRUMR = DRUM RADIUS, FEET

OMEGA = ANGULAR VELOCITY, R.P.M.

SUBMR = DRUM SUBMERGENCE, DEGREES

RMEDM = MEDIUM RESISTANCE, 1/FEET

S = WEIGHT FRACTION SOLIDS IN SLURRY, DIMENSIONLESS

INCR = INCREMENTS OF TIME, DIMENSIONLESS

PVACU=70.727*VACU

PHIO=PI*SUBMR/360.

RH0F=1./(S/RH0S+(1.-S)/RH0L)

OMEGAS=2.*PI*OMEGA/60.

ENDTIM=2.*PHIO/OMEGAS

DELTHE=ENDTIM/INCR

DELPHI=2.*PHIO/INCR

DPCAKE=PVACU+RH0F*DRUMR*(SIN.(PHIO)/PHIO-COS.(PHIO))

EPSAVG=((A(5)*DPCAKE+A(4))*DPCAKE+A(3))*DPCAKE+A(2))*DPCAKE+

1 A(1)

ALPHA=((B(5)*DPCAKE+B(4))*DPCAKE+B(3))*DPCAKE+B(2))*DPCAKE+

1 B(1)

MRATIO=1.+RH0L*EPSAVG/(RH0S*(1.-EPSAVG))

PRINT RESULTS ALPHA, EPSAVG

PRINT RESULTS DPCAKE, MRATIO

AA=ALPHA*MU*S*RH0L*OMEGAS/(64.348*(1.-MRATIO*S))

BB=RMEDM*OMEGAS*MU/32.174

AB=BB/(2.*AA)

C=DPCAKE/AA

THROUGH ONE, FOR I=1,1,I.G.INCR

ANGLE=DELPHI*I

THETA(I)=DELTHE*I

PHI(I)=ANGLE

ONE V(I)=-AB+SQRT.(AB*AB+ANGLE*C)

PRINT COMMENT \$0 RUTH PROGRAM \$

PRINT COMMENT \$0 TIME FILTRATE PHI \$

PRINT COMMENT \$ SECONDS CU.FT/SQ.FT. RADIANS \$

PRINT COMMENT \$0\$

THROUGH TWO, FOR I=1,1,I.G.INCR

TWO PRINT FORMAT ANSWR, THETA(I), V(I), PHI(I)

VECTOR VALUES ANSWR = \$1H, S9, F7.3, S6, F8.6, S7, F7.5*\$

TRANSFER TO START
END OF PROGRAM

THE FOLLOWING NAMES HAVE OCCURRED ONLY ONCE IN THIS PROGRAM.
COMPILATION WILL CONTINUE.

DRUMR	*013
OMEGA	*009
RMEDM	*020
SUBMR	*007
VACU	*006

\$COMPILE MAD,EXECUTE,PRINT OBJECT,DUMP

MAD (01 OCT 1965 VERSION) PROGRAM LISTING

```

DIMENSION DPCAKE(100),EPSAVG(100),EPSCAL(100),ALPHA(100),ALFC
1 AL(100),AISS(10),BISS(10)
INTEGER I,N

```

.....THIS PROGRAM DETERMINES THE COEFFICIENTS USED IN
CALCULATING THE AVERAGE POROSITY AND THE ALPHA FROM
EXPERIMENTAL OR CALCULATED CONSTANT PRESSURE DATA

```
BEGIN READ AND PRINT DATA
```

.....THIS READS IN THE AVERAGE POROSITY DATA

N = NUMBER OF EQUALLY SPACED DATA TO BE FITTED
DPCAKE = PRESSURE, P - P1, ACROSS CAKE, LB.F/SQ.FT.
EPSAVG = AVERAGE POROSITY OF FILTER CAKE

```
EXECUTE EGAUSS.(AISS,N,5,DPCAKE,EPSAVG)
READ AND PRINT DATA
```

.....THIS READS IN THE ALPHA DATA

ALPHA = SPECIFIC CAKE RESISTANCE, FT./LB.M

```
EXECUTE EGAUSS.(BISS,N,5,DPCAKE,ALPHA)
THROUGH FIGUR, FOR I=1,1,I.G.N
```

```

PRESS=DPCAKE(I)
EPSCAL(I)=(((AISS(5)*PRESS+AISS(4))*PRESS+AISS(3))*PRESS+
1 AISS(2))*PRESS+AISS(1)
FIGUR 1 ALFCAL(I)=(((BISS(5)*PRESS+BISS(4))*PRESS+BISS(3))*PRESS+
1 BISS(2))*PRESS+BISS(1)
PRINT COMMENT $0 COMPARISON OF CALCULATED AND EXPERI
1 MENTAL VALUES $
PRINT COMMENT $ PRESSURE POROSITY
1 CAKE RESISTANCE $
PRINT COMMENT $ LB/SQ.FT. CALCUL. EXPERIT. CALC
1 ULATED EXPERIMENTAL $
PRINT COMMENT $0$
THROUGH LAST, FOR I=1,1,I.G.N
LAST PRINT FORMAT OUT, DPCAKE(I),EPSCAL(I),EPSAVG(I),ALFCAL(I),ALP
1 HA(I)
VECTOR VALUES OUT = $S11,F7.2,F10.5,F9.5,S1,2E12.5 *$
TRANSFER TO BEGIN
END OF PROGRAM

```

AD (01 OCT 1965 VERSION) PROGRAM LISTING

GAUSSIAN ELIMINATION FOR CURVEFIT

DEFINITION OF SYMBOLS

NDATA IS THE NUMBER OF DATA SETS (MAXIMUM ALLOWED FOR IS 100)

NTERMS IS THE NUMBER OF TERMS , THAT IS NTERMS MINUS ONE IS THE DEGREE OF POLYNOMIAL FIT DESIRED

EXTERNAL FUNCTION(COEFF,NDATA,NTERMS,X,Y)
ENTRY TO EGAUSS.

INTEGER I,J,K,NDATA,NTERMS

DIMENSION A(56,DIX),B(7),C(800,TRIX),YCAL(100)

VECTOR VALUES DIX=2,1,8

VECTOR VALUES TRIX=2,1,8

EXECUTE ZERO.(A(1,1)...A(NTERMS,NTERMS+1))

THROUGH D0S , FOR I=1,1,I.G.NDATA

C(I,1) = 1.0

THROUGH TRES , FOR J=2,1,J.G.NTERMS

TRES C(I,J) = C(I,J-1)*X(I)

D0S C(I,NTERMS+1) = Y(I)

THROUGH CUART0 , FOR K=1,1,K.G.NTERMS

THROUGH CUART0 , FOR I=1,1,I.G.NTERMS+1

THROUGH CUART0 , FOR J=1,1,J.G.NDATA

CUART0 A(K,I) = C(J,I)*C(J,K)+A(K,I)

THROUGH CINCO,FOR I=1,1,I.G.NTERMS

WHENEVER A(I,I).E.O.O

K=I+1

TRANSFER TO PROX0

OTHERWISE

0TRAV THROUGH SIES ,FOR J=NTERMS+1,-1,J.L.I

SIES A(I,J) = A(I,J)/A(I,I)

END OF CONDITIONAL

WHENEVER I.E.NTERMS , TRANSFER TO MAS

THROUGH CINCO , FOR K=NTERMS,-1,K.E.I

THROUGH CINCO , FOR J=NTERMS+1,-1,J.L.I

A(K,J) = A(K,J) - A(K,I)*A(I,J)

CINCO CONTINUE

MAS THROUGH SIETE , FOR K=NTERMS,-1,K.L.2

THROUGH SIETE , FOR I=1,1,I.E.K

THROUGH SIETE , FOR J=NTERMS+1,-1,J.L.K

SIETE A(I,J) = A(I,J) - A(K,J)*A(I,K)

THROUGH 0CH0 , FOR I=1,1,I.G.NTERMS

0CH0 COEFF(I) = A(I,NTERMS+1)

THROUGH D0CE, FOR J=1,1,J.G.NDATA

SUMY = COEFF(1)

THROUGH 0NCE, FOR I=2,1,I.G.NTERMS

0NCE SUMY = SUMY + COEFF(I)*X(J).P.(I-1)

D0CE YCAL(J) = SUMY

PRINT RESULTS NTERMS, COEFF(1)...COEFF(NTERMS)

THROUGH TRECE, FOR J=1,1,J.G.NDATA

TRECE PRINT FORMAT ANSWR,X(J), Y(J), YCAL(J)

VECTOR VALUES ANSWR = \$S10,E14.5,S3,E14.5,S3,E14.5*\$

```
FUNCTION RETURN  
PR0X0  WHENEVER A(K,I).E.O.O  
      K = K+1  
      TRANSFER TO ULTIM0  
      OTHERWISE  
      THROUGH NUEVE , FOR J=1,1,J.G.NTERMS  
      TEMP = A(I,J)  
      A(I,J) = A(K,J)  
      NUEVE  A(K,J) = TEMP  
      TRANSFER TO 0TRAV  
      END OF CONDITIONAL  
      ULTIM0 WHENEVER K.LE.NTERMS , TRANSFER TO PR0X0  
      PRINT COMMENT $ ** YOU GOOFED NO SOLUTION TO IT **$  
      ERROR RETURN  
      END OF FUNCTION
```

TABLE IV
RESULTS OF CALCULATIONS FROM
RUTH PROGRAM

TIME	RADIANS	CU.FT./SQ.FT. ^v
8	.2094	.00835
16	.4189	.01465
24	.6283	.01985
32	.8378	.02445
40	1.0472	.02855
48	1.2566	.03235
56	1.4661	.03595
64	1.6755	.03925
72	1.8849	.04275
80	2.0944	.04625

The above calculations were made of ten per cent talc slurry at 5 p.s.i. with an eight foot diameter drum. The results of these calculations are plotted in Figure III-8.

APPENDIX C

CALCULATIONS FOR KELVIN RHEOLOGICAL MODEL

MAD (01 OCT 1965 VERSION) PROGRAM LISTING

..... CALCULATIONS FOR KELVIN RHEOLOGICAL MODEL

```

DIMENSION HEAD(12), THETA(200), LCAKE(200), DELTA(200), D(200)
INTEGER HEAD, I, N
START  READ FORMAT HEADNG, HEAD(1)...HEAD(12)
      VECTOR VALUES HEADNG=$12A6*$
      PRINT COMMENT $1$
      READ DATA
      PRINT FORMAT HEADNG, HEAD(1)...HEAD(12)
      DDIFF=DLDIAL-LCAKE(1)
      THROUGH END, FOR I=1,1,I.G.N
          DIFF=DLDIAL-LCAKE(I)
          DELTA(I-1)=DIFF-DDIFF
          D(I)=DIFF
      END  DDIFF=DIFF
      THROUGH FINAL, FOR I=1,1,I.G.N
FINAL  PRINT FORMAT ANSWR, THETA(I), D(I), DELTA(I)
      VECTOR VALUES ANSWR=$S10,3E14.5*$
      EXECUTE ZERO.(THETA(0)...THETA(200))
      EXECUTE ZERO.(LCAKE(0)...LCAKE(200))
      TRANSFER TO START
      END OF PROGRAM
    
```

SØLKA FLØC (ALPHA CELLULOSE)

XVII-1-63

.30000E-02	.27932E 02	-.24000E 00
.40000E-02	.27692E 02	-.96000E 00
.50000E-02	.26732E 02	-.29000E 00
.60000E-02	.26442E 02	-.70000E 00
.70000E-02	.25742E 02	-.10000E 00
.80000E-02	.25642E 02	-.15000E 00
.90000E-02	.25492E 02	-.16000E 00
1.00000E-02	.25332E 02	-.16000E 00
.11000E-01	.25172E 02	-.13000E 00
.12000E-01	.25042E 02	-.13000E 00
.13000E-01	.24912E 02	-1.00000E-01
.14000E-01	.24812E 02	-.90000E-01
.15000E-01	.24722E 02	-.90000E-01
.16000E-01	.24632E 02	-.80000E-01
.17000E-01	.24552E 02	-.80000E-01
.18000E-01	.24472E 02	-.50000E-01
.19000E-01	.24422E 02	-.70000E-01
.20000E-01	.24352E 02	-.50000E-01
.21000E-01	.24302E 02	-.40000E-01
.22000E-01	.24262E 02	-.50000E-01
.23000E-01	.24212E 02	-.50000E-01
.24000E-01	.24162E 02	-.40000E-01
.25000E-01	.24122E 02	-.40000E-01
.26000E-01	.24082E 02	-.40000E-01
.27000E-01	.24042E 02	-.30000E-01
.28000E-01	.24012E 02	-.30000E-01
.29000E-01	.23982E 02	-.30000E-01
.30000E-01	.23952E 02	-.30000E-01
.31000E-01	.23922E 02	-.20000E-01
.32000E-01	.23902E 02	-.30000E-01
.33000E-01	.23872E 02	-.20000E-01
.34000E-01	.23852E 02	-.30000E-01
.35000E-01	.23822E 02	-.90000E-01
.40000E-01	.23732E 02	-.14000E 00
.50000E-01	.23592E 02	-.90000E-01
.60000E-01	.23502E 02	-.51000E 00
.30000E 00	.22992E 02	-.13000E 00
.64000E 00	.22862E 02	-.90000E-01
.10000E 01	.22772E 02	-.70000E-01
.15000E 01	.22702E 02	-.50000E-01
.20000E 01	.22652E 02	-.40000E-01
.25000E 01	.22612E 02	-.30000E-01
.30000E 01	.22582E 02	-.49999E-02
.40000E 01	.22577E 02	-.50001E-02
.50000E 01	.22572E 02	-.49999E-02
.60000E 01	.22567E 02	-.30000E-02
.70000E 01	.22564E 02	-.20001E-02
.80000E 01	.22562E 02	-.20000E-01
.90000E 01	.22542E 02	-.30000E-01
.10000E 02	.22512E 02	.18845E-36

OLKA FLGC (ALPHA CELLULOSE)

XVII-1-130

.50000E-01	.27056E 02	.00000E 00
.60000E-01	.27056E 02	-.16000E 00
.61000E-01	.26896E 02	-.60000E 00
.62000E-01	.26296E 02	-.70000E-01
.63000E-01	.26226E 02	-.30000E 00
.64000E-01	.25926E 02	-.36000E 00
.65000E-01	.25566E 02	-.26000E 00
.66000E-01	.25306E 02	-.34000E 00
.67000E-01	.24966E 02	-.38000E 00
.68000E-01	.24586E 02	-.42000E 00
.69000E-01	.24166E 02	-.33000E 00
.70000E-01	.23836E 02	-.29000E 00
.71000E-01	.23546E 02	-.19000E 00
.72000E-01	.23356E 02	-.16000E 00
.73000E-01	.23196E 02	-.19000E 00
.74000E-01	.23006E 02	-.28000E 00
.75000E-01	.22726E 02	1.00000E-02
.76000E-01	.22736E 02	-.70000E-01
.77000E-01	.22666E 02	-.50000E-01
.78000E-01	.22616E 02	-1.00000E-01
.79000E-01	.22516E 02	-.50000E-01
.80000E-01	.22466E 02	-.70000E-01
.81000E-01	.22396E 02	-.40000E-01
.82000E-01	.22356E 02	-.60000E-01
.83000E-01	.22296E 02	-.19000E 00
.84000E-01	.22106E 02	-.17000E 00
.85000E-01	.21936E 02	-.21000E 00
.86000E-01	.21726E 02	-.20000E 00
.87000E-01	.21526E 02	-.48000E 00
.88000E-01	.21046E 02	-.32000E 00
.89000E-01	.20726E 02	-.20000E 00
.90000E-01	.20526E 02	-.13000E 00
.91000E-01	.20396E 02	-1.00000E-01
.92000E-01	.20296E 02	-.23000E 00
.93000E-01	.20066E 02	-1.00000E-02
.94000E-01	.20056E 02	-.80000E-01
.95000E-01	.19976E 02	-.16000E 00
.96000E-01	.19816E 02	-.11000E 00
.97000E-01	.19706E 02	-.11000E 00
.98000E-01	.19596E 02	-.14500E 00
.99000E-01	.19451E 02	-.11000E 00
1.00000E-01	.19341E 02	.00000E 00
.10100E 00	.19341E 02	-1.00000E-01
.10200E 00	.19241E 02	-.19500E 00
.10300E 00	.19046E 02	-.55000E-01
.10400E 00	.18991E 02	-.65000E-01
.10500E 00	.18926E 02	-.60000E-01
.10600E 00	.18866E 02	-.90000E-01
.10700E 00	.18776E 02	-.80000E-01
.10800E 00	.18696E 02	-.85000E-01
.10900E 00	.18611E 02	-.65000E-01
.11000E 00	.18546E 02	-.70000E-01
.11100E 00	.18476E 02	-.50000E-01
.11200E 00	.18426E 02	-.20000E-01
.11300E 00	.18406E 02	-.30000E-01
.11400E 00	.18376E 02	-.60000E-01
.11500E 00	.18316E 02	-.65000E-01
.11600E 00	.18251E 02	-.45000E-01

.11700E 00	.18206E 02	-.40000E-01
.11800E 00	.18166E 02	-.30000E-01
.11900E 00	.18136E 02	-.50000E-01
.12000E 00	.18086E 02	-.50000E-01
.12100E 00	.18036E 02	-.40000E-01
.12200E 00	.17996E 02	-.40000E-01
.12300E 00	.17956E 02	-.40000E-01
.12400E 00	.17916E 02	-.40000E-01
.12500E 00	.17876E 02	-.30000E-01
.12600E 00	.17846E 02	-.45000E-01
.12700E 00	.17801E 02	-.35000E-01
.12800E 00	.17766E 02	-.15000E-01
.12900E 00	.17751E 02	-.70000E-01
.13000E 00	.17681E 02	-.55000E-01
.13100E 00	.17626E 02	-.50000E-01
.13200E 00	.17576E 02	-.40000E-01
.13300E 00	.17536E 02	-.40000E-01
.13400E 00	.17496E 02	-.40000E-01
.13500E 00	.17456E 02	-.50000E-01
.13600E 00	.17406E 02	-.40000E-01
.13700E 00	.17366E 02	-.40000E-01
.13800E 00	.17326E 02	-.40000E-01
.13900E 00	.17286E 02	-.70000E-01
.14000E 00	.17216E 02	-.90000E-01
.14200E 00	.17126E 02	-.50000E-01
.14300E 00	.17076E 02	-.40000E-01
.14400E 00	.17036E 02	-.40000E-01
.14500E 00	.16996E 02	-.40000E-01
.14600E 00	.16956E 02	-.40000E-01
.14700E 00	.16916E 02	-.30000E-01
.14800E 00	.16886E 02	-.50000E-01
.14900E 00	.16836E 02	-.30000E-01
.15000E 00	.16806E 02	-.30000E-01
.15100E 00	.16776E 02	-.20000E-01
.15200E 00	.16756E 02	-.20000E-01
.15300E 00	.16736E 02	-.20000E-01
.15400E 00	.16716E 02	-1.00000E-02
.15500E 00	.16706E 02	-.20000E-01
.15600E 00	.16686E 02	-1.00000E-02
.15700E 00	.16676E 02	-.20000E-01
.15800E 00	.16656E 02	-1.00000E-02
.15900E 00	.16646E 02	-1.00000E-02
.16000E 00	.16636E 02	-.20000E-01
.16100E 00	.16616E 02	-1.00000E-02
.16200E 00	.16606E 02	-1.00000E-02
.16300E 00	.16596E 02	-1.00000E-02
.16400E 00	.16586E 02	.00000E 00
.16500E 00	.16586E 02	-.40000E-01
.17000E 00	.16546E 02	-.30000E-01
.17500E 00	.16516E 02	-.20000E-01
.18000E 00	.16496E 02	-.30000E-01
.18500E 00	.16466E 02	-.40000E-01
.19000E 00	.16426E 02	-.20000E-01
.19500E 00	.16406E 02	-.70000E 00
.40000E 00	.15706E 02	-.10000E 00
.60000E 00	.15606E 02	-.19000E 00
.80000E 00	.15416E 02	-.40000E-01
.10000E 01	.15376E 02	-.40000E-01
.12500E 01	.15336E 02	-.40000E-01
.15000E 01	.15296E 02	-.30000E-01

.17500E 01	.15266E 02	-.27000E-01
.20000E 01	.15239E 02	-.45000E-01
.25000E 01	.15194E 02	-.53000E-01
.30000E 01	.15141E 02	-.70000E-02
.35000E 01	.15134E 02	-.35000E-01
.40000E 01	.15099E 02	-.13000E-01
.45000E 01	.15086E 02	-.10000E-01
.50000E 01	.15076E 02	.18845E-36

SØLKA FLØC (ALPHA CELLULOSE)

XVII-1-65

.40000E-02	.31645E 02	-.24000E 01
.50000E-02	.29245E 02	-.28400E 01
.60000E-02	.26405E 02	-.44000E 00
.70000E-02	.25965E 02	-.12000E 00
.80000E-02	.25845E 02	-.25000E 00
.90000E-02	.25595E 02	-.16000E 00
1.00000E-02	.25435E 02	-.18000E 00
.11000E-01	.25255E 02	-.15000E 00
.12000E-01	.25105E 02	-.13000E 00
.13000E-01	.24975E 02	-.12000E 00
.14000E-01	.24855E 02	-.11000E 00
.15000E-01	.24745E 02	-.11000E 00
.16000E-01	.24635E 02	-.90000E-01
.17000E-01	.24545E 02	-.10500E 00
.18000E-01	.24440E 02	-.75000E-01
.19000E-01	.24365E 02	-.90000E-01
.20000E-01	.24275E 02	-.90000E-01
.21000E-01	.24185E 02	-.90000E-01
.22000E-01	.24095E 02	-.70000E-01
.23000E-01	.24025E 02	-.60000E-01
.24000E-01	.23965E 02	-.80000E-01
.25000E-01	.23885E 02	-.70000E-01
.26000E-01	.23815E 02	-.50000E-01
.27000E-01	.23765E 02	-.60000E-01
.28000E-01	.23705E 02	-.50000E-01
.29000E-01	.23655E 02	-.50000E-01
.30000E-01	.23605E 02	-.60000E-01
.31000E-01	.23545E 02	-.50000E-01
.32000E-01	.23495E 02	-.40000E-01
.33000E-01	.23455E 02	-.40000E-01
.34000E-01	.23415E 02	-.40000E-01
.35000E-01	.23375E 02	-.40000E-01
.36000E-01	.23335E 02	-.30000E-01
.37000E-01	.23305E 02	-.30000E-01
.38000E-01	.23275E 02	-.30000E-01
.39000E-01	.23245E 02	-.40000E-01
.40000E-01	.23205E 02	-.30000E-01
.41000E-01	.23175E 02	-.20000E-01
.42000E-01	.23155E 02	-.20000E-01
.43000E-01	.23135E 02	-.30000E-01
.44000E-01	.23105E 02	-.20000E-01
.45000E-01	.23085E 02	-.20000E-01
.46000E-01	.23065E 02	-.20000E-01
.47000E-01	.23045E 02	-.20000E-01
.48000E-01	.23025E 02	-.20000E-01
.49000E-01	.23005E 02	-1.00000E-02
.50000E-01	.22995E 02	-.30000E-01
.51000E-01	.22965E 02	-.20000E-01
.52000E-01	.22945E 02	-.20000E-01
.53000E-01	.22925E 02	-.20000E-01
.54000E-01	.22905E 02	-1.00000E-02
.55000E-01	.22895E 02	-.50000E-01
.60000E-01	.22845E 02	-.60000E-01
.65000E-01	.22785E 02	-.50000E-01
.70000E-01	.22735E 02	-.50000E-01
.75000E-01	.22685E 02	-.30000E-01
.80000E-01	.22655E 02	-.35000E-01
.85000E-01	.22620E 02	-.25000E-01

.90000E-01	.22595E 02	-.20000E-01
.95000E-01	.22575E 02	-.30000E-01

*** ALL INPUT DATA HAVE BEEN PROCESSED.
AT LOCATION 11550

APPENDIX D

COMPUTER OUTPUT OF EXPERIMENTAL RESULTS

\$COMPILE MAD,EXECUTE,PRINT OBJECT,DUMP

D (01 OCT 1965 VERSION) PROGRAM LISTING

.....PROGRAM FOR CALCULATING POROSITY AND ALPHA

DIMENSION MAT(6),THETA(100),LZ(100),FLOW(100),EPSLON(100),
 1 ALPHA(100),LCAKE(100)
 INTEGER I,J,MAT,N,MAXN0,TEMPER
 START PRINT COMMENT \$1\$
 READ FORMAT NAME, MAT(1)..MAT(6)
 VECTOR VALUES NAME = \$6C6*\$
 READ DATA

.....THIS READS IN THE FOLLOWING DATA

FORCE = WEIGHT APPLIED TO COMPRESS CAKE FOR EACH RUN, LB.F
 WCAKE = WEIGHT OF DRY CAKE, GRAMS
 RHOS = TRUE SOLIDS DENSITY, LB.M/CU.FT.
 RHOL = LIQUID DENSITY, LB.M/CU.FT.
 TEMPER = AMBIENT TEMPERATURE, DEGREES F
 VISC = LIQUID VISCOSITY, CP
 DLDIAL = FINAL CAKE HEIGHT PLUS FINAL DIAL READING, MM
 DPRESS = HYDROSTATIC PRESSURE, INCHES WATER
 N = NUMBER OF PERIODS DURING RUN
 THETA = TIME PERIODS DURING RUN, SECONDS
 FLOW = PERMEATION, CC/SEC
 LCAKE = DIAL READING, MM

VSOL=WCAKE*RHOL/RHOS
 DELP=5.2*DPRESS
 AFACTR=32.174*DELP/(.000672*VISC*RHOS)
 THROUGH ALEF, FOR I=1,1,I.G.N
 DELH=DL DIAL-LCAKE(I)
 VCAKE=2.074738*DELH
 POROS=1.-VSOL/VCAKE
 EPSLON(I)=POROS
 LZ(I)=DELH/25.4
 Z=DELH/304.8
 QUE=FLOW(I)/632.52331
 WHENEVER QUE.E.O.O, TRANSFER TO ALEF
 ALPHA(I)=AFACTR/(QUE*Z*(1.-POROS))
 FLOW(O)=QUE
 ALEF CONTINUE

PRINT FORMAT TITLE, MAT(1)..MAT(6),WCAKE,RHOS,TEMPER,VISC,
 1 RHOL
 VECTOR VALUES TITLE = \$1H1,S27,26H EXPERIMENTAL RESULTS FROM,
 1 /,S22,38H COMPRESSION-PERMEABILITY CELL TESTING,/,18H M
 2 ATERIAL - ,6C6,/,21H CAKE WEIGHT = F7.4,19H GRAMS (DRY
 3 WEIGHT),/,21H SOLID DENS. = F5.1,12H LB.M/CU.FT.,/,21H
 4 TEMPERATURE = I2,2H F,/,21H VISCOSITY = F6.4,4H
 5 CP.,/,21H LIQ. DENS. = F5.1,12H LB.M/CU.FT. *\$
 PRINT COMMENT \$0\$
 PRINT RESULTS FORCE
 MAXN0=40
 WHENEVER FLOW(O).E.O.O, TRANSFER TO P00NLY
 PRINT COMMENT \$0 TIME-SEC THICKNESS FLOW RATE PORO

```

1 SITY SPEC. CAKE $
PRINT COMMENT $          INCHES          CC/SEC $
PRINT COMMENT $0$
THROUGH UM, FOR I=1,1,I.G.N
WHENEVER I.LE.MAXNO, TRANSFER TO UMM
PRINT COMMENT $1          EXPERIMENTAL RESULT
1 TS FROM $
PRINT COMMENT $          COMPRESSION-PERMEABILITY
1 CELL TESTING $
PRINT COMMENT $          (CONTINUED)
1 $
MAXNO=MAXNO+50
PRINT COMMENT $0$
PRINT COMMENT $0          TIME-SEC          THICKNESS          FLOW RATE          PORO
1 SITY SPEC. CAKE $
PRINT COMMENT $          INCHES          CC/SEC $
PRINT COMMENT $0$
UMM          WHENEVER FLOW(I).E.0.0
PRINT FORMAT ANSWR2, THETA(I), LZ(I), EPSLON(I)
OTHERWISE
PRINT FORMAT ANSWR1, THETA(I), LZ(I), FLOW(I), EPSLON(I), ALPHA(I)
VECTOR VALUES ANSWR1 = $ S7, F8.1, S4, F6.4, S5, F8.6, S4, F6.4, S3,
1 E12.5 *$
VECTOR VALUES ANSWR2 = $ S7, F8.1, S4, F6.4, S17, F6.4 *$
UM          END OF CONDITIONAL
TRANSFER TO ULTIMO
POONLY          PRINT COMMENT $0          TIME-SEC          THICKNESS          POROSITY $
PRINT COMMENT $          INCHES $
PRINT COMMENT $0$
THROUGH EN, FOR I=1,1,I.G.N
WHENEVER I.LE.MAXNO, TRANSFER TO EN
PRINT COMMENT $1          EXPERIMENTAL RESULT
1 TS FROM $
PRINT COMMENT $          COMPRESSION-PERMEABILITY
1 CELL TESTING $
PRINT COMMENT $          (CONTINUED)
1 $
MAXNO=MAXNO+50
PRINT COMMENT $0$
EN          PRINT FORMAT ANSWR3, THETA(I), LZ(I), EPSLON(I)
VECTOR VALUES ANSWR3 = $ S7, F8.1, S4, F6.4, S5, F6.4 *$
ULTIMO          EXECUTE ZERO.(FLOW(0)...FLOW(100))
TRANSFER TO START
END OF PROGRAM

```

THE FOLLOWING NAMES HAVE OCCURRED ONLY ONCE IN THIS PROGRAM.
 COMPILATION WILL CONTINUE.

```

DLDIAL          *011
DPRESS          *008
FORCE           *025
TEMPER         *022

```

EXPERIMENTAL RESULTS FROM
COMPRESSION-PERMEABILITY CELL TESTING

MATERIAL - SOLKA FLOC (ALPHA CELLULOSE)
 CAKE WEIGHT = 14.4362 GRAMS (DRY WEIGHT)
 SOLID DENS. = 95.8 LB./CU.FT.
 TEMPERATURE = 73 F
 VISCOSITY = .9410 CP.
 LIQ. DENS. = 62.3 LB./CU.FT.

FORCE = 25.300000

TIME-SEC	THICKNESS INCHES	FLOW RATE CC/SEC	POROSITY	SPEC. CAKE
6.0	.8264		.7846	
12.0	.8213		.7832	
24.0	.8185		.7825	
36.0	.8160		.7818	
48.0	.8142		.7814	
60.0	.8128		.7810	
90.0	.8104		.7803	
120.0	.8086		.7798	
150.0	.8070		.7794	
180.0	.8058		.7791	
210.0	.8045	.392000	.7787	.65685E 10
240.0	.8036		.7785	
270.0	.8028		.7782	
300.0	.8020	.352000	.7780	.73149E 10
360.0	.8008		.7777	
420.0	.7996	.346000	.7774	.74417E 10
480.0	.7984		.7770	
540.0	.7976	.347000	.7768	.74203E 10
600.0	.7969		.7766	
720.0	.7957	.328000	.7763	.78501E 10
840.0	.7943	.335000	.7759	.76861E 10
960.0	.7931	.351000	.7755	.73357E 10
1080.0	.7921	.332000	.7752	.77556E 10
1200.0	.7913	.331000	.7750	.77790E 10
1320.0	.7904	.330000	.7748	.78026E 10
1440.0	.7895	.326000	.7745	.78983E 10
1520.0	.7888	.323000	.7743	.79717E 10
1640.0	.7884	.313000	.7742	.82263E 10
1800.0	.7878	.305000	.7740	.84421E 10
2100.0	.7864	.318000	.7736	.80970E 10
2400.0	.7854	.312000	.7734	.82527E 10
2700.0	.7843	.309000	.7730	.83328E 10
3000.0	.7835	.304000	.7728	.84699E 10
3300.0	.7827	.302000	.7726	.85260E 10
3600.0	.7821	.297000	.7724	.86695E 10
4200.0	.7806	.290000	.7720	.88788E 10
4800.0	.7795	.285000	.7716	.90345E 10
5400.0	.7784	.278000	.7713	.92620E 10
6000.0	.7709	.273000	.7691	.94317E 10
6600.0	.7685	.264000	.7684	.97532E 10

EXPERIMENTAL RESULTS FROM
COMPRESSION-PERMEABILITY CELL TESTING
(CONTINUED)

TIME-SEC	THICKNESS INCHES	FLOW RATE CC/SEC	POROSITY	SPEC. CAKE
7200.0	.7676	.258000	.7681	.99800E 10
7800.0	.7665	.255000	.7678	.10097E 11
8400.0	.7661	.250000	.7676	.10299E 11
9000.0	.7654	.248000	.7674	.10382E 11
9600.0	.7650	.242000	.7673	.10640E 11
10200.0	.7646	.240000	.7672	.10729E 11
10740.0	.7634	.234000	.7668	.11004E 11

EXPERIMENTAL RESULTS FROM
COMPRESSION-PERMEABILITY CELL TESTING

MATERIAL - SØLKA FLØC (ALPHA CELLULOSE)
 CAKE WEIGHT = 14.5307 GRAMS (DRY WEIGHT)
 SOLID DENS. = 95.8 LB./CU.FT.
 TEMPERATURE = 72 F
 VISCOSITY = .9530 CP.
 LIQ. DENS. = 62.3 LB./CU.FT.

FORCE = 50.300000

TIME-SEC	THICKNESS INCHES	FLOW RATE CC/SEC	POROSITY	SPEC. CAKE
12.0	.7540		.7624	
24.0	.7465		.7600	
36.0	.7438		.7591	
48.0	.7414		.7583	
60.0	.7402		.7579	
90.0	.7375		.7570	
120.0	.7343	.233000	.7560	.11119E 11
150.0	.7327		.7555	
180.0	.7312		.7549	
210.0	.7304	.247000	.7547	.10489E 11
240.0	.7288		.7541	
270.0	.7280	.224000	.7539	.11566E 11
300.0	.7264		.7533	
360.0	.7249	.217000	.7528	.11939E 11
420.0	.7237	.233000	.7524	.11119E 11
480.0	.7225	.217000	.7520	.11939E 11
540.0	.7215	.210000	.7517	.12337E 11
600.0	.7205		.7513	
720.0	.7190	.208000	.7508	.12456E 11
840.0	.7174	.203000	.7502	.12763E 11
960.0	.7162	.202000	.7498	.12826E 11
1080.0	.7150	.201000	.7494	.12890E 11
1200.0	.7138	.200000	.7490	.12954E 11
1320.0	.7131	.198000	.7487	.13085E 11
1440.0	.7123	.198000	.7484	.13085E 11
1560.0	.7115	.197000	.7482	.13151E 11
1680.0	.7107	.195000	.7479	.13286E 11
1800.0	.7099	.193000	.7476	.13424E 11
2100.0	.7083	.188000	.7470	.13781E 11
2400.0	.7068	.185000	.7465	.14005E 11
2700.0	.7058	.184000	.7461	.14081E 11
3000.0	.7046	.183000	.7457	.14158E 11
3600.0	.7028	.175000	.7451	.14805E 11
4200.0	.7012	.170000	.7445	.15240E 11
4800.0	.7001	.166000	.7441	.15607E 11
5400.0	.6988	.163000	.7436	.15895E 11
6000.0	.6980	.159000	.7433	.16295E 11
6600.0	.6969	.154000	.7429	.16824E 11
7200.0	.6961	.151000	.7426	.17158E 11
7800.0	.6953	.147000	.7423	.17625E 11

EXPERIMENTAL RESULTS FROM
COMPRESSION-PERMEABILITY CELL TESTING
(CONTINUED)

TIME-SEC	THICKNESS INCHES	FLOW RATE CC/SEC	POROSITY	SPEC. CAKE
8400.0	.6947	.143000	.7421	.18118E 11
9000.0	.6942	.140000	.7419	.18506E 11
9600.0	.6936	.138000	.7417	.18774E 11
10200.0	.6928	.133000	.7414	.19480E 11
10800.0	.6925	.130000	.7412	.19930E 11
11400.0	.6920	.128000	.7411	.20241E 11
12000.0	.6916	.127000	.7409	.20400E 11
12600.0	.6910	.123000	.7407	.21064E 11
13200.0	.6906	.120000	.7405	.21590E 11
13800.0	.6905	.118000	.7405	.21956E 11
14400.0	.6900	.117000	.7403	.22144E 11
15000.0	.6895	.113000	.7401	.22928E 11
15600.0	.6891	.112000	.7400	.23132E 11
16200.0	.6886	.108000	.7398	.23989E 11
21000.0	.6860		.7388	
21600.0	.6858	.091700	.7387	.28253E 11
22200.0	.6857	.089200	.7387	.29045E 11
22800.0	.6854	.088300	.7386	.29341E 11
23400.0	.6852	.086700	.7385	.29883E 11
24000.0	.6851	.085900	.7384	.30161E 11
24600.0	.6849	.082800	.7384	.31290E 11
25200.0	.6846	.081600	.7383	.31750E 11
25800.0	.6845	.080000	.7382	.32385E 11
26400.0	.6842	.079400	.7381	.32630E 11
27000.0	.6840	.077500	.7380	.33430E 11

EXPERIMENTAL RESULTS FROM
COMPRESSION-PERMEABILITY CELL TESTING

MATERIAL - SOLKA FLOC (ALPHA CELLULOSE)
 CAKE WEIGHT = 15.1138 GRAMS (DRY WEIGHT)
 SOLID DENS. = 95.8 LB./CU.FT.
 TEMPERATURE = 72 F
 VISCOSITY = .9530 CP.
 LIQ. DENS. = 62.3 LB./CU.FT.

FORCE = 75.299999

TIME-SEC	THICKNESS INCHES	FLOW RATE CC/SEC	POROSITY	SPEC. CAKE
6.0	.6888		.7294	
12.0	.6821		.7268	
24.0	.6770		.7247	
36.0	.6741		.7235	
48.0	.6717		.7225	
60.0	.6701		.7219	
90.0	.6674		.7207	
120.0	.6652		.7198	
150.0	.6636		.7192	
180.0	.6621		.7185	
210.0	.6605		.7178	
240.0	.6599		.7176	
270.0	.6589		.7172	
300.0	.6581		.7168	
360.0	.6562	.149200	.7160	.16462E 11
420.0	.6550		.7155	
480.0	.6538	.145000	.7149	.16939E 11
540.0	.6530		.7146	
600.0	.6520	.133000	.7142	.18468E 11
660.0	.6512	.132000	.7138	.18608E 11
720.0	.6506	.130400	.7136	.18836E 11
840.0	.6493	.126200	.7130	.19463E 11
960.0	.6478	.125500	.7123	.19571E 11
1080.0	.6471	.123000	.7120	.19969E 11
1200.0	.6465	.120500	.7117	.20383E 11
1320.0	.6455	.117800	.7113	.20851E 11
1440.0	.6447	.112200	.7109	.21891E 11
1560.0	.6439	.107800	.7106	.22785E 11
1680.0	.6436	.103800	.7104	.23663E 11
1800.0	.6430	.100800	.7101	.24367E 11
2100.0	.6419	.098600	.7097	.24911E 11
2400.0	.6408	.096400	.7092	.25479E 11
2700.0	.6398	.093800	.7087	.26185E 11
3000.0	.6390	.091800	.7084	.26756E 11
3600.0	.6376	.090000	.7077	.27291E 11
4200.0	.6363	.088200	.7071	.27848E 11
4800.0	.6353	.086500	.7066	.28395E 11
5400.0	.6344	.085000	.7062	.28896E 11
6000.0	.6337	.083500	.7059	.29415E 11
6600.0	.6329	.082100	.7055	.29917E 11

EXPERIMENTAL RESULTS FROM
 COMPRESSION-PERMEABILITY CELL TESTING
 (CONTINUED)

TIME-SEC	THICKNESS INCHES	FLOW RATE CC/SEC	POROSITY	SPEC. CAKE
7200.0	.6323	.080500	.7053	.30512E 11
7800.0	.6317	.079000	.7050	.31091E 11
8400.0	.6312	.041600	.7047	.59043E 11
9000.0	.6306	.040200	.7045	.61099E 11
9600.0	.6302	.039900	.7043	.61559E 11
10200.0	.6298	.039000	.7041	.62979E 11
10800.0	.6293	.038700	.7038	.63467E 11
11400.0	.6290	.037600	.7037	.65324E 11
12000.0	.6286	.036900	.7035	.66563E 11
12600.0	.6284	.036500	.7034	.67293E 11
13200.0	.6281	.035200	.7033	.69778E 11
13800.0	.6278	.034500	.7031	.71194E 11
14400.0	.6275	.034200	.7030	.71818E 11
36000.0	.6214	.034200	.7001	.71818E 11
36600.0	.6214	.033000	.7001	.74430E 11
37200.0	.6212	.032400	.7000	.75808E 11
37800.0	.6211	.032300	.6999	.76043E 11
38400.0	.6210	.031600	.6999	.77728E 11
39000.0	.6209	.031000	.6998	.79232E 11
39600.0	.6208	.030400	.6998	.80796E 11
40200.0	.6207	.030200	.6997	.81331E 11
40800.0	.6206		.6997	
41400.0	.6204		.6996	
42000.0	.6203		.6996	
42600.0	.6203		.6995	
43200.0	.6202		.6995	
43800.0	.6200		.6994	
44400.0	.6199		.6994	
45000.0	.6199		.6993	
45600.0	.6199		.6993	
46200.0	.6195		.6992	
46800.0	.6195		.6992	

EXPERIMENTAL RESULTS FROM
COMPRESSION-PERMEABILITY CELL TESTING

MATERIAL - SOLKA FLOC (ALPHA-CELLULOSE)
 CAKE WEIGHT = 13.2860 GRAMS (DRY WEIGHT)
 SOLID DENS. = 95.8 LB./CU.FT.
 TEMPERATURE = 75 F
 VISCOSITY = .9190 CP.
 LIQ. DENS. = 62.3 LB./CU.FT.

FORCE = 100.299999

TIME-SEC	THICKNESS INCHES	FLOW RATE CC/SEC	POROSITY	SPEC. CAKE
60.0	.5933		.7240	
90.0	.5803		.7178	
120.0	.5756		.7155	
150.0	.5734	.112500	.7144	.29694E 11
180.0	.5725		.7139	
210.0	.5716		.7135	
240.0	.5704	.101700	.7129	.32847E 11
270.0	.5693		.7123	
300.0	.5675		.7114	
360.0	.5649		.7101	
420.0	.5637	.100000	.7095	.33405E 11
480.0	.5630		.7091	
540.0	.5626		.7089	
600.0	.5616	.096670	.7084	.34556E 11
720.0	.5604	.093330	.7078	.35793E 11
840.0	.5593	.090830	.7072	.36778E 11
960.0	.5586	.090830	.7068	.36778E 11
1080.0	.5576	.089670	.7063	.37254E 11
1200.0	.5569	.088330	.7059	.37819E 11
1320.0	.5563	.086500	.7056	.38619E 11
1440.0	.5557	.084670	.7053	.39454E 11
1560.0	.5551	.083570	.7050	.39973E 11
1680.0	.5547	.082500	.7048	.40491E 11
1800.0	.5543	.079100	.7045	.42232E 11
2100.0	.5531	.081000	.7039	.41241E 11
2400.0	.5523	.079100	.7035	.42232E 11
2700.0	.5515	.077700	.7031	.42993E 11
3000.0	.5509	.076300	.7027	.43782E 11
3600.0	.5496	.075100	.7020	.44481E 11
4200.0	.5486	.073700	.7015	.45326E 11
4800.0	.5476	.071900	.7009	.46461E 11
5400.0	.5469	.070600	.7005	.47316E 11
6000.0	.5464	.069400	.7003	.48134E 11
6600.0	.5456	.068900	.6999	.48484E 11
7200.0	.5450	.067800	.6995	.49270E 11
7860.0	.5445	.065000	.6992	.51393E 11
8400.0	.5441	.062900	.6990	.53109E 11
9000.0	.5437	.062300	.6988	.53620E 11
9600.0	.5432	.060700	.6985	.55033E 11
10200.0	.5429	.059600	.6983	.56049E 11

EXPERIMENTAL RESULTS FROM
COMPRESSION-PERMEABILITY CELL TESTING
(CONTINUED)

TIME-SEC	THICKNESS INCHES	FLOW RATE CC/SEC	POROSITY	SPEC. CAKE
10800.0	.5427	.058600	.6982	.57006E 11
11400.0	.5423	.057700	.6980	.57895E 11
12000.0	.5420	.056800	.6978	.58812E 11
27900.0	.5359		.6944	
28200.0	.5358		.6943	
28800.0	.5357	.039600	.6943	.84357E 11
29400.0	.5357	.040100	.6943	.83305E 11
30000.0	.5356	.039300	.6943	.85001E 11
30600.0	.5356	.039600	.6942	.84357E 11
31200.0	.5354	.038200	.6941	.87448E 11
31800.0	.5353	.038400	.6941	.86993E 11
32400.0	.5353	.037800	.6940	.88374E 11
33000.0	.5352	.037300	.6940	.89558E 11
33600.0	.5350	.036900	.6939	.90529E 11

EXPERIMENTAL RESULTS FROM
COMPRESSION-PERMEABILITY CELL TESTING

MATERIAL - SOLKA FLOC (ALPHA CELLULOSE)
 CAKE WEIGHT = 14.4288 GRAMS (DRY WEIGHT)
 SOLID DENS. = 95.8 LB./CU.FT.
 TEMPERATURE = 72 F
 VISCOSITY = .9530 CP.
 LIQ. DENS. = 62.3 LB./CU.FT.

FORCE = 15.300000

TIME-SEC	THICKNESS INCHES	POROSITY
----------	---------------------	----------

-.00	1.3309	.8663
.06	1.3293	.8661
.12	1.2931	.8624
.18	1.2675	.8596
.24	1.2616	.8589
.30	1.2470	.8573
.36	1.2289	.8552
.42	1.1899	.8505
.48	1.1537	.8458
.60	1.1502	.8453
.66	1.1411	.8441
.72	1.1376	.8436
.78	1.1340	.8431
.84	1.1309	.8426
.90	1.1273	.8421
.96	1.1234	.8416
1.02	1.1218	.8414
1.08	1.1187	.8409
1.14	1.1147	.8404
1.56	1.1010	.8384
1.68	1.0982	.8380
1.74	1.0966	.8377
1.80	1.0923	.8371
1.86	1.0903	.8368
1.92	1.0884	.8365
1.98	1.0864	.8362
2.04	1.0840	.8358
2.10	1.0825	.8356
2.16	1.0805	.8353
2.34	1.0750	.8345
2.40	1.0734	.8342
2.52	1.0718	.8340
2.58	1.0687	.8335
2.64	1.0671	.8332
2.70	1.0659	.8331
2.76	1.0643	.8328
2.88	1.0616	.8324
3.00	1.0588	.8319
3.06	1.0580	.8318
3.12	1.0569	.8316

EXPERIMENTAL RESULTS FROM
COMPRESSION-PERMEABILITY CELL TESTING
(CONTINUED)

TIME-SEC	THICKNESS INCHES	POROSITY
3.18	1.0557	.8314
3.24	1.0549	.8313
3.30	1.0533	.8311
3.42	1.0517	.8308
30.36	1.0163	.8249
60.36	1.0159	.8248
90.36	1.0096	.8237
126.36	1.0073	.8233

EXPERIMENTAL RESULTS FROM
COMPRESSION-PERMEABILITY CELL TESTING

MATERIAL - SOLKA FLOC (ALPHA CELLULOSE)
 CAKE WEIGHT = 14.4288 GRAMS (DRY WEIGHT)
 SOLID DENS. = 95.8 LB./CU.FT.
 TEMPERATURE = 72 F
 VISCOSITY = .9530 CP.
 LIQ. DENS. = 62.3 LB./CU.FT.

FORCE = 40.300000

TIME-SEC	THICKNESS INCHES	POROSITY
----------	---------------------	----------

.00	1.0073	.8233
.30	1.0073	.8233
.60	1.0073	.8233
.90	1.0073	.8233
1.20	1.0073	.8233
1.50	1.0073	.8233
1.56	1.0029	.8226
1.68	1.0053	.8230
1.74	.9828	.8189
1.80	.9541	.8135
1.86	.9435	.8114
1.92	.9269	.8080
1.98	.9100	.8045
2.04	.8974	.8017
2.10	.8868	.7993
2.16	.8773	.7972
2.22	.8699	.7954
2.28	.8643	.7941
2.34	.8592	.7929
2.40	.8549	.7918
2.46	.8514	.7910
2.52	.8486	.7903
2.58	.8458	.7896
2.64	.8419	.7886
2.70	.8411	.7884
2.76	.8391	.7879
2.82	.8376	.7875
2.88	.8364	.7872
2.94	.8352	.7869
3.00	.8336	.7865
3.06	.8317	.7860
3.12	.8313	.7859
3.18	.8311	.7859
3.24	.8297	.7855
3.42	.8281	.7851
20.70	.8069	.7795
52.50	.7986	.7772
68.70	.7974	.7768
83.70	.7962	.7765
98.70	.7954	.7763

EXPERIMENTAL RESULTS FROM
COMPRESSION-PERMEABILITY CELL TESTING
(CONTINUED)

TIME-SEC	THICKNESS INCHES	POROSITY
119.70	.7939	.7758
120.00	.7939	.7758

EXPERIMENTAL RESULTS FROM
COMPRESSION-PERMEABILITY CELL TESTING

MATERIAL - SOLKA FLOC (ALPHA CELLULOSE)
CAKE WEIGHT = 14.6001 GRAMS (DRY WEIGHT)
SOLID DENS. = 95.8 LB./CU.FT.
TEMPERATURE = 72 F
VISCOSITY = .9530 CP.
LIQ. DENS. = 62.3 LB./CU.FT.

FORCE = 15.300000

TIME-SEC	THICKNESS INCHES	POROSITY
----------	---------------------	----------

.00	1.0997	.8363
.06	1.0902	.8348
.12	1.0524	.8289
.18	1.0410	.8270
.24	1.0135	.8223
.30	1.0095	.8216
.36	1.0036	.8206
.42	.9973	.8195
.48	.9910	.8183
.54	.9859	.8174
.60	.9808	.8164
.66	.9769	.8157
.72	.9733	.8150
.78	.9698	.8143
.84	.9666	.8137
.90	.9635	.8131
.96	.9615	.8127
1.02	.9587	.8122
1.08	.9568	.8118
1.14	.9552	.8115
1.20	.9532	.8111
1.26	.9513	.8107
1.32	.9497	.8104
1.38	.9481	.8101
1.44	.9465	.8098
1.50	.9454	.8095
1.56	.9442	.8093
1.62	.9430	.8091
1.68	.9418	.8088
1.74	.9410	.8087
1.80	.9399	.8084
1.86	.9391	.8082
1.92	.9379	.8080
2.22	.9343	.8073
2.82	.9288	.8061
3.42	.9253	.8054
17.82	.9052	.8011
38.22	.9001	.7999
59.82	.8965	.7992
89.82	.8938	.7985

EXPERIMENTAL RESULTS FROM
COMPRESSION-PERMEABILITY CELL TESTING
(CONTINUED)

TIME-SEC	THICKNESS INCHES	POROSITY
----------	---------------------	----------

119.82	.8918	.7981
149.82	.8902	.7977
179.82	.8891	.7975
239.82	.8889	.7974
299.82	.8887	.7974
359.82	.8885	.7973
419.82	.8884	.7973
479.82	.8883	.7973
539.82	.8875	.7971
599.82	.8863	.7968

EXPERIMENTAL RESULTS FROM
COMPRESSION-PERMEABILITY CELL TESTING

MATERIAL - SOLKA FLOC (ALPHA CELLULOSE)
 CAKE WEIGHT = 14.6001 GRAMS (DRY WEIGHT)
 SOLID DENS. = 95.8 LB./CU.FT.
 TEMPERATURE = 72 F
 VISCOSITY = .9530 CP.
 LIQ. DENS. = 62.3 LB./CU.FT.

FORCE = 40.30000

TIME-SEC	THICKNESS INCHES	POROSITY
----------	---------------------	----------

.00	.8863	.7968
.30	.8859	.7967
.36	.8855	.7967
.42	.8832	.7961
.48	.8776	.7948
.54	.8658	.7920
.60	.8524	.7888
.66	.8406	.7858
.72	.8284	.7826
.78	.8182	.7799
.84	.8099	.7777
.90	.8040	.7760
1.02	.7997	.7748
1.08	.7958	.7737
1.14	.7930	.7729
1.20	.7906	.7723
1.26	.7887	.7717
1.32	.7871	.7712
1.38	.7855	.7708
1.44	.7847	.7705
1.50	.7832	.7701
1.56	.7824	.7698
1.62	.7816	.7696
1.68	.7808	.7694
1.74	.7800	.7691
1.80	.7796	.7690
2.10	.7765	.7681
2.70	.7729	.7670
3.30	.7710	.7664
20.88	.7580	.7624
33.00	.7552	.7616
59.70	.7517	.7604
89.70	.7497	.7598
120.24	.7481	.7593
179.76	.7461	.7587
239.70	.7446	.7582
299.76	.7430	.7577
359.70	.7418	.7573
419.70	.7410	.7570
479.70	.7399	.7566

EXPERIMENTAL RESULTS FROM
COMPRESSION-PERMEABILITY CELL TESTING
(CONTINUED)

TIME-SEC	THICKNESS INCHES	POROSITY
539.70	.7391	.7564
599.70	.7383	.7561

EXPERIMENTAL RESULTS FROM
COMPRESSION-PERMEABILITY CELL TESTING

MATERIAL - SOLKA FLOC (ALPHA CELLULOSE)
 CAKE WEIGHT = 14.6725 GRAMS (DRY WEIGHT)
 SOLID DENS. = 95.8 LB./CU.FT.
 TEMPERATURE = 72 F
 VISCOSITY = .9530 CP.
 LIQ. DENS. = 62.3 LB./CU.FT.

FORCE = 15.30000

TIME-SEC	THICKNESS INCHES	POROSITY
----------	---------------------	----------

.00	1.2459	.8548
.06	1.1514	.8428
.12	1.0396	.8259
.18	1.0222	.8230
.24	1.0175	.8222
.30	1.0077	.8204
.36	1.0014	.8193
.42	.9943	.8180
.48	.9884	.8169
.54	.9833	.8160
.60	.9785	.8151
.66	.9742	.8142
.72	.9699	.8134
.78	.9663	.8127
.84	.9622	.8119
.90	.9592	.8114
.96	.9557	.8107
1.02	.9521	.8099
1.08	.9486	.8092
1.14	.9459	.8087
1.20	.9435	.8082
1.26	.9403	.8076
1.32	.9376	.8070
1.38	.9356	.8066
1.44	.9333	.8061
1.50	.9313	.8057
1.56	.9293	.8053
1.62	.9270	.8048
1.68	.9250	.8044
1.74	.9234	.8040
1.80	.9218	.8037
1.86	.9203	.8034
1.92	.9187	.8030
1.98	.9175	.8028
2.04	.9163	.8025
2.10	.9151	.8023
2.16	.9136	.8019
2.22	.9124	.8017
2.28	.9116	.8015
2.34	.9108	.8013

EXPERIMENTAL RESULTS FROM
COMPRESSION-PERMEABILITY CELL TESTING
(CONTINUED)

TIME-SEC	THICKNESS INCHES	POROSITY
2.40	.9096	.8011
2.46	.9088	.8009
2.52	.9081	.8007
2.58	.9073	.8005
2.64	.9065	.8004
2.70	.9057	.8002
2.76	.9053	.8001
2.82	.9041	.7999
2.88	.9033	.7997
2.94	.9025	.7995
3.00	.9018	.7993
3.06	.9014	.7992
3.36	.8994	.7988
3.66	.8970	.7983
3.96	.8951	.7978
4.26	.8931	.7974
4.56	.8919	.7971
4.86	.8905	.7968
5.16	.8896	.7966
5.46	.8888	.7964

EXPERIMENTAL RESULTS FROM
COMPRESSION-PERMEABILITY CELL TESTING

MATERIAL - SOLKA FLOC (ALPHA CELLULOSE)
 CAKE WEIGHT = 14.6725 GRAMS (DRY WEIGHT)
 SOLID DENS. = 95.8 LB./CU.FT.
 TEMPERATURE = 72 F
 VISCOSITY = .9530 CP.
 LIQ. DENS. = 62.3 LB./CU.FT.

FORCE = 40.30000

TIME-SEC	THICKNESS INCHES	POROSITY
----------	---------------------	----------

.00	.8880	.7962
.30	.8868	.7959
.54	.8860	.7958
.60	.8836	.7952
.66	.8833	.7951
.72	.8825	.7949
.78	.8781	.7939
.84	.8746	.7931
.90	.8710	.7923
.96	.8651	.7908
1.02	.8494	.7870
1.08	.8305	.7821
1.14	.8144	.7778
1.20	.8025	.7745
1.26	.7931	.7718
1.32	.7860	.7698
1.38	.7801	.7680
1.44	.7754	.7666
1.50	.7718	.7655
1.56	.7687	.7646
1.62	.7663	.7639
1.68	.7640	.7631
1.74	.7620	.7625
1.80	.7604	.7620
1.86	.7596	.7618
1.92	.7584	.7614
1.98	.7569	.7609
2.04	.7561	.7607
2.10	.7553	.7604
2.16	.7545	.7602
2.28	.7533	.7598
2.40	.7525	.7595
2.52	.7514	.7592
2.64	.7502	.7588
2.76	.7494	.7585
2.88	.7486	.7583
3.00	.7478	.7580
3.30	.7462	.7575
3.60	.7447	.7570
3.90	.7439	.7567

EXPERIMENTAL RESULTS FROM
COMPRESSION-PERMEABILITY CELL TESTING
(CONTINUED)

TIME-SEC	THICKNESS INCHES	POROSITY
4.20	.7431	.7565
4.50	.7423	.7562
4.80	.7415	.7560
5.10	.7407	.7557
5.40	.7399	.7554
5.70	.7396	.7553

EXPERIMENTAL RESULTS FROM
COMPRESSION-PERMEABILITY CELL TESTING

MATERIAL - SOLKA FLOC (ALPHA CELLULOSE)
 CAKE WEIGHT = 13.3946 GRAMS (DRY WEIGHT)
 SOLID DENS. = 95.8 LB./CU.FT.
 TEMPERATURE = 72 F
 VISCOSITY = .9530 CP.
 LIQ. DENS. = 62.3 LB./CU.FT.

FORCE = 100.299999

TIME-SEC	THICKNESS INCHES	POROSITY
----------	---------------------	----------

.00	1.0652	.8449
.60	1.0652	.8449
.66	1.0589	.8440
.72	1.0353	.8404
.78	1.0325	.8400
.84	1.0207	.8382
.90	1.0065	.8359
.96	.9963	.8342
1.02	.9829	.8319
1.08	.9679	.8293
1.14	.9514	.8264
1.20	.9384	.8240
1.26	.9270	.8218
1.32	.9195	.8203
1.38	.9132	.8191
1.44	.9057	.8176
1.50	.8947	.8154
1.56	.8951	.8154
1.62	.8924	.8149
1.68	.8904	.8145
1.74	.8864	.8136
1.80	.8845	.8132
1.86	.8817	.8126
1.92	.8801	.8123
1.98	.8778	.8118
2.04	.8703	.8102
2.10	.8636	.8087
2.16	.8553	.8069
2.22	.8475	.8051
2.28	.8286	.8006
2.34	.8160	.7975
2.40	.8081	.7956
2.46	.8030	.7943
2.52	.7990	.7933
2.58	.7900	.7909
2.64	.7896	.7908
2.70	.7864	.7899
2.76	.7801	.7882
2.82	.7758	.7871
2.88	.7715	.7859

EXPERIMENTAL RESULTS FROM
COMPRESSION-PERMEABILITY CELL TESTING
(CONTINUED)

TIME-SEC	THICKNESS INCHES	POROSITY
2.94	.7658	.7843
3.00	.7614	.7830
3.06	.7614	.7830
3.12	.7575	.7819
3.18	.7498	.7797
3.24	.7477	.7790
3.30	.7451	.7783
3.36	.7427	.7776
3.42	.7392	.7765
3.48	.7361	.7756
3.54	.7327	.7745
3.60	.7301	.7737
3.66	.7274	.7729
3.72	.7254	.7723
3.78	.7246	.7720
3.84	.7235	.7717
3.90	.7211	.7709
3.96	.7185	.7701
4.02	.7168	.7695
4.08	.7152	.7690
4.14	.7140	.7686
4.20	.7120	.7680
4.26	.7101	.7674
4.32	.7085	.7668
4.38	.7069	.7663
4.44	.7053	.7658
4.50	.7038	.7653
4.56	.7026	.7649
4.62	.7008	.7643
4.68	.6994	.7638
4.74	.6989	.7636
4.80	.6961	.7627
4.86	.6939	.7619
4.92	.6920	.7613
4.98	.6904	.7607
5.04	.6888	.7602
5.10	.6872	.7596
5.16	.6853	.7589
5.22	.6837	.7584
5.28	.6821	.7578
5.34	.6805	.7573
5.40	.6778	.7563
5.52	.6742	.7550
5.58	.6723	.7543
5.64	.6707	.7537
5.70	.6691	.7531
5.76	.6676	.7525
5.82	.6660	.7519
5.88	.6648	.7515
5.94	.6628	.7508

EXPERIMENTAL RESULTS FROM
COMPRESSION-PERMEABILITY CELL TESTING
(CONTINUED)

TIME-SEC	THICKNESS INCHES	POROSITY
6.00	.6616	.7503
6.06	.6605	.7499
6.12	.6597	.7496
6.18	.6589	.7493
6.24	.6581	.7490
6.30	.6577	.7488
6.36	.6569	.7485
6.42	.6565	.7484
6.48	.6557	.7481
6.54	.6553	.7479
6.60	.6550	.7478
6.66	.6542	.7475
6.72	.6538	.7473
6.78	.6534	.7472
6.84	.6530	.7470
6.90	.6530	.7470
7.20	.6514	.7464
7.50	.6502	.7459
7.80	.6494	.7456
8.10	.6483	.7452
8.40	.6467	.7445
8.70	.6459	.7442
21.00	.6183	.7328
33.00	.6144	.7311
45.00	.6069	.7278
57.00	.6053	.7271
72.00	.6038	.7264
87.00	.6022	.7257
102.00	.6010	.7251
117.00	.6000	.7246
147.00	.5982	.7238
177.00	.5961	.7229
207.00	.5958	.7227
237.00	.5944	.7221
267.00	.5939	.7219
297.00	.5935	.7217

EXPERIMENTAL RESULTS FROM
COMPRESSION-PERMEABILITY CELL TESTING

MATERIAL - SOLKA FLOC (ALPHA CELLULOSE)
 CAKE WEIGHT = 13.3946 GRAMS (DRY WEIGHT)
 SOLID DENS. = 95.8 LB./CU.FT.
 TEMPERATURE = 72 F
 VISCOSITY = .9530 CP.
 LIQ. DENS. = 62.3 LB./CU.FT.

FORCE = 200.299999

TIME-SEC	THICKNESS INCHES	POROSITY
----------	---------------------	----------

.00	.5833	.7168
.06	.5825	.7164
.12	.5817	.7160
.18	.5809	.7156
.24	.5794	.7149
.30	.5766	.7135
.36	.5715	.7109
.42	.5685	.7094
.48	.5662	.7082
.54	.5630	.7066
.60	.5597	.7048
.66	.5571	.7035
.72	.5561	.7030
.78	.5536	.7016
.84	.5526	.7010
.90	.5508	.7001
.96	.5494	.6993
1.02	.5481	.6986
1.08	.5475	.6983
1.14	.5465	.6977
1.20	.5455	.6972
1.26	.5453	.6971
1.32	.5443	.6965
1.38	.5439	.6963
1.44	.5431	.6958
1.50	.5427	.6956
1.56	.5426	.6955
1.62	.5420	.6952
1.68	.5414	.6949
2.28	.5394	.6937
2.28	.5386	.6933
2.58	.5374	.6926
2.88	.5363	.6919
3.18	.5357	.6916
3.48	.5353	.6914
4.08	.5337	.6905
4.68	.5329	.6900
5.28	.5321	.6895
5.88	.5313	.6891
6.42	.5309	.6889

EXPERIMENTAL RESULTS FROM
COMPRESSION-PERMEABILITY CELL TESTING
(CONTINUED)

TIME-SEC	THICKNESS INCHES	POROSITY
7.68	.5290	.6877
19.68	.5231	.6842
31.68	.5160	.6798
43.68	.5132	.6781
55.68	.5120	.6774
70.68	.5095	.6758
85.68	.5081	.6749
100.68	.5067	.6740
115.68	.5057	.6734
145.68	.5042	.6723
175.68	.5018	.6708
205.68	.5013	.6704
235.68	.5005	.6700
265.68	.4998	.6695